CONFIDENTIAL

CCN

NATIONAL AERONAUTICS
AND SPACE ADMINISTRATION

(NASA-CR-71245) DEVELOPMENT ON SNAP-8 NUCLEAR POWER CONVERSION SYSTEM, MODEL AGAN-0010 Quarterly Report, 1 Sep. - 30 Nov. 1961 (Aerojet-General Corp., Azusa, Calif.) 131 p

N75-75647

Unclas
00/98 25969

DEVELOPMENT OF [U] SNAP-8

Nuclear Power Conversion System

MODEL AGAN-0010

Available to NASA Offices and NASA Centers Only

RECEIVED JUL 1975 NASA STI FACILITY INPUT BRANCH

Report 0390-04-6 (Quarterly)

February 1962

FACILITY FORM 602

X66 81428 (ACCESSION NUMBER) (THRU)

131 (PAGES) 1A (CODE)

CR-71245 (NASA CR OR TMX OR AD NUMBER) (CATEGORY)

POWER/EQUIPMENT DIVISION

Aerojet-General® CORPORATION

AZUSA, CALIFORNIA • SACRAMENTO, CALIFORNIA

A SUBSIDIARY OF THE GENERAL TIRE AND RUBBER COMPANY

11

CONFIDENTIAL

Contract 62-213

CONFIDENTIAL

C65-9492

7 February 1962

Report No. 0390-04-6

DEVELOPMENT OF SNAP-8 NUCLEAR POWER CONVERSION SYSTEM MODEL AGAN-0010

[U]

CLASSIFICATION CHANGE
To UNCLASSIFIED
By authority of NASA ltr TD 21-320
Changed by Orlando Lee Date 6/24/75
Classified Document Master Control Station, NASA
Scientific and Technical Information Facility

Contract NAS 5-417

Available to NASA Offices and NASA Centers Only.

No. of Pages: 125

Period Covered:

1 September 1961 through 30 November 1961

NOTE: This document contains information affecting the national defense of the United States within the meaning of the Espionage Laws, Title 18, USC, Sections 793 and 794. The transmission or the revelation of its contents in any manner to an unauthorized person is prohibited by law.

AEROJET-GENERAL CORPORATION
Azusa, California

EXCLUDED FROM THE GDS

CONTENTS

		Page
Contract Fulfillment Statement		viii
I.	INTRODUCTION	1
II.	OBJECTIVES	1
III.	SUMMARY OF ACCOMPLISHMENTS PRIOR TO 1 SEPTEMBER 1961	2
A.	Boiler	2
B.	Radiator	2
C.	Power-Drive Assembly	3
D.	Turbine	3
E.	Mercury Pump	3
F.	NaK Pump	3
G.	Bearings and Seals	3
H.	NaK Expansion Reservoir	3
I.	Speed Controller and Voltage Regulator	3
J.	Alternator	4
K.	NaK-Pump Motor	4
L.	Electromagnetic Start Pump	4
M.	Materials Evaluation	4
N.	Systems Engineering and Reliability	4
O.	Component Development Tests (Non-Nuclear)	5
P.	Low-Power Mercury-Vapor Test Loop (LPL)	5
Q.	Rated-Power Test Loop (RPL)	5
R.	Non-Nuclear System No. 1	5
S.	Ground Prototype Test Facility (GPTF)	5
T.	Flight Prototype Test Facility (FPTF)	5

CONTENTS (cont.)

		Page
IV.	THERMOMECHANICAL COMPONENTS	6
	A. Boiler	6
	B. Radiator	9
	C. Power-Drive Assembly	16
	D. Turbine	17
	E. Mercury Pump	22
	F. NaK Pump	23
	G. Bearings and Seals	23
	H. NaK Expansion Reservoir	27
	I. Mercury Recirculating Pump	28
V.	ELECTRICAL COMPONENT DEVELOPMENT	28
	A. Controls	28
	B. Alternator	32
	C. NaK-Pump Motor	34
VI.	MATERIALS EVALUATION	35
	A. Materials Development	35
	B. Materials Survey Experiments	42
VII.	SYSTEMS ENGINEERING AND RELIABILITY	47
	A. Systems Analysis Engineering	47
	B. Reliability	50
	C. 60-kw Feasibility Demonstration Program	52
VIII.	SUBSYSTEMS TESTS	53
	A. Summary of Accomplishments - 1 September Through 30 November 1961	53

CONTENTS (cont.)

Page

B. Discussion ____ 53

C. Work Planned for the Next Quarter ____ 55

IX. NON-NUCLEAR SYSTEMS TESTS ____ 55

A. Summary of Accomplishments - 1 September Through 30 November 1961 ____ 55

B. Discussion ____ 55

C. Work Planned for the Next Quarter ____ 57

X. NUCLEAR SYSTEMS, GROUND EVALUATION ____ 57

A. Summary of Accomplishments - 1 September Through 30 November 1961 ____ 57

B. Discussion ____ 57

C. Work Planned for the Next Quarter ____ 58

Table

1 Tabulation of Test Data: Unstable-Section Concept ____ 13

2 Saturation Density vs Temperature and Time ____ 37

3 Loop Sections Removed ____ 38

4 Deposits Removed ____ 39

5 Corrosion Layer Penetration ____ 43

6 Capsule Test Conditions ____ 45

Figure

Plot of Test Data from the Boiling-Mercury Heat-Transfer Test Loop ____ 1

Water Test Loop for Boiler Mockup ____ 2

Full-Scale Boiler Mockup ____ 3

Boiler for 6-tube Condensing Experiment (Disassembled) ____ 4

CONTENTS (cont.)

	Figure
Bend-Test Fixture	5
One-Inch-Diameter Haynes 25 Bellows	6
Three-Inch-Diameter Haynes 25 Bellows	7
Bend Test Data - One-Inch Haynes 25 Bellows	8
Bend Test Data - Three-Inch Haynes 25 Bellows	9
Three-Inch Deflection Joint Made From 0.020-in. Haynes 25	10
Three-Inch Flexible Joint Assembly	11
Tapered Radiator Tubes in the "As Cast" Condition	12
Closeup of Break in Casting to Minimize Shear Stress	13
Finished Machined Haynes 25 Tapered Tubes with 0.350-in. Aluminum Armor	14
Flared-Weld Diagram, Tube-to-Vapor Header	15a
Tube-to-Vapor Header Joint - Flared-Type Weld	15b
Tube-to-Manifold Plate Weld	16
Two-Stage Turbine Inertia Tests. Original Blade Height on the First-Stage Wheel	17
Two-Stage Turbine Inertia Tests Incorporating Increased Blade Height on First-Stage Wheel	18
Two-Stage Turbine Efficiency. Effect of Increased Blade Height in the First-Stage Wheel	19
Two-Stage Turbine Efficiency	20
Axial Pressure Distribution, Runs 33-35	21
Axial Pressure Distribution, Runs 50-55	22
Two-Stage Turbine Efficiency. Original Blade Height in First-Stage Wheel	23

CONTENTS (cont.)

	Figure
Two-Stage Turbine Efficiency. Effect of Increased Blade Height in First-Stage Wheel	24
Two-Stage Turbine Inertia Tests with Increased Blade Height on First-Stage Wheel	25
Axial Pressure Distribution, Nitrogen Gas	26
Mercury Bearing Test. Four-Axial Groove Bearing - No Evidence of Half-Frequency Whirl at 20,000 rpm	27
Mercury Bearing Test. Circumferential-Groove Bearing - Half-Frequency Whirl at 20,000 rpm	28
Electrical Schematic - Speed Controller (NNS-1)	29
Electrical Schematic - Voltage Regulator (NNS-1)	30
Electrical Schematic - Overspeed Trip Assembly	31
Electrical Schematic - Alternator Flashing Circuit	32
Electrical Schematic - Eddy-Current Brake, Rated-Power Loop Control Circuitry	33
Electrical Coordination Diagram - High-Temperature Control	34
Loop Sections Removed	35
Sample A - Condenser Outlet (Magnified 1000x)	36
Sample B - Pump Inlet (Magnified 250x)	37
Sample C - Pump Outlet (Magnified 10x)	38
Photomicrographs of Corrosion Layer Haynes 25 Compatibility Capsules	39
Microhardness Survey - Haynes 25 and Type 405 Stainless Steel Exposed to Mercury at 1025°F	40
Microhardness Survey - Haynes 25 Tubing Exposed to Mercury at 1100°F	41
Microhardness Survey; Haynes 25 Exposed to Mercury at 1175°F	42
Broken Tensile Specimen from Compatibility Capsule Exposed at 1100°F for 2000 hr	43

CONTENTS (cont.)

	Figure
Tensile Test Assembly	44
Microhardness Survey - Type 405 Stainless Steel Tubing Exposed to Mercury at 1100°F	45
Mercury Compatibility Capsules	46
Concentration of Elements Found in Mercury After 16 hr Contact with Haynes 8187	47

APPENDIX A - IBM 7090 RADIATOR OPTIMIZATION CODE - SNOR

APPENDIX B - MERCURY SOLUBILITY DATA FOR HAYNES ALLOY 8187

CONTRACT FULFILLMENT STATEMENT

This is the sixth in a series of quarterly progress reports submitted in partial fulfillment of Contract NAS 5-417.

I. INTRODUCTION

The Aerojet-General Corporation (AGC) is proceeding with the design and development of the SNAP-8 Power Conversion System (PCS) authorized by National Aeronautics and Space Administration (NASA) Contract No. NAS 5-417. The effective starting date of the contract was 9 May 1960.

The following nomenclature is used in this series of reports:

Electrical Generating System (EGS) - the complete SNAP-8 power plant including all Nuclear System and Power Conversion System components.

Power Conversion System (PCS) - all components of the SNAP-8 system being developed by Aerojet-General Corporation.

Nuclear System (NS) - all parts of the SNAP-8 system being developed by Atomics International.

Non-Nuclear System (NNS) - a series of Power Conversion Systems, incorporating a non-nuclear heat source, used for development testing at Aerojet-General Corporation.

II. OBJECTIVES

The ultimate objective of the SNAP-8 program is to design and develop a 30-kw Electrical Generating System for use in various space missions. The power source for this system will be a nuclear reactor furnished by the AEC. The SNAP-8 system will use a eutectic mixture of sodium and potassium (NaK) as the reactor coolant; the system will operate on a Rankine cycle with mercury as the working fluid for the turbogenerator. The SNAP-8 system will be lightweight and highly reliable. It will be launched from a ground base and will operate unattended at full power for a minimum of 10,000 hours. After the system is placed in orbit, both activation and shutdown may be accomplished by ground command.

III. SUMMARY OF ACCOMPLISHMENTS PRIOR TO 1 SEPTEMBER 1961

Phase II of the SNAP-8 program began in May 1961. During this phase, which will continue through May 1962, component development testing, will continue. Emphasis during Phase II will be on the design and development of both subsystems and Non-Nuclear Systems, and on the initiation of system testing.

Final design of the nuclear-test facilities will be completed, and test-program planning for both the Ground Prototype Test Facility (GPTF) and the Flight Prototype Test Facility (FPTF) will be initiated. Designs will be completed for support test equipment used in tests of the Power Conversion Systems in these nuclear-test facilities.

Integration of the Power Conversion System into the complete SNAP-8 Electrical Generating System will begin in this phase.

Program highlights during the first 3 months of Phase II are summarized in paragraphs A through T below.

A. BOILER

Assembly of the heat-transfer test loop was completed and testing was initiated. Design of a full-scale model of the boiler, and assembly of the water-flow test loop for the boiler model were completed. Design of the experimental boiler for Non-Nuclear System No. 1 (NNS-1) was completed, and fabrication of this boiler and the experimental boiler for the Rated-Power Loop began.

B. RADIATOR

Results of a single tube mercury-condensing experiment indicated that the mercury liquid-to-vapor interface is stable. Studies of mercury drop tests showed that the mercury liquid-to-droplet interface is stable to impacting drops in a zero-g environment. Uniform armor thickness on all prime surfaces for micrometeorite protection yields minimum radiator weight, and two methods of armoring the radiator flexible joints were formulated. A computer program for weight optimization began. Preliminary layout drawings showing the general radiator configuration for both folded and erect positions were completed. Design of the experimental radiator for NNS-1 was completed and fabrication initiated.

C. POWER-DRIVE ASSEMBLY

Detail drawings for the power-drive assembly were completed. A new critical-speed analysis was performed using the larger generator rotor. A dynamic stress analysis of the generator rotor was made based on an estimated temperature distribution and cooling requirements for the PDA.

D. TURBINE

Development testing continued with the turbine mounted on the inertia test fixture. Inertia tests were initiated using ambient-temperature nitrogen. A program was initiated for steady-state, extended-duration performance testing using either cold nitrogen vapor, or mercury vapor. Nozzle reaction tests were completed using ambient-temperature nitrogen.

E. MERCURY PUMP

Performance testing of the mercury pump continued, using 150°F mercury; minimum net positive suction head (NPSH) data were obtained. Performance testing using mercury at 500°F was initiated.

F. NaK PUMP

Preliminary data from completed performance tests ranging from ambient temperature to 350°F indicated a head rise of 60 ft at the design flow rate of 68 gpm. Tests were performed with NaK at 500°F to obtain NPSH data. Pump test results are satisfactory for the present PCS.

G. BEARINGS AND SEALS

Preliminary performance testing of the mercury-lubricated bearings began. The test fixture was operated in both the horizontal and vertical attitudes.

H. NaK EXPANSION RESERVOIR

Drawings of the experimental reservoir assembly were completed and an initial test program was formulated.

I. SPEED CONTROLLER AND VOLTAGE REGULATOR

Load resistors were installed for use in the development of the saturable reactors, and preliminary single-phase testing of these reactors

continued using 1000-cps power. Electrical controls for the Rated-Power Test Loop were designed and fabricated, and design of the electrical controls for NNS-1 was initiated.

J. ALTERNATOR

Installation of the alternator and motor test stands was completed. The second experimental alternator was assembled and tested, and fabrication of components for two alternators for the PDA was started. Fabrication of the copper-disk-cooled field coils was initiated. Design of a Mod II alternator began.

K. NaK-PUMP MOTOR

Fabrication of the first NaK-pump motor was completed and testing was initiated.

L. ELECTROMAGNETIC START PUMP

Design was initiated of an electromagnetic start pump that will circulate NaK through the reactor and boiler during the start phase.

M. MATERIALS EVALUATION

The survey continued for materials with acceptable magnetic and strength properties for the rotor of the prototype alternator. Cavity-seal metallic diaphragms were fabricated for the stators of the NaK-pump motor and the alternator. Compatibility capsules of Haynes 25 alloy and Type 405 stainless steel were evaluated after 2000 hr in the test furnace at 1100°F. A new lot of compatibility capsules was fabricated, and tests at 1025, 1100, and 1175°F were initiated.

N. SYSTEMS ENGINEERING AND RELIABILITY

Revised reactor equations were programed for the analog computer. Computer runs included a step change in the NaK inlet temperature with the power held constant, a step change in power with the inlet temperature held constant, and a secondary-loop start-up. Development of a digital computer program for system optimization and off-design analysis was initiated.

A reliability program was established; personnel training was initiated and a failure-reporting system was put into effect.

O. COMPONENT DEVELOPMENT TESTS (NON-NUCLEAR)

A high-temperature mercury pump was constructed to obtain performance data for the pump configuration for the first PDA. The initial series of the NaK-pump development tests was completed. The mercury bearing-and-seal test loop was operated in the horizontal and vertical attitudes to evaluate journal-bearing performance. Inertia testing began using the cold-gas turbine system to obtain performance data for design and off-design operating conditions. Tests of a mercury-recirculating pump were performed. This pump will be used as an auxiliary pump for the RPL and the NNS-1.

P. LOW-POWER MERCURY-VAPOR TEST LOOP (LPL)

Operation of the LPL was initiated to determine mercury boiling and condensing characteristics.

Q. RATED-POWER TEST LOOP (RPL)

Installation of RPL components was initiated.

R. NON-NUCLEAR SYSTEM NO. 1

Design and planning for NNS-1 continued, and a preliminary test plan was completed.

S. GROUND PROTOTYPE TEST FACILITY (GPTF)

Final review of Title I design-phase drawings for the GPTF was completed by AI and AGC. Title II design-phase drawings were also completed. Test planning continued and building-site excavation began.

T. FLIGHT PROTOTYPE TEST FACILITY (FPTF)

Design criteria and technical requirements for the FPTF were analyzed, and documents were prepared for review by AI and the AEC. Studies of test equipment requirements for the facilities continued and preparation of a test facility began.

IV. THERMOMECHANICAL COMPONENTS

A. BOILER

1. Summary of Accomplishments - 1 September through 30 November 1961

The 1-in.-OD Haynes 25 tube, used in the heat-transfer test, was repaired and operated. A tube rupture terminated the test after 5 hr.

The test section was replaced with a 0.875-in.-OD by 0.049-in.-wall No. 316 stainless steel tube, and a 14-hr test was performed with no failures.

The full-scale mockup of the boiler was completed, and flow testing with water was performed.

2. Objectives

The ultimate objective of the boiler development program is to design, fabricate, and test a flight-prototype NaK-mercury boiler suitable for the SNAP-8 PCS. Prototype boiler weight will not exceed 200 lb. The mercury flow rate will be 7200 lb/hr, while the NaK flow rate will be 24,000 lb/hr. The mercury exit temperature will be 1250°F at a nominal pressure of 275 psia; the pressure drop is not to exceed 35 psia.

A more current objective is to prepare a preliminary prototype boiler design based on heat-transfer and water-flow tests, and on information derived from tests on experimental boilers fabricated for other systems and subsystems.

3. Discussion

During early September, the 1-in.-OD Haynes 25 test section was repaired and a second test was made on 19 September. After 5 hours of operation, a mercury leak developed in the boiling region. At that time, the following conditions prevailed in the test section:

Flow rate	-	1200 lb/hr
Boiling temperature	-	1100°F
Pressure	-	290 psia
Exit quality	-	42%
Pressure drop	-	10 psi
Boiling h*	-	varied between 35 and 185 Btu/hr ft^2 °F.

*h = Boiling heat-transfer coefficient.

The Stratham pressure transducer at the exit station indicated pressure pulsations of ±5 psi with a frequency of 1 cps. There was no flow-stabilization orifice at the test-section entrance.

The test section was replaced with a stainless steel tube. The pressure-drop and heat-transfer data from the 5/8-in.-OD tube and the 1-in.-OD tube indicated that a 7/8-in.-OD tube should be quite close to the optimum size for a four-tube boiler with a pressure drop of 35 psi.

After shipping delays and some welding difficulties, the 7/8-in. OD by 0.049-in. wall 316 stainless steel test section was assembled and checked out. A successful 14-hr test was made on 14 November. During the test, the first 5 hr were required to bring the test section from ambient temperature* to 1100°F; the next 4 hr were used to achieve wetting of the test section, and an additional 5 hr was used for investigation of the critical heat flux at various qualities up to 50%. During the test, the flow rate was held constant at 1865 lb/hr and the discharge pressure was controlled at 275 psia.

Figure 1 is a plot of the uncorrected wall temperature, the fluid temperature, the power applied to the mercury, and the calculated vapor quality.

The boiling h for a quality in excess of 10% is between 600-700 Btu/hr ft^2 °F, a result that agrees with the data from the 5/8-in.-OD tube test. However, an h of 30-40 Btu/hr ft^2 °F occurred below 10% quality, a result that was not experienced in the 5/8-in. tube. A comparison of these test results with the data reported by Kutateladze show that the low heat-transfer coefficients occur when the velocity is below 1 ft/sec.** Once the quality approaches 10%, the resultant increase in specific volume produces stream velocities greater than 5 ft/sec, and high heat-transfer rates can be observed. Analysis indicates that a boiler tube diameter should be of small initial size, and should become larger in the high-quality region to satisfy pressure-drop restrictions.

---

* Approximately 60°F.

** S. S. Kutateladze, et al, "Liquid Metal Heat Transfer Media," Soviet Journal of Atomic Energy, Supplement No. 2, translation published by Chapman and Hall, Ltd., London, 1959.

During September, the full-scale boiler mockup was fabricated and assembly was completed in October.

A series of water-flow tests through the shell-side were performed over a range of Reynolds' numbers, from 10^4 to 4×10^4; the average shell-side Reynolds' number that is predicted for NaK in the prototype boiler is 17,000. Visual observations of the flow distribution were made using dye and small nitrogen bubbles. Velocity traverses were made in the entrance plenum with a two-dimensional Pitot tube, but the readings were unreliable due to the low water velocities (less than 1 ft/sec) in the plenum. Photographs of the test loop and the boiler mockup are shown in Figures 2 and 3.

Reduced pressure-drop data indicate that the prototype boiler should have a pressure drop of 0.25 psi on the NaK side.

Visual observations of the flow patterns revealed that considerable mixing and radial flow occurs in the tube coils. Maldistribution of the NaK flow does not appear to be a problem that will require baffles or spacers to correct.

A reference design for the prototype boiler was initiated during the latter part of November.

The workhorse boiler for the Rated-Power Test Loop was completed on 24 September and installed in the RPL early in October. Fabrication delays occurred when a leak in the mercury-tube coil necessitated the removal of the outer shell of the boiler. Repair welds were satisfactorily made. Fabrication of the experimental boiler for the NNS-1 was completed on 30 November 1961, and will arrive at Aerojet by 1 December. This boiler will be installed in the NNS-1 during December.

Haynes 25 alloy required for fabrication of four additional boilers has been ordered. To ensure maintenance of development schedules, and to make certain that enough material of the necessary quality will be available, Haynes 25 tubing was ordered from three suppliers; Michigan Seamless, Superior Tube, and Trent Tube.

4. Work Planned for the Next Quarter

Testing of the 7/8-in.-OD test section will continue until sufficient data are obtained. Based on the results to date, the 5/8-in.-OD tube will be used in the first 36 ft of the test section.

The final test of the shell-side experiment will be completed and the recommended friction factors will be published.

A design specification and layout will be prepared for the prototype boiler.

B. RADIATOR

1. Summary of Accomplishments - 1 September through 30 November 1961

Early in the quarter a decision was made to change the radiator design for the 30-kw system from a single-wing to a two-wing concept. A vibration analysis was completed for the single-wing design.

Late in the quarter the digital-computer code was completed that will be used to analyze the performance of the two-wing radiator design.

The detail drawings for the six-tube condensing experiment were released and fabrication of the test section was 80% completed.

Samples of several types of aluminum-to-Haynes 25 bonding techniques were received and tested. Based on the test results, two Haynes 25 tapered tubes were successfully armored with 0.350-in. aluminum.

A bend-test fixture was designed and fabricated. At the end of the quarter samples of 1-in.-ID and 3-in.-ID Haynes 25 bellows were bend-tested, with favorable results. Also, a flexible-joint design supplied by NASA Lewis Laboratory was tested.

Flexible ball-and-socket armor for a 3-in. bellows was fabricated and assembled along with an extension linkage.

Weld-test samples of the condensing tube-to-header joints were made; two of the designs were found acceptable for fabrication.

2. Objectives

The ultimate objective of the radiator development program is to design and develop a flight-prototype radiator for the SNAP-8 PCS. Specific objectives include the performance of small-scale tests, development of optimum degrees of weight reduction, studies of meteorite protection, and the preliminary design of a zero-g flight-test experiment. Extensive fluid-flow and hydrodynamic analyses, coupled with a series of mercury-condensing experiments, are required to meet these objectives.

A current task of the experimental program is construction of a suitable pressure-drop model that will relate data obtained in 1-g environment to a zero-g environment. A stability analysis of the mercury liquid-vapor interface is also required. Another program task is the performance of mercury-condensing tests, in both straight and narrow tubes, to arrive at a suitable pressure-drop correlation. Information concerning stabilization characteristics of subcooler flow restrictions is also required.

3. Discussion

a. Analytical Work

During the quarter, an intensive effort was expended in preparation of the digital computer code to evaluate the performance of the SNAP-8 radiator. At the end of November the code had been written and checked out. The evaluation program named SNOR has a running time of 7 minutes. Two subroutines from the program have been written in the form of small programs. They are TUBCAL, which computes the pressure drop in a single tube, and RADIAT, which calculates the heat rejected per linear inch of a condensing tube. These subroutines have running times of 20 sec and 5 sec respectively and are, therefore, quite useful for preliminary low-cost optimizations.

A description of the SNOR program and the subroutines is presented in Appendix A.

b. Condensing Tests

During the quarter, tests were performed on the 6-ft-long 0.402-in.-ID straight tube at flow rates of 85 to 100 lb/hr. The principal

purpose of the tests was to obtain a pressure-drop correlation. The test data reported during August were in error because two pressure taps were incorrectly installed. During September, the faulty test section was replaced with an identical tube and static pressure taps of improved design. An error analysis of the manometer system indicated that the experimental technique had errors of the same magnitude as the pressure drops being measured.

In November, a manometer system was designed and installed that would measure differential pressures between adjacent pressure taps. Briefly, this system uses liquid mercury to sense the pressures in the condensing tube: the liquid mercury transmits the pressure through a nitrogen ballast to a water manometer, while the mercury-to-nitrogen interface is controlled by a probe which switches a solenoid valve that controls the ballast pressure. This system should provide sufficiently accurate pressure-drop determinations.

Also during November, a 7 1/2-ft-long tapered Haynes 25 tube with a major ID of 0.450 in. and a minor ID of 0.140 in. was fitted with an aluminum fin and four pressure taps. After considerable difficulty, the fin attachment was finally accomplished by a combination of mechanical fit and aluminum spray coat.

During the quarter the drawings of the six-parallel-tube condensing experiment were released and procurement was initiated. Fabrication was initiated in November and 80% completed. A photograph of the mercury boiler for the test rig is shown in Figure 4. The purpose of the experiment is to:

(1) Investigate flow distribution in a six-tube assembly

(2) Determine stability of mercury vapor-liquid interface location

(3) Determine the location of the vapor-liquid interface for various flow rates and pressure-drop conditions

(4) Determine pressure distribution in vapor manifold and liquid manifold

(5) Determine the effect of capillary diameter variation on interface, flow, and pressure drop.

During November, a system for detecting subcooler density variations, typical of oscillation of liquid-to-vapor interface using gamma absorption, was designed and checkout of this design was initiated.

c. Mechanical Design

A preliminary analysis was made in August to determine the approximate range of natural frequencies that would be typical of the single-wing 30-kw radiator in the extended position. The analysis assumed that the radiator was built into an infinitely stiff vehicle frame because no information has been made available on the Q value for the vehicle.

Normal mode frequencies were found to range from 0.045 cps to 1 cps if the flexible bellows were not locked, and from 6 to 8 cps if locks were provided. This analysis will be revised when more data become available on the folding-joint design.

During September a flexible-joint bend-test fixture, shown in Figure 5, was designed and built. The device is used to determine angular deflections vs bending moments for flexible metal hose and for the NASA-type joints.

Flexible metal hose of 1/2-, 1-, 2-, and 3-in. nominal ID was ordered from Aeroflex; 2- and 3-in.-ID hose was ordered from Flexible Metal Hose. The samples were to be fabricated from Haynes 25 stock of 0.020-in. thickness. Both vendors experienced fabrication difficulties. Late in November three 1-in. samples and one 3-in. sample were received by Aerojet. These are shown in Figures 6 and 7 respectively. Both sizes were X-rayed, dye-penetrant-checked, and helium-leak-tested. The 1-in. units were very sound, but the 3-in. unit contained many surface microcracks and one small leak in the seam weld.

Bend tests were performed on one 1-in. unit and the 3-in. unit. The angular deflection data is reported in Figures 8 and 9. The data indicate that the use of bellows does not require unreasonable bending moments to fold the vapor manifold around an 8-ft diameter circle that is typical of the SNAP-8 vehicle.

A folding joint of the unstable-section concept was supplied to Aerojet by Mr. L. Goertsma of Lewis Research Center. This unit was made of double-aged AM-350 with a yield strength of 170,000 psi, and had the same flow area as a 3-in. tube. Deformation and deflection tests were performed in the bend-test fixture, but were not completed due to the failure of an edge weld. A picture of the part in the test fixture is shown in Figure 5. A tabulation of the test data is presented in Table 1.

TABLE 1

Distance Between Support Centers	Buckling Load, Lb	Torque (Lb/In.) Required To Obtain Included Angle in Bend				
		160°	140°	120°	100°	90°
32-1/2	82.5	176	240	260	312	350
30-1/2	124.5	230	256	256	332	356
28-1/2	135.0	264	230	270	328	362
26-1/2	165.0	308	296	*	-	-

*Test model developed a crack in the edge seam weld.

Aerojet fabricated two identical units from 0.020-in. Haynes 25 sheet. The first unit was tested in the bend-test fixture and immediately assumed a permanent set. Figure 10 presents a comparison of the failed part with the new part. A stress analysis indicated that fiber stresses of some 130,000 psi exceeded the 63,000 psi yield strength of the Haynes 25 sheet. More 0.020-in. Haynes 25 sheet was ordered in the 20% cold-reduced and aged condition with a yield strength of 152,000 psi. Some No. 301 stainless steel sheet, which has a yield strength of 140,000 psi, was ordered, and fabrication of two joints was initiated.

The purpose of this testing program is to reduce the length of the flexible joint. The unit supplied by Lewis Laboratory was 3 ft long; it would be desirable to reduce this to less than 2 ft.

During the quarter, a flexible-armor design, based on the ball-and-socket concept, was designed. Fabrication and assembly of a unit to fit a 3-in.-dia flexible metal bellows was completed during November. A photograph of the device complete with a three-bar extension linkage is shown in Figure 11. The linkage provides a maximum moment of 200 lb-in.

In September, eight 7 1/2-ft-long Haynes 25 tapered tubes, with a 0.500-in. major OD and a 0.200-in. minor OD, were received from Superior Tube. These were made from welded and redrawn tubing, and had a final wall thickness which varied from 0.021 to 0.025 in.

During the first part of the quarter, samples of aluminum armor joined to 5/8-in.-OD Haynes 25 tubes were received from various vendors and evaluated by ultrasonic inspection, X-ray, metallographic examination, and thermal cycling. The vendors and the types of processes that were represented were:

Straza Industries	-	Aluminum spray coated
Stewart-Warner	-	Aluminum braze
Tickle Engineering	-	AL-FIN casting process

The specimens furnished by Tickle Engineering were superior to the other samples. A shear test of these "as-received" samples by Tickle produced a shear strength of 9000 psi and the shear occurred in the aluminum. A second sample was thermal cycled from 700°F to -50°F three times with a total elapsed time at 700°F of nearly 30 hours. A shear test was performed on the specimen and a similar failure occurred. Due to a slippage in the tensile machine, the load was not ascertained, but it was in excess of 7700 psi shear strength.

Based on the above results, two of the Haynes 25 tapered tubes were sent to Tickle for the application of aluminum armor. In November, the two tubes were completed; one tube was cast with five voids in the armor and the other had two voids. The two tubes are shown in Figure 12 and a close-up of one void is shown in Figure 13. X-ray inspection of the two tubes revealed only a minor porosity in the tube with five voids. The tubes were finished machined late in November and are shown in Figure 14. The five-void sample was cut up into

several pieces for further evaluation. Based on the results to date, the AL-FIN process seems to be the most satisfactory method for armoring the condensing tubes and manifolds.

During November, a program was begun to evaluate several tube-to-header welding techniques. The purpose of this activity is to select the most satisfactory type of joint from the standpoint of pressure loss and ease of fabrication. The design shown in Figure 15a was fabricated and the finished unit shown in Figure 15b. All welds were made with 0.020-0.025-in. Haynes 25 material by the TIG process with inert gas backup. Both joint types proved to be sound welds by X-ray and dye penetrant inspection.

The heat-transfer analysis of the NNS-2 radiator was completed. A kerosene coolant system was selected for the heat sink. Since no air cooling is available, kerosene was selected because it has good heat-transfer characteristics, and is compatible with NaK. Commercial availability of kerosene-to-air heat exchangers is being investigated.

d. Fabrication

Fabrication of the experimental NNS-1 radiator (condenser) was completed 29 November. The fin design for this radiator was changed. Formerly, the copper fins were brazed to the Haynes 25 tubing; the fins are presently bolted to the tubing because the brazing operation caused circumferential cracks in the tubing that passed under the copper fins. The Haynes 25 tube-to-manifold plate weld joint is shown in Figure 16. Fabrication of a spare NNS-1 radiator was initiated and orders were placed for the necessary Haynes 25 tubing.

Haynes 25 tapered tubing is being procured for future radiator fabrication. This tubing will have a constant taper from 0.500- to 0.200-in.-OD within a 7-ft length, and will have a wall thickness of 0.020 to 0.025 in.

4. Work Planned for the Next Quarter

The radiator performance evaluation code will be used to arrive at the prototype radiator layout. Specification for various components of the assembly will be drafted.

The single-tube condensing experiment will be terminated after testing of the Haynes 25 tapered tube is completed. Following the shutdown of the single-tube experiment, the six-tube parallel experiment will be checked out with straight tubes while awaiting delivery of the tapered tubes. The tapered tubes will be tested in the middle of the next quarter.

Flow tests for entrance loss determinations will be performed on various weld joints in the vapor manifold.

The flow tests and bend tests will be completed on the Haynes 25 bellows, and on the NASA deflection joint. Also, the extension linkage and flexible armor assembly will be tested.

If the favorable bend tests of the bellows continue, then a complete vapor manifold can be assembled and bend tested.

The data from the mechanical testing will be factored into a stress analysis of the radiator.

Initial layout drawings of a radiator cold-wall assembly will be started during the next report period. Present plans call for a NNS-2 radiator design as close as possible to the current prototype concept, including tapered Haynes 25 tubing with aluminum fins and armor.

C. POWER-DRIVE ASSEMBLY

1. Summary of Accomplishments - 1 September through 30 November 1961

The dynamic-stress analysis of the Mod I alternator rotor for the PDA is nearly complete.

Mod I PDA hardware is being converted to PDA-X machines.

Preliminary design of a temporary, "lift-off" mercury seal was initiated.

2. Discussion

A new dynamic-stress analysis of the Mod I alternator rotor for the PDA neared completion. Preliminary results indicate that Type 347 stainless

steel is superior to Type 316 for the pole-separator material. Vapor cooling for the rotor was established as necessary for extended PDA operation at rated conditions.

Water-flow tests of the PDA end-bell housing showed a pressure drop of 40 to 50 psi. Enlargement of the inlet and outlet passages of the pump-end housing resulted in a total drop of 19 psi. The turbine-end housing was similarly reworked.

Preliminary design of a temporary, or "lift-off" seal was initiated. The seal will be used to prevent mercury flow into the alternator and turbine cavities during the start-up cycle.

Fabrication of the first experimental Power-Drive Assembly was delayed due to difficulty encountered in procurement of a suitable stator seal for the alternator. PDA hardware is being converted into the newer version: the PDA-X. The PDA-X will be used to test the turbine, bearings, seals, and mercury pump in the Rated-Power Loop (RPL). A liquid-cooled eddy-current brake, incorporated in the alternator and stator housings, will be used to provide system load.

Fabrication orders were placed in November for the long-lead-time items required for the future PDA-Y. The PDA-Y will incorporate an improved liquid-cooled eddy-current brake, and will provide additional hardware necessary for testing in the RPL.

3. Work Planned for the Next Quarter

Assembly of the first PDA-X will be completed, and the unit will be installed for testing in the Rated-Power Loop in December.

The new dynamic-stress analysis will be completed and the results published.

D. TURBINE

1. Summary of Accomplishments - 1 September through 30 November 1961

Inertia tests of the two-stage turbine progressed satisfactorily. Accumulated data can now be applied toward the design of modifications to improve overall turbine performance.

Fabrication of turbine wheels and nozzles was completed for the PDA-X and initiated for the PDA-Y.

2. Discussion

Performance testing of the modified turbine (which has a first-stage wheel with a greater OD), using the inertia test method, was completed. Both cold nitrogen vapor and ambient-temperature nitrogen gas were used as working fluids. The results of the first three cold-nitrogen-vapor inertia tests with the original design configuration indicated an average peak efficiency of approximately 66%. The inlet conditions averaged 10°F above and 15 psi below the estimated design point for nitrogen vapor; as a result, the moisture conditions in the second stage were estimated about 5% drier than the design case had anticipated (Figure 17).

To assess the effects of the increased blade height in the first-stage wheel, attempt was made to reproduce the inlet conditions achieved during the tests with the original configuration, as well as to achieve the estimated design-point inlet conditions (Figure 18).

The mean efficiencies of Run No. 53 and No. 50 compare closely with Run No. 35. In this manner the inlet conditions are within 5 psi and 1°F of each other. Figure 19 indicates an improvement in peak efficiency of about 1%. However, it is a matter of conjecture whether or not this actually occurs since the increase in efficiency is within the probable order of magnitude of the accuracy of the inertia test.

Although the estimated nitrogen-vapor design-point inlet conditions were not achieved, a definite trend is indicated. As the estimated design inlet conditions are approached, the turbine efficiency increases (Figure 20). The shaft-horsepower output indicates no perceptible effect of increased moisture in the second stage as the design point is approached, while the available energy to the turbine is effectively reduced. Note that the turbine was operated at pressure ratios lower than the design condition. The nitrogen vapor design point inlet conditions should therefore give rise to a turbine efficiency of about 66%.

Examination of the static pressure variation, with respect to time recorded behind the first- and second-stage nozzles during the acceleration portion of each test, indicate that the pressures (at these two stations only) shown in Figures 21 and 22 are not steady-state values. The general trend of this transient pressure distribution suggests that the final steady-state pressure behind the first-stage nozzle should be higher than the values plotted in Figures 21 and 22, while the pressures shown behind the second-stage nozzle should be only slightly higher. Results then indicate that the axial distribution curve, situated between the turbine inlet and the second-stage blade mid-chord positions, actually lies above the estimated design distribution. This curve, and the indicated pressure drop through the second-stage wheel, suggests insufficient flow area in the second-stage nozzle, and indicates that the first-stage nozzle may be operating unchoked. This was not entirely unexpected since previously-conducted flow tests of both nozzle rows indicated that both nozzles have effective flow areas less than design values. The second-stage nozzle effective flow area was also further from its design value (18% less) than was the first stage (6% less), indicating an area mismatch in addition to the smaller flow areas. The effect of the smaller effective flow area in the second-stage nozzle could also be aggravated by drier vapor conditions in the second stage than the nitrogen-vapor design condition requires.

Inertia tests of the original turbine configuration with ambient nitrogen gas, Figures 23 and 24, indicate a peak efficiency of about 68% at a pressure ratio of approximately 14.0:1 and a speed of 27,800 rpm.

Since test data of the performance of the turbine when the blade height was less than the annulus height was already available from earlier inertia tests, it was more advantageous to test next the opposite extreme case, in which the blade height is increased by an amount definitely in excess of the optimum. With the two extreme positions indicated, the blade height and recess depth could then be progressively decreased to establish an optimum configuration.

The recess in the shroud over the first-stage wheel of increased blade height was expected to reduce the tip clearance losses by reducing the through-flow over the blade tip in the clearance space. The unloading of the

blade tips (flow over the blade tip from pressure to suction surface) is controlled mainly by the clearance space over the blade tip, and this clearance was not changed from the original configuration. In addition, the longer blade should provide a larger blade area for doing work, the blade row covering at least the complete annulus height compared to a 93% coverage afforded by the original design configuration.

Increasing the blade height by an optimum amount in the first-stage wheel was expected to produce an increase in the two-stage turbine overall efficiency of about 0.5 to 1.0%, an increase which, considering the accuracy of the testing technique and instrumentation, would not be clearly indicated by the inertia tests. The performance of the turbine with the larger first-stage blade row is shown in Figure 25.

A comparison of peak efficiencies achieved by the two configurations during tests with similar inlet conditions (Runs No. 39 and No. 57, Figure 24), indicates that a degradation of 8% in peak efficiency occurs when the original first-stage wheel is replaced by one containing 25% longer blades.

The first-stage wheel blade height was increased by 0.025 in., an increase of 25% over the original blade height. With a 0.0075-in. nominal blade tip clearance, the recess over the annulus area has been increased by almost 23%. The excessive area available in the blade row will significantly reduce the mean relative blade inlet and exit velocities (particularly in the tip region), the momentum change through the blade, and hence work output from the stage. There is evidence of the decreased work output in the smaller temperature drop (some 16° less) recorded at peak efficiency for Run No. 57. Part of the lower temperature drop is due to more frictional reheat as a consequence of the larger blade surface area, in addition to the reheat involved due to mixing of the main stream flow in the tip region with the greater amount of eddy and vortex elements created by the higher secondary losses.

The axial pressure distributions measured in the ambient N_2 tests (Figure 26) are similar to those obtained during tests with cold nitrogen vapor. Transient effects are still evident in both recorded nozzle-exit pressures.

In summary, it would appear from the ambient-temperature nitrogen inertia tests that the 25% increase in blade height on the first-stage blade row has been excessive. The tests carried out with cold nitrogen vapor do not indicate any inferior performance with the longer first-stage blades compared with the original design configuration. It is not yet clear why there should be a degradation in performance using ambient-temperature nitrogen and not with cold nitrogen vapor. As a next step, blade heights 12.5% and 7.5% greater than that indicated in the original design will be tested.

The axial pressure-distribution data indicate that the diffuser contributes nothing to the turbine performance. The higher-than-expected total pressure losses result from subjection of the flow leaving the second-stage blade row to a comparatively high degree of turning over a comparatively short flow path. This is particularly the case at the outer wall of the annulus immediately behind the blade row. If exit swirl from the second-stage blade row were designed into the turbine, it might reduce these turning losses; alternately, an additional inch or so in axial length may enable some gain to be realized from the diffuser.

Following completion of the inertia tests, the turbine with the larger OD first-stage wheel was installed on the water-absorption dynamometer test rig, and preliminary check-out test runs were initiated.

Fabrication of the turbine wheels and nozzles for the PDA-X was completed, and initiated for the PDA-Y. Fabrication of the turbine inlet and exhaust housings was completed for the first PDA-X. Materials for the PDA-Y were ordered.

On 13 October, an experimental turbine was loaned to Lewis Laboratory for performance testing.

3. Work Planned for the Next Quarter

Nozzle throat areas will be enlarged to the design values. This modification will be tested with a first stage containing a wheel having a blade of the original design dimensions.

Small-gain items, such as blade-tip clearance effects and improved diffuser performance, will, for the time being, be placed on a low priority. The performance of both nozzle rows will receive first priority in the immediate future.

Testing of the turbine-dynamometer unit will begin early in December.

E. MERCURY PUMP

1. Summary of Accomplishments - 1 September through 30 November 1961

Development testing with high-temperature mercury was completed.

Fabrication of the experimental mercury pumps for the PDA-X was completed.

2. Discussion

One high-temperature mercury pumping test, conducted early in the report period, completed the current series of mercury-pump development tests. Data from pump development testing at 20,000 rpm with 465°F mercury showed a head rise of 56 ft at design flow rate, and 83 ft at shutoff. Data concerning NPSH indicated a minimum value less than 1.5 ft.

Development testing of the mercury pump was temporarily suspended; the test loop was modified to permit testing of mercury dynamic seals.

Fabrication of additional hardware for check-out testing of the experimental PDA-X pumps was initiated. This hardware will be used in conjunction with the present mercury-pump test rig when the present rig becomes available, after completion of the mercury dynamic-seal testing.

Fabrication of the experimental mercury pumps for the PDA-X was completed.

Material required for manufacture of the PDA-Y mercury pumps was pre-released in November.

3. Work Planned for the Next Quarter

Fabrication of the check-out test fixture for the experimental PDA-X pumps will occur during the quarter.

F. NaK PUMP

No NaK-pump tests were scheduled or conducted during the report period.

Fabrication of the all-cast extended-vane impeller was completed; the impeller is available for future development tests of the pump. Fabrication of the NaK-pump journal bearings was completed.

G. BEARINGS AND SEALS

1. Summary of Accomplishments - 1 September through 30 November 1961

Testing of the mercury bearings progressed satisfactorily during the last reporting period. Several successful tests have produced a valuable amount of significant data.

Data from initial tests of the original mercury dynamic seal design led to a series of modifications in the design to improve operating performance.

Further study and the preliminary design of a temporary, or "lift-off" mechanical contact seal were continued.

2. Discussion

a. Bearings

Ambient temperature tests of the original circumferential-groove journal bearings, with the test rig positioned vertically, were completed early in September. Two separate tests were performed successfully, at speeds as high as 20,300 rpm, for a total duration of 90 min. A final test, lasting 160 min, included inlet pressures up to 80 psig and extensive operation at 20,000 rpm. Radial loads of only a few pounds were applied briefly during operation due to difficulties with the load-magnetic circuit.

As speed was increased during the tests, half-frequency whirl was detected initially at 17,000 rpm and continued during higher speeds to 20,000 rpm. Decreasing speed showed a transition to stable operation at about 16,000 rpm.

After a total accumulated running time of 5 hours in the vertical position, the test unit was disassembled for inspection. Wiping score marks were evident on the turbine-end journal bearing (upper), while only minor circumferential scratches were apparent on the pump-end journal bearing (lower). This evidence was consistent with the observation that the amplitude of half-frequency vibration was substantially higher in the upper journal. Both thrust bearings and the thrust runner showed negligible evidence of contact running. Inspection of the 10-micron filter in the main line which feeds the bearings showed no evidence of foreign material in the system.

Preliminary reduction of speed-decay data, taken at the conclusion of vertical testing, indicated total windage and friction losses of 4 to 5 hp at 20,000 rpm. The following individual losses contributing to this total have been evaluated: friction of journal and thrust bearings; pumping losses of dynamic seals; rotor and turbine windage; and fluid friction losses associated with shaft parts running in liquid mercury.

Lubricant temperature rise and lubricant flow data for the journal bearings during operation at 20,000 rpm showed a loss of 0.67 hp for the 1.200-in.-dia bearing, and 0.43 hp for the 1.000-in.-dia bearing.

The bearing test fixture was disassembled and three new sets of journal bearings were line ground: a three-axial-groove, a four-axial-groove, and an axial-step bearing (based on a hydrostatic bearing type) incorporating a wide, shallow annulus. Also, a new one-piece rotor-shaft was made to improve the dynamic balance of the rotating assembly and reduce radial bearing loads during vertical testing.

Vertical testing was resumed in mid-October with the three-axial groove bearing. Several tests were successfully performed at speeds to 17,000 rpm. After modification of the turbine drive, a rapid shutdown occurred at 19,000 rpm following normal acceleration from 15,000 rpm. Oscillograph traces showed no evidence of half-frequency whirl up to the maximum speed attained.

Disassembly of the fixture revealed that the turbine-end journal had seized both on the shaft and in its bearing, and that the tungsten-carbide thrust washer was broken in several pieces. In addition, the turbine-carbide

journal retaining nut was loose on the shaft. The failure was apparently due to loosening of the retaining nut which permitted the journal sleeve to rotate on the shaft, causing excessive friction and subsequent expansion which resulted in galling and seizure. Fracture of the thrust washer was attributed to the sudden axial load resulting from the journal seizure.

The fixture was reassembled and an additional locking device for the journal retaining nut was incorporated. Tests continued in the vertical position with a bearing having four equally-spaced axial grooves fed by a central circumferential groove. The axial grooves extend from the central feed groove to within approximately 1/16 in. of the bearing ends.

Three tests were conducted for an accumulated running time of 9.2 hr, including about 4.5 hr at 20,000 rpm. During these tests no half-frequency whirl or excessive vibration were observed at any speed. The last test was terminated abruptly, after about 4 hr continuous running at 20,000 rpm, due to a power loss to the loop-pump motor. The resultant loss of lubricant to the bearings precipitated a bearing failure.

Disassembly of the fixture revealed that the turbine-end journal had seized to the bearing insert. The pump-end journal and bearing were free and only lightly scored, the outboard thrust bearing surfaces were slightly marked, and the inboard thrust bearing surfaces were unmarked.

Figure 27 shows a typical oscillograph trace of the accelerometer output at each bearing during 20,000-rpm tests of the four-axial-groove design. For comparison, a similar trace for the plain, circumferential-groove bearings is shown in Figure 28. In the previously-run plain-bearing tests, the ratio of whirl frequency to shaft rotational frequency ranged from 0.43 to 0.48.

Bearing Test Fixture No. 2 is being modified to correspond to Fixture No. 1. Line-grinding operations with three new sets of bearings are scheduled for completion in December. These bearings are the three-axial-groove design tested previously, a new three-axial-groove design with individually fed grooves, and a new axial-step bearing of higher L/D ratio.

Two variable-reluctance sensing units were purchased to obtain biaxial dynamic measurements of shaft displacement. Half-frequency whirl detection will be made with these devices as soon as the test fixture can be altered to permit their installation.

b. Dynamic Seals

The experimental mercury-pump test fixture was modified for dynamic seal development testing. The fixture was used during this period to test various modifications of the dynamic seal. During one of the tests, mercury contaminated the drive motor; the motor was removed and cleaned after this test. Reassembly of the fixture was completed in November.

Initial tests of the original seal configuration (both sides vaned) indicated an excessively high head-rise characteristic. The vanes were removed from the lubricant scavenging (liquid) side of the seal leaving a plain disk, while the vanes were retained on the opposite (vapor) side.

Testing was resumed with axial clearances set at 0.030 in. on each side of the seal. The pressure rise across the seal, about 500 psi, was still higher than necessary. Also, some leakage was noted past the vaned side of the seal.

Next, the test rig was modified to provide 0.010-in. vane-side axial clearance and 0.060-in. plain-side axial clearance. Testing will be resumed early in December.

Preliminary design of a temporary, or "lift-off" mechanical contact seal continued. The basic design concept is the integration of a simple sealing device into or adjacent to each dynamic seal. This should prevent, or at least minimize, liquid mercury flow into the turbine and rotor cavities during the initial phase of the start-up cycle. As full operating speed is approached, the contact seals are automatically disengaged and the dynamic seals assume the sealing function. Initial design efforts are based on the deactivation of the contact seal by centrifugal force or by liquid mercury pressure.

Other seal types which were considered, but which were judged either too complex or impractical for repeatable operation, included: bimetal thermally-operated seals, "soluble-face" seals, friction-sensitive seals, mercury-wetted-face seals, and torque-actuated seals.

3. Work Planned for the Next Quarter

Bearing configurations planned for future testing include another test of the four-axial-groove (circumferential feed) design, a four-axial-groove bearing with individually fed grooves, and a stepped-film bearing, plus various modifications of these designs as results of development tests indicate promising configurations. A tilting-pad bearing is also being considered for testing.

Testing of bearings and seals in the mercury bearing-and-seal test fixture will resume early in December.

Fabrication of spare housings and rotors for development testing, initiated in November, will be completed in December.

H. NaK EXPANSION RESERVOIR

1. Summary of Accomplishments - 1 September through 30 November 1961

All detail drawings for the experimental NaK expansion reservoir were completed.

2. Discussion

Minor redesign of several components of the experimental version of the NaK expansion reservoir was required because of an error in the information furnished by the bellows manufacturer. Functional and thermal design analyses were recalculated and appropriate dimensional changes were made in the drawings affected.

All detail drawings for the experimental unit were completed and rechecked. Major items are scheduled for release in December. The final assembly drawing is in process, and is nearing completion. Also, detailed specifications are being prepared to define test procedures and evaluation criteria.

3. Work Planned for the Next Quarter

Design will be completed, and all drawings will be released for fabrication during December and January.

Fabrication will begin in February.

I. MERCURY RECIRCULATING PUMP

Fabrication of two additional 3600-rpm mercury recirculating pumps was initiated in November. These pumps will be completed in January.

After a design modification to seal the cover-gas cavity through the impeller shaft mounting, the first two pumps were installed in the RPL and in the bearing-and-seal test loop.

V. ELECTRICAL COMPONENT DEVELOPMENT

A. CONTROLS

1. Summary of Accomplishments - 1 September through 30 November 1961

The design of all electrical control systems to be used in the NNS-1 testing has been completed. The individual control assemblies consist of a voltage regulator, a speed controller, an overspeed trip, and an alternator flashing unit. All of these assemblies are designed for ambient-temperature operation; all will be installed in the NNS-1 loop to provide PCS control evaluation. An electrical coordination diagram has been completed to illustrate the electrical interconnections of the NNS-1 control system.

2. Discussion

a. Speed Controller (NNS-1)

The speed controller is comprised of two assemblies: a magnetic amplifier assembly, which includes the speed-sensing circuit, and a saturable-reactor assembly consisting of six saturable reactors (Figure 29).

Continued testing of the reactors indicated an excessive rise in temperature in the reactors. To reduce this rise, the 6-mil laminations were replaced with 4-mil laminations. This reduced the temperature rise by 10%.

Using 4-mil laminations, the design of the NNS-1 saturable reactors was completed. Six reactors were fabricated to this design and assembled in a reactor assembly. Three-phase open-loop testing was completed. The magnetic amplifier transfer curve (gate output vs frequency) indicates that the reactors can be cycled from on to off within 10 cycles. Using a d-c supply for control, the "off" current was eleven amperes per phase and the "on" current was 300 amperes. At 300 amperes, the voltage drop across the reactor was approximately 15% of the line-to-neutral voltage.

The magnetic amplifier design for NNS-1 was completed and four units were fabricated. The magnetic amplifier was completed and open-loop tested. The current transfer curve is linear with shutoff occurring at about 1.5 amperes. Operation of the magnetic amplifier with the saturable reactor assembly will be concluded in December.

b. Voltage Regulator (NNS-1)

The voltage regulator (Figure 30) design and fabrication were completed. The magnetic amplifier for the voltage regulator is identical to the one used in the speed controller, except that the number of control windings differ. The first voltage regulator for ambient operation used zener diodes in series for the sensing circuit; operation was satisfactory while regulating the voltage of the laboratory alternators. Further testing revealed unstable areas of operation when new zener diodes were substituted in the circuit because of inconsistent diode characteristics. The problem of instability was eliminated by using a zener bridge for the voltage sensing network. Further open-loop testing of the present design has proven satisfactory, although no closed-loop testing has been done to date.

c. Overspeed Trip

An overspeed-trip assembly (Figure 31) was designed to control PDA units in the NNS-1 loop and the Rated-Power Loop. This assembly is a low-pass filter set to trip at 1020 cycles, the presently-designated overspeed limit. The low-pass filter constitutes a fail-safe assembly because excessive speed, upon loss of a-c signal, will produce a shut-down signal. Three of these assemblies have been fabricated and calibrated for loop testing.

d. Alternator Flashing Assembly (NNS-1)

An alternator flashing circuit (Figure 32) was designed for use with the voltage regulator. The flashing circuit provides a d-c signal for alternator startup, and blocking diodes that allow automatic transfer from the flashing circuit to the voltage regulator as the alternator approaches rated speed.

e. Rated-Power Loop Controls

Design, fabrication, and closed-loop testing of the Rated-Power Loop alternator load control was completed, although the alternator used for closed-loop testing was the laboratory alternator, which has a load of about 100 amp.

To permit the PDA assembly test to proceed, an eddy-current brake was designed to provide the load for the turbine. Use of the eddy-current-brake required the design of a control circuit for the brake. The control circuitry consists of a frequency-to-dc transducer which controls, through a magnetic amplifier driver, the firing angle of silicon-controlled rectifiers. The frequency or speed signal is produced by three turns of wire that have been imbedded in the stator iron of the eddy-current brake. By sensing the speed and controlling the field current, the required load can be applied to the turbine to maintain a constant speed. The design of this circuit has been completed and is illustrated in Figure 33.

Two breadboard control units for the Rated Power Loop were fabricated and tested. Initial operating characteristics show a 10 kw increase in load with a 10-cycle change in speed. The overspeed-trip breadboard, designed for the original RPL control, was converted to operate with the eddy-current control breadboard.

f. High-Temperature Controls (NNS-2)

An analysis of the efficiency, weight, and reliability of the magnetic amplifier control system has been completed for the NNS-2 system. The present design (NNS-1) uses a 3-phase full-wave bridge magnetic amplifier.

A 3-phase half-wave magnetic amplifier was studied to determine the advantages or disadvantages of each system. The 3-phase half-wave system using ceramic diodes has advantages in efficiency, weight, and reliability; therefore, it will be used as the first NNS-2 high-temperature system.

System design of the high-temperature controls was completed, and an electrical coordination drawing illustrating this system was made (Figure 34). The start-up sequence unit on this drawing is of a very preliminary nature and should be used only as a guide. While the NNS-1 controls contain semiconductors, the NNS-2 design replaces these semiconductors with ceramic diodes; therefore, all components in the NNS-2 system can be used up to 890°F. Design of specific items not used in the NNS-1 was initiated. To ascertain the NNS-2 operating characteristics, a low-temperature test program will precede the high-temperature evaluation. The low-temperature NNS-2 testing will be started in December.

g. High-Temperature Controls Program

The high temperature materials and components program has been delayed due to the lack of adequate oven facilities. Some preliminary testing has been done on core materials and ceramic diodes.

Ten-amp General Electric ceramic diodes were tested at 770°F for approximately 2 hours. The operating parameters were within the specifications published by General Electric. Ambient testing of the ceramic 2-amp and 150-ma diodes has proven satisfactory.

Two ovens from Pacific Scientific were received by the Electrical Engineering Laboratory. Installation of these ovens is 90% completed. When installation is completed, the following materials will be immediately investigated:

Ceramic diodes, 10-amp, 2-amp, and 150-ma
Ceramic glow tube voltage reference
Terminals (crimp type)
Stator wire
Magnet wire
Magnetic amplifier cores
Connectors
Insulating materials
Potting materials

h. Electromagnetic Start Pump

A preliminary design for a d-c electromagnetic start pump was completed. With the information acquired from the study program, an electromagnetic start pump procurement specification was prepared. This specification was forwarded to qualified vendors. Proposals for the start pump will be received in December.

i. Parasitic Load Resistor

A procurement specification, for two types of parasitic load resistors for installation in the NaK loop, was completed. The first type of load resistor will meet all flight requirements except wire terminations and weight; the second type will be designed to the flight requirements. The specification for the parasitic load resistor will be forwarded to qualified vendors in December.

3. Work Planned for the Next Quarter

Closed-loop testing of the NNS-1 voltage regulator and speed controller will begin.

Component design for the high-temperature control system will be completed.

Ambient-temperature testing of the high-temperature control system will be conducted.

High-temperature component and materials evaluation will continue.

Proposals for the electromagnetic start pump and the parasitic load resistor will be evaluated.

B. ALTERNATOR

1. Summary of Accomplishments - 1 September through 30 November 1961

Use of metal sealing diaphragms in the alternator proved unfeasible, and Eitel-McCullough was awarded a contract to develop a non-metallic diaphragm. Hughes Aircraft is investigating ceramic sealing techniques for the alternator stator.

Design of a back-up alternator for the Mod I alternator was initiated and fabrication of the first two Mod II alternators was completed.

Installation of additional test equipment continues.

2. Discussion

The first design of an alternator seal used Hastelloy-C for the sealing membrane. Ambient-temperature testing of this type of metal diaphragm produced a temperature rise in excess of 700°F with excessive eddy-current losses.

Another diaphragm, consisting basically of Type 316 stainless steel screens, 100 and 200 mesh, was investigated. A test on this type of screen diaphragm revealed that a temperature rise in excess of 700°F was produced. Test results proved conclusively that metal diaphragms in the alternator created excessive losses; therefore, stator sealing with metal diaphragms is not feasible.

Eitel-McCullough, Inc. (Eimac) was contacted regarding development of a non-metallic seal for the alternator. Initial discussions with Dr. Reed of Eimac resulted in a contract being awarded to them for the development of a non-metallic diaphragm. Using alumina disks supplied by AGC, Eimac is investigating the geometry, and the ceramic-to-metal seal problem. In the initial phases of this program, Eimac successfully brazed a diaphragm consisting of an 0.030-in.-thick alumina disk and Kovar inner and outer rings.

A general engineering requirement has been prepared permitting Hughes Aircraft to proceed in the investigation of ceramic sealing techniques to be used in the alternator stator. Hughes is investigating a ceramic bonding technique that may be employed for bonding the stator iron with closed slots.

Due to the reduced output of the Mod I alternator (approximately 20 kw), design of a Mod II alternator was initiated. Hardware fabricated for the Mod I alternator will be used for the fabrication of the first eddy-current brake assemblies. The first two Mod II assemblies will be used to investigate electrical characteristics. Some high-temperature materials are used in the first two units, but the wire and insulation system are designed for operation at ambient temperature. Fabrication of the first Mod II alternators was completed,

and testing was started. The electrical design of the ambient-temperature Mod II alternator will be retained in the high-temperature version of this alternator. Design of the high-temperature insulation system has been initiated.

Installation of additional test equipment is continuing. Four 100-hp, 1000-cycle, 20,000-rpm motors have been purchased. These motors are to be used for driving the SNAP-8 alternators, eddy-current brakes, and other rotating equipment requiring a drive source. A reactive load bank capable of 46.5 kvar has been designed and an order will be placed for its fabrication.

3. Work Planned for the Next Quarter

Electrical characteristics testing of the Mod II alternator will be completed.

The high-temperature insulation design for the alternator will be completed, and design and testing of the alternator diaphragm will continue.

C. NaK-PUMP MOTOR

1. Summary of Accomplishments - 1 September through 30 November 1961

Design of the Mod II NaK-pump motor was completed.

Design of an insulation system for the motor was initiated.

2. Discussion

The Mod I NaK motor was tested to obtain shaft-horsepower output. The test was performed at ambient conditions without NaK in the rotor cavity. The maximum shaft power was 1100 watts. Due to the low output and large physical size, the Mod I NaK motor program was discontinued and the design of Mod II was completed. The Mod II NaK motor will be physically smaller and require less input power. It will be a radial air-gap type rather than an axial air-gap type motor. Its approximate size is 6-in.-dia by 5 1/2-in. long. Fabrication of two motors for ambient-temperature electrical testing will be completed in December.

Design of an insulation system for the Mod II NaK motor was initiated. Investigation of the high-temperature insulation system is applicable to both the alternator high-temperature design and the NaK motor high-temperature

design; therefore, the first high-temperature tests will use components of the Mod II NaK motor that are compatible with elevated temperatures. Test results should be applicable to high-temperature alternator components.

To investigate the electrical and windage losses with NaK in the rotor cavity, a commercial motor of equivalent size was purchased. The motor housing was redesigned and the stator potted to permit operation with NaK. The motor was operated in the experimental NaK loop (LNL-1). Test results and calculated values were in close agreement. The motor was first operated in air, then with NaK. The no-load motor losses increased by a factor of 3.5:4 when NaK was present in the rotor cavity.

3. Work Planned for the Next Quarter

Electrical-characteristics testing of the Mod II NaK-pump motor will be concluded.

The high-temperature insulation system design for the NaK-pump motor will be completed.

VI. MATERIALS EVALUATION

A. MATERIALS DEVELOPMENT

1. Summary of Accomplishments - 1 September through 30 November 1961

During the past quarter the exposure temperature of the magnetic aging test was changed from 985°F to 910°F and, again, from 910°F to 970°F.

Fabrication technique for NNS-1 radiator tubes was changed from brazing to mechanical clamping after the brazing subcontractor experienced difficulty.

After 225 hours of intermittent operation of the Low-Power Loop, a shutdown for loop modification enabled removal of several sections and accumulated precipitates for study.

Material has been ordered, in conjunction with current orders of Haynes 25 tubes, for specimen fabrication for high-temperature aging tests.

Acetylene black was chosen as the high-emissivity coating for the the NSS-1 radiator. Establishment of parameters for successful application of this coating was completed, and two radiator panels successfully coated.

2. Discussion

a. Magnetic Aging Test

During this past quarter, the following periods of time and temperature of exposure were accumulated in the magnetic aging test:* 2616 hours of exposure to 985°F, 1680 hours at 910°F, and 400 hours at 970°F.

During the period of exposure to 985°F temperature, above, the magnet wire wrapped on several metallic ring specimens failed, apparently by shorting of adjacent turns, making readings impossible. This occurred after an exposure of 2200 hours. To the present, these coils have remained shorted. The rest of the coils appear to be operating satisfactorily. To establish the cause of the difficulty and to ensure that the material properties had not radically changed, one of the shorted rings was rewound. Saturation density values determined subsequently agreed with the readings taken with the original magnet wire.

At the start of period of exposure to 910°F temperature, above, another ring was removed from the oven and the magnet wire replaced. Again, a determination was made at 75°F prior to replacement of the rewound coil in the furnace. The subsequent values agreed with the original saturation density.

An insufficient number of readings have been taken during the period of exposure to 970°F temperature, to make reliable observations, except that there has been no apparent drastic change of properties.

Table 2 contains a summary of the history of the two low-alloy steel rings which were rewound with new magnetic wire.

*The materials include the low alloy steels and conventional magnetic materials described in previous reports.

TABLE 2

SATURATION DENSITY* VS TEMPERATURE AND TIME
(AISI 8620 STEEL)

Temperature (°F)	Time (hr)	Saturation Density (Kilogauss) Core No. 34 (N+Q+T)**	Core No. 36 (A)***	Remarks
75		17.5	16.4	Prior to start of test.
75			16.0	After 5300 hr exposure at elevated temperature, Core No. 36 was rewound.
985	2616/89	14.8	13.2	2616 total hr for Core No. 34; 89 total hr on new winding of Core No. 36.
75		18.0		
910****	500	15.9	14.2	Values on low alloy steels rose suddenly.
910****	1680	17.5	15.3	Reason for increase not apparent.
970				Insufficient time accumulated for reliable readings.

* At 75 Oersted.

** Normalized at 1700°F, quenched from 1600°F, and tempered 4 hr at 1225°F.

*** Annealed at 1600°F.

**** The same test. After 500 hr, values rose and remained higher for the remaining 1680 hr.

b. Fabrication Technique for NNS-1 Radiator

During the early stages of fabrication of the brazed fin-to-tube radiator assemblies, the subcontractor noticed that several tubes had visible cracks running circumferentially around and radiating from the edge of the braze joint. Dye-penetrant inspection of all completed assemblies revealed that approximately 50% were unacceptable. Weld repair was attempted, but found to be extremely difficult.

The assemblies which passed dye-penetration inspection were subsequently leak tested with helium. A large number contained leaks; the helium diffusing through the braze material indicated cracks completely hidden by the braze joint.

To avoid schedule slippage, the brazed-joint design was abandoned, and copper fins mechanically clamped to Haynes 25 tubes were used instead.

As soon as the difficulty was found, an engineer from the brazing subcontractor investigated the problem. He reported that the production department had changed the brazing procedure developed for the demonstration sample and the cracking was caused by improper heat application. This analysis was proven correct after brazing the final eight assemblies using a corrected heat-application technique. These assemblies were received and all assemblies tested with both dye penetrant and helium passed inspection.

c. Low-Power Mercury-Vapor Test Loop (LPL)

After 225 hours of operation, a Type 316 stainless steel simulated turbine-nozzle-blade test section was installed in the LPL. This section replaced a simple flow-control orifice used to throttle the super-heated mercury vapor. Various parts of the loop were examined and where practical, sections were removed and wall deposits were collected. The location of the sections removed are shown in Figure 35, and are identified and subsequently referred to by numbers 1 through 4. Flow rate in the system was 350 lb/hr. The flow conditions which existed at each of these points are described in Table 3.

TABLE 3

LOOP SECTIONS REMOVED

Section	Stage of Hg	Temperature °F	Pressure psia
1.	Superheated vapor	1180	275
2. a. Orifice inlet	Superheated vapor	1180	275
b. Orifice outlet	Wet vapor	625	18
3.	Wet vapor	625	18
4.	Liquid	80	24

Visual examination of the four sections revealed the following:

Section 1 - A dispersion of extremely fine mercury droplets adhered to the wall of the tube, covering about 75% of the wall circumference. The balance of the wall appeared black and shiny, but, when rubbed, the same mercury droplet dispersion appeared. The black, shiny surface appeared to be a very fine powder.

Section 2 - The upstream face of the nozzle was well wetted with an adherent mercury film; however, there were isolated bare areas that appeared as if the film had been removed by abrasion. Some of these areas appeared as long thin lines, resembling those which would result if the film were scraped with a sharp pointed object. Approximately an inch of tubing immediately upstream of this face was also wetted. Again, there were isolated unwetted areas and lines. Metallographic examination revealed no corrosion of the tube wall.

Section 3 - There were very small isolated globules of mercury adhering to the wall. Many could be made to drop off by tapping the end of the tube on a solid surface, but most resisted displacement by this impact.

Section 4 - The surface was unwetted, but a black powder deposit, which was easily removed, was found on the wall. This material was removed and analyzed.

Along with the precipitate removed from Section 4 (condenser outlet), deposits were removed from the mercury-pump inlet and outlet. These were also analyzed. The three specimens collected are described as Samples A, B, and C. Sources of these deposits and loop conditions at these points are described in Table 4.

TABLE 4

DEPOSITS REMOVED

Sample	Loop Location	Hg Temperature, °F
A	Condenser outlet	80
B	Pump inlet	80
C	Pump outlet	132

The visual appearances of the specimens were as follows:

Sample A (from condenser outlet) - A fine black powder of apparent uniform consistency. A magnified photograph (1000x) was taken of the particles as removed from the loop. This photograph appears as Figure 36. Analysis of this deposit showed the following:

(1) The wet (as removed) state consisted of Hg, Hg O, Cr_2O_3 and $(Ni, Cr)_2O_3$.

(2) Vacuum drying at 600°F for 1/2 hour removed all Hg and Hg O.

(3) The X-ray diffraction analysis of the dried residue was: Cr_2O_3, 60%; $(Ni, Cr)_2O_3$, 30%; $NiC \cdot Cr_2O_3$, 10% (spinal-type structure, maybe $Ni\ O \cdot Cr_2O_3$).

(4) The ratio of total nickel to total chromium found by X-ray spectrograph was 1 to 8 by weight.

Sample B (from pump inlet) - A fine black powder of apparent uniform consistency differing visually from Sample A only in that this sample contained shiny metallic-looking specks. A magnified photograph (250x) was taken after vacuum baking. This photograph appears as Figure 37. Analysis of this deposit showed the following:

(1) X-ray diffraction of residue after vacuum baking showed evidence of Cr_2O_3, traces of $(Ni, Cr)_2O_3$ and a metallic phase of a face-centered cubic structure.

(2) X-ray spectrograph analysis showed a ratio of nickel to chromium of 5 to 2.

Sample C (from pump outlet) - A fine black powder intermixed with relatively large shiny metallic-looking flakes and black needle-like particles. A magnified photograph (10x) was taken of this material as removed from the loop with no special preparation of the sample. This photograph is shown as Figure 38. Analysis of this deposit showed the following:

(1) X-ray diffraction of the residue after vacuum baking gave identical results to those found on the previous sample (pump inlet).

(2) X-ray spectrograph analysis showed a ratio of nickel to chromium of 8.3 to 3.7. The needles and flakes in this sample were sufficiently large to isolate. They were removed and analyzed separately. The results were:

(a) X-ray diffraction showed them to be entirely of the same face-centered cubic structure previously found.

(b) X-ray spectrograph analysis showed these particles to be an amalgam of Ni-Cr-Hg.

d. NNS-1 Radiator Coating

Acetylene black was chosen as the high-emmissivity coating for the NNS-1 radiator. Development work led to the following procedure for producing an adherent coating:

(1) Nickel plate copper fins to depth of 0.0005 to 0.0006 in.

(2) Lightly sandblast nickel plate with fine grit at 5 to 10 psi air pressure.

(3) Bolt fins to tube.

(4) Mix acetylene black, furnished by Acheson Colloid Company (Dag No. EC1652) mixed with Xylol to a No. 4 Ford viscosity of 18 to 20 sec.

(5) Apply the mixture by spraying on several coats to a total thickness of 0.002 to 0.004 in., using an air pressure of 45 psi.

Test samples fabricated using this procedure withstood a 12 hr exposure to 650 to 700°F with no apparent degradation of coating. In development of this coating procedure, the experience of Pratt and Whitney* was used to the fullest extent.

*As reported in the various progress reports covering their high-emissivity coatings development program.

3. Work Planned for the Next Quarter

Magnetic-aging tests will continue.

High-temperature aging tests using Haynes 25 will be initiated. An investigation will begin leading to the selection of a high-emissivity coating for the NNS-2 radiator.

B. MATERIALS SURVEY EXPERIMENTS

1. Summary of Accomplishments - 1 September through 30 November 1961

Tensile Specimens cut from the compatibility capsule bodies after exposure to mercury at 1100°F for 500, 1000, and 2000 hr were removed and evaluated.

Haynes 25 capsules exposed to mercury at 1025°F for 1000 and 2000 hr and 1175°F for 500 and 1000 hr were removed from the furnace and evaluated.

Type 405 stainless steel capsules exposed to mercury at 1025°F for 1000 and 2000 hr were removed from the furnace and evaluated.

The solubility tests of Haynes 8187 alloy in mercury were completed and evaluated.

A new lot of seven Haynes 25 capsules was fabricated for the 1250°F compatibility test.

2. Objectives

The primary objective of the materials survey program is to provide experimental evaluation of the suitability of certain materials for use in the SNAP-8 Power Conversion System. The program includes testing to determine the ability of these materials to contain mercury for substantial lengths of time at certain temperatures and pressures. Resulting data will be used to select alloys for more sophisticated testing and to provide initial recommendations concerning the selection of materials for component designs.

Current objectives of the program are to perform compatibility tests on capsules made of Haynes 25 and Type 405 stainless steel at 1025°, 1100°, and 1175°F for periods ranging from 500 to 10,000 hr. These tests are performed

to determine long-term corrosion, stress corrosion characteristics, and mass-transfer characteristics of the materials with small temperature differences. Changes in the microstructure of the alloys and welds, and resultant effects on the mechanical properties will also be determined.

3. Discussion

a. Experimental Evaluation

In the compatibility test program, capsules were removed after remaining in the furnaces for times up to 2000 hr for temperatures of 1025°F, and to 1000 hr for a temperature of 1175°F. Evaluation of the capsules has been completed, except for the tensile tests of the 1175°F and 1025°F capsule. The corrosion effects and the results of the tensile and hardness tests for the Haynes 25 capsules are discussed below.

Corrosion penetration of the Haynes 25 capsule walls is shown in Figure 39. The photomicrographs were taken from a section of the capsule near the bottom where the maximum temperature is reached. The photomicrographs show typical areas of the corrosion layer. The maximum corrosion-layer penetration in inches found for each temperature and time appear in Table 5.

TABLE 5

CORROSION LAYER PENETRATION

Test Time (hr)	Test Temperature, °F		
	1025	1100	1175
500	No test	None	0.0001
1000	0.0003	0.0005	0.0003
2000	0.0006	0.0008	Not completed

These results are not consistent with known corrosion mechanisms. There is no clear variation due to temperature. The variation with time appears to be about linear. Corrosion mechanisms are limited by solubility or diffusion parameters, both of which have an appreciable temperature coefficient.

The effect may be hidden by different flow patterns within the capsule at different temperatures. As a check, a number of capsules will be examined along their entire length to see whether the samples were cut at the point of maximum penetration. No conclusions regarding corrosion mechanism will be made until this is done, and the 5000 hr capsules are evaluated.

The capsules exposed for 2000 hr at 1025°F have a double corrosion layer as can be seen in Figure 39 (Sheet 1, Bottom Plate) and both layers were counted toward the penetration. This type of corrosion layer has not been found in any of the other capsules. The cause is not known.

X-ray studies of the single corrosion layer found on the Haynes 25 1100°F capsules indicated the layer consists of cobalt and tungsten compounds such as Co_3W and Co_7W. This is consistent with the phase diagram of Co and W; however, no CoW was found. This would indicate that the Co and W are forming intermetallic compounds as the leaching of the Ni and Cr progresses. Since the formation of the layer does not appreciably retard the corrosion, as shown by the photomicrographs in Figure 39, the corrosion layer must be porous. The porous layer, then, does not act as a diffusion barrier to retard further penetration of the material under the conditions existing in the capsules. This is consistent with the linear rate with time, and with the diffusion layer studies by NASA Lewis.

Microhardness readings were made on a ring cut from each capsule, as was described in the last quarterly report. The microhardness readings are plotted versus tube wall thickness for the capsules that have been evaluated. See Figures 40, 41 and 42.

The microhardness readings indicate age hardening of the Haynes 25 takes place after an initial softening. The softening is believed to be a stress relief of the stresses set up in the tube wall during fabrication. The rate of age hardening depends on the temperature of the test. The 1025°F capsules did not harden as much in 2000 hr of exposure as did the 1100°F capsules. The 1175°F capsules appear to have started to age harden within the first 500 hr because they did not show an initial softening even though the capsules were from the same lot of tubing.

The age hardening and reduction of ductility of Haynes 25, when exposed to elevated temperatures for extended times, was further proved by the tensile tests conducted on the tensile specimens cut from four 1100°F capsules. The design of the tensile specimen was described in the last quarterly report. The results of the tensile tests removed at room temperature appear in Table 6.

TABLE 6

CAPSULE TEST CONDITIONS

Time (hr)	Temperature °F	Ultimate Tensile Strength, psi	Yield Strength 0.2% offset psi	Elongation in 1 in., %
500	1100	154,000	75,000	48
1000	1100	152,000	77,500	46*
1000	1100	146,000	76,000	69*
2000	1100	131,000	83,200	20

*Fractured outside gage marks.

A broken tensile specimen from the 2000 hr 1100°F capsule is shown in Figure 43, and the grips to hold the tensile specimens are shown in Figure 44.

After 2000 hr exposure at 1100°F, there is a sharp drop in the ductility of Haynes 25 with a slight increase in yield strength. The results of the tensile tests exposed for 500 and 1000 hr at 1100°F agree with the values published for solution-annealed Haynes 25 sheet. The age-hardening effect appears negligible for Haynes 25 for the lesser exposure times at 1100°F.

Note that only one of the tensile specimens tested indicated a substantial decrease in ductility of Haynes 25 after exposure to elevated temperature for extended times. Future tests should provide the extent of the ductility loss that can be expected in Haynes 25 after exposure to temperatures of 1025°, 1100°, and 1175°F.

Evaluation of the Type 405 stainless steel capsules showed no intergranular corrosion as was reported in the last quarterly report. There is no corrosion layer formed on the Type 405 stainless steel, and the surface shows no evidence of attack in the photomicrographs. However, an even attack must take place since a mass-transport deposit formed near the liquid surface at the top (cold) end of the capsule.

The microhardness of the Type 405 stainless steel capsules was measured, and is plotted in Figure 45. The Type 405 capsules exposed to 1025°F temperature for times up to 2000 hr decreased in hardness as did the capsules exposed to 1100°F.

Figure 46 shows eight of the 1100°F capsules after they were split so that the inside diameter could be examined. The inside surfaces of all capsules were smooth and had not been selectively attacked or pitted. Indications of the mass-transfer deposit can be seen as a bright ring near the top (the cold end) of the capsule, especially capsule No. HD2A2. The capsules of Haynes 25 exposed at 1025°F (1000 and 2000 hr) and 1175°F (500 and 1000 hr) had similar mass-transport deposits at the cold end of the capsule.

Measurements of the wall thickness of the compatibility capsules to the nearest 0.0005 in. before and after the corrosion test did not reveal a loss of wall thickness for any of the capsules.

Solubility runs were made with Haynes 8187 alloy (62Co, 21Cr, 1.5W, 1.5Fe, 3Ni, Si, Mn) in mercury and the analysis was completed. Tests at 917°F, 1062°F, and 1152°F were conducted. Duplicate samples were run, but one each of the capsules at the upper two temperatures developed leaks during the run and the mercury was lost.

The data are given in Appendix B; the quantitative data plotted in Figure 47. The curves for Cr and Co from Haynes 25 (taken from the last quarterly report) are also shown for comparison. The Co is about 50% higher for Haynes 8187 than for Haynes 25. The Cr is nearly an order of magnitude lower for Haynes 8187 than Haynes 25, although the Cr content of the alloys is about the same. Although not proven, it is suspected that the Cr did not approach

saturation. (Thus, no curve is drawn through the Cr points.) This could arise from the fact that the diffusion rate of Cr to the surface could be much slower in the Haynes 8187 than in Haynes 25. Considerable Ni is present in the Haynes 25. When this dissolves, a greater actual surface area could be created at the interface to allow a more rapid Cr diffusion into the liquid. It is concluded from the data that Haynes 8187 should show somewhat better overall resistance to mercury corrosion than Haynes 25.

b. Testing

The three compatibility furnaces operated at 1025°F, 1100°F, and 1175°F throughout the quarter. The 1175°F furnace was shut down, the capsule removed, and the furnace used for the solubility tests for 3 weeks. The furnace was then restarted at 1175°F to continue the compatibility test. The three furnaces are operating under a vacuum of less than one micron.

Testing to yield strength of the tensile specimens machined from the capsule bodies was conducted on a tensile machine, with an autographic stress-strain recorder, at a strain rate of approximately 0.005 in./in./min at 0.2% offset. The cross-head speed after the yield strength was reached was increased to approximately 0.02 in./min until fracture occurred.

4. Work Planned for the Next Quarter

The first 5000-hr Haynes 25 and Type 405 stainless steel capsules run at 1100°F will be removed and evaluated.

The 1250°F compatibility capsules will be started. The 500-hr and 1000-hr capsules will be removed and evaluation initiated.

The tensile properties of Haynes 25 will be determined after exposure for 1000 hr and 2000 hr to temperatures of 1025 and 1175°F.

VII. SYSTEMS ENGINEERING AND RELIABILITY

A. SYSTEMS ANALYSIS ENGINEERING

1. Summary of Accomplishments - 1 September through 30 November 1961

In the analog computer program, system startups were simulated for three different radiator extension temperatures, and an additional startup was simulated using the most recent reactor data from Atomics International.

Development of a digital computer code continued for system optimization and off-design performance.

2. Objectives

The overall objective of the computer program is to simulate the performance of the SNAP-8 EGS in space, and to determine the static and dynamic characteristics during simulated startup and operation.

3. Discussion

a. Analog Computer

During October, several system startups were simulated. The reactor equations used were those current in October. Each startup was assumed to begin with the reactor at 2% rated power; reactor NaK inlet and outlet temperatures at 1300°F and 1320°F, respectively; NaK flow rate at 10% rated; and the radiator insulated and preheated to 250°F. The mercury inventory was injected into the secondary loop at 10% rated flow. At the completion of mercury injection NPSH at the mercury pump determined subsequent mercury flow rates. The turbine was assumed to start acceleration when the liquid mercury initially reached the heat exchanger, and to reach rated speed 60 sec after starting acceleration. The NaK pump was assumed to begin acceleration 30 sec after the turbine, and to reach rated speed 30 sec later.

During separate startup simulations, the radiator was extended when the radiator temperature reached 450°F, 500°F, and 550°F. The startup was unsuccessful for the 450°F case since the turbine output power diminished to zero. The 500°F radiator simulation was also unsuccessful; the turbine output power and mercury flow remained constant and did not increase to rated conditions. However, when radiator extension occurred at a radiator temperature of 550°F, a successful startup was achieved and rated system conditions were subsequently attained. After rated system conditions were attained, full vehicle load changes were made at three separate speed-control gains with no apparent system instability occurring. The speed control gains used were approximately equivalent to ± 0.1%, ± 0.2%, and ± 0.4% changes in speed.

Results of the successful startup are as follows:

Transients of NaK temperature leaving the heat exchanger varied from a minimum of 1120°F to a maximum of 1375°F

Transients of NaK temperature entering the heat exchanger varied from 1210°F to 1410°F

Turbine inlet temperature varied from 1210°F to 1410°F

A time duration of 20 min was required to reach rated secondary-loop output from the time at which the reactor was at rated NaK outlet temperature and 2% power level

After rated system conditions were attained, full vehicle-load changes produced no noticeable system instability with several values of speed-control gain.

An additional system startup was simulated after reactor time equations were updated in accordance with the reactor design data available from Atomics International at the end of October. Equations describing transient NaK-pump motor performance were formulated, eliminating the requirement for assumed NaK-pump and turbine acceleration rates.

This last simulated startup was unsuccessful since excessive reactor power transients occurred during the final phase of the mercury-injection period, resulting in loss of mercury-vapor superheat. System parameters will be investigated and further computer investigations will be made.

Since the last analog computer run, new information has been received from Atomics International concerning changes in reactor controls and in temperature coefficients. The temperature coefficients have been reduced considerably from previous values, and may be expected to produce more severe reactor power transients than those observed in the last computer run. The analog simulation is being modified to reflect these latest reactor changes.

Analog work has been temporarily suspended until approximately 15 January because the computer is being relocated.

b. Digital Computer

Development continued of a digital computer code for system optimization and off-design performance evaluation. An overall optimization logic diagram was completed. Subroutines were prepared for analysis of the heat exchanger, turbine, radiator, and pumps.

Optimization logic is based on a parametric analysis which will provide a systematic variation of parameters so that a minimum-weight system can be achieved for a given power output. This optimization can also be accomplished with limited boiling temperatures. Provisions have been made for optimizing a system in which a fixed design is incorporated for heat exchanger, turbine, or radiator.

Heat-exchanger subroutine equations have been coded and checked out. Several test cases have been run to determine convergence criteria for the optimization analysis, and to determine the effect of variations of system parameters on boiling temperature.

Turbine subroutine equations have been coded and are currently being checked. Other system equations for computing component cooling, pump and alternator power, and system weights have been prepared and are presently being coded. Optimum radiator data is being prepared on the AGN radiator code for use in the system optimization.

B. RELIABILITY

1. Summary of Accomplishments - 1 September through 30 November 1961

Intensive effort was devoted to perfecting the Failure Reporting and Analysis System. Indoctrination training was continued, an environmental specification was started, and a preliminary study of the predicted reliability of the SNAP-8 System was initiated.

2. Objective

The principle objective of the reliability program is to increase the inherent reliability of the SNAP-8 Power Conversion System.

3. Discussion

The cold-nitrogen turbine test failure investigation (Failure Reports 007 and 016) was continued beyond the mere establishment of the precise mode of failure. There was indisputable evidence that vibration of the PDA shaft was a contributor to Failure 007, while Failure 016 showed the need for multiple approaches to solution of the problem of vibration.

From the design viewpoint, need was established for a dynamic analysis of the PDA rotating assembly. Accordingly, the Flight Dynamics Department was requested to perform a critical speed analysis and investigate the effects of other elements on critical speed. Among the other elements considered were gyroscopic effects, damping, and flexible supports.

A report was received on the first part of the critical speed analysis which indicates that vibration problems may occur with bearings having a stiffness less than 4×10^5 lb/in. in the absence of effective lubricant-film damping. This report will be reviewed during the next quarter and further investigation made in those areas where questions arise.

Problems of dynamic balancing procedures, techniques, and capabilities were attacked from the human engineering standpoint. The equipment in use was considered first, and arrangements were made to have it overhauled and brought up to factory-new standards. In addition, the equipment has been moved to a dust-free, temperature-controlled atmosphere.

A specification on balancing and inspection techniques was written and is now being reviewed. Arrangements were also being made to provide expert training of personnel involved with balancing, inspection, and calibration. A test rotor for checking the accuracy of the balancing machine is being fabricated. Arrangements have been made with the Aerojet Secondary Standards Laboratory to periodically check and certify the accuracy of the machine.

4. Work Planned for the Next Quarter

The Critical Speed Analysis Program will continue.

The human engineering in dynamic balancing program will continue, a specification on balancing will be released, and the failure reporting system will be implemented. A specification on the environmental requirements for the SNAP-8 electrical generating system will be released.

A formal reliability program will be developed and released.

Reliability of the SNAP-8 System will be predicted, and reliability goals for all components and subsystems will be assigned.

C. 60-KW FEASIBILITY DEMONSTRATION PROGRAM

A program designed to demonstrate the feasibility of a 60-kw power conversion system was initiated, and the following major areas of effort were established:

1. Electrical System Paralleling

An analysis of the various methods of paralleling two SNAP-8 alternators was conducted in which the primary objective was to establish a method of paralleling that required a minimum modification of existing SNAP-8 hardware. As a result of this analysis, the random-paralleling method of electrical paralleling has been selected for further study. Other methods, such as automatic paralleling, and motorizing of one alternator, were rejected due to weight penalties imposed by additional switchgear and insufficient motoring torque. A detailed study program is being conducted to determine real-load and reactive-load division, transient response, damper winding location, and to establish the voltage-regulator and speed-controller modifications necessary to permit parallel operation.

2. Primary Loop Paralleling

A preliminary system analysis was completed for six primary-loop configurations. The configurations analyzed consisted of either two 300-kwt boilers connected in parallel, or one 600-kwt boiler provided with two independent mercury passages. In each system, the pumping effect was examined for two NaK pumps in parallel, two pumps in series, and a single large pump. The effects of PDA overspeeds or underspeeds, decreases in NaK or mercury flow rates, decreases

in heat-transfer coefficients, and the different starting procedures were studied for each of the various configurations. Results of the analytical studies indicate that a primary loop using paralleled 300-kw boilers and paralleled NaK pumps is most promising. The selected configuration is the only system which will maintain a 30-kw output after failure of one NaK pump. In addition, this configuration displays little system degradation with flow-rate or heat-transfer coefficient degradation. Existing SNAP-8 primary loop components can be used to construct the selected configurations.

3. Work Planned for the Future

The theoretical analysis of the problems inherent in paralleling two SNAP-8 alternators and their control subsystems will continue. When the analysis has progressed to the point where problem areas and modification requirements can be defined, a paralleled-alternator test program will be initiated.

A detailed analysis of the selected primary loop configuration will be conducted to verify the indications of the preliminary studies. Upon the conclusion of the detailed studies, a liquid-metals test loop, representing the proposed primary loop, will be constructed and operated to verify the findings of the study programs.

VIII. SUBSYSTEMS TESTS

A. SUMMARY OF ACCOMPLISHMENTS - 1 SEPTEMBER THROUGH 30 NOVEMBER 1961

Testing of the low-power mercury-vapor test loop (LPL), at mercury boiling-condensing design conditions, continued throughout the quarter.

The NaK system assembly for the rated-power mercury-vapor test loop (RPL) was completed by mid-October. Integrated NaK-mercury system tests were initiated in November, and eight mercury boiling-condensing tests were performed by the end of the quarter.

B. DISCUSSION

1. Low-Power Mercury-Vapor Test Loop (LPL)

Testing of the LPL at mercury boiling-condensing design conditions continued throughout the report period. A static test section of Type

347 stainless steel, simulating the turbine second-stage blades, was installed in the vapor section of the loop in September. Following several check-out and adjustment tests, two extended-duration tests were conducted for a total accumulated operating time of 250 hr 15 min on the test piece before it was removed for evaluation.

When the first test section was removed, a second test section (similar to the first but made of Haynes 25) was installed. The vapor portion of the test loop was also modified by removal of the 3 ft^3 accumulator and installation (in place of the accumulator) of a second superheater. This superheater will permit mercury vapor temperatures up to 1300°F.

During this report period the test loop was operated for 316 hr 15 min, resulting in a total accumulated operating time of 474 hr 33 min.

2. Rated-Power Mercury - Vapor Test Loop (RPL)

Early in the report period, the test-loop NaK system assembly was completed, except for the mercury boiler. Upon completion of satisfactory helium-leak tests, NaK pumping tests at temperatures up to 1100°F were conducted to check out the system components and instrumentation, and to "wet" the internal surfaces of the electromagnetic pump and flowmeter. The mercury boiler was received following repair welding by the manufacturer. By mid-October, the boiler was helium-leak tested, mounted on the support stand, and welded into the NaK loop.

The mercury workhorse radiator (condenser) was delivered to the test facility, after repair welding to correct leakage, and installed in the test-support stand. The mercury system buildup was completed in late October. In addition to the mercury boiler and condenser, the system includes a nozzle in the mercury-vapor line (substituting for the turbine unit until a PDA becomes available), and a workhorse mercury recirculating pump of AGC design. Upon completion of satisfactory mercury-system helium-leak tests, shake-down pumping tests were conducted to determine the pump operating characteristics and control requirements prior to initiation of mercury boiling-condensing tests.

Integrated NaK-mercury system tests began early in November, and eight mercury boiling-condensing tests were performed during the report period. The tests were conducted to check out the operation of loop components and instrumentation, and to determine the operating characteristics of the test loop and control systems.

The NaK-system temperatures have been raised to a maximum of 1350°F as the tests progressed; the mercury-boiler-outlet vapor temperatures and flow rate have also been gradually increased to approach design operating conditions. These conditions should be achieved during December. Minor loop adjustments have been made between tests to improve system controls and to resolve several instrumentation problems. The total accumulated operating time of the integrated NaK-mercury systems was 45 hr 10 min at the close of this report period.

C. WORK PLANNED FOR THE NEXT QUARTER

Operation of the LPL will continue on an extended-duration basis. Data will be gathered for corrosion-erosion effects on selected test specimens, and the effects of extended-duration operation on the loop materials and working fluids will be investigated.

RPL operation will continue with particular emphasis placed on achieving design operating conditions and testing of the PDA-X.

IX. NON-NUCLEAR SYSTEMS TESTS

A. SUMMARY OF ACCOMPLISHMENTS - 1 SEPTEMBER THROUGH 30 NOVEMBER 1961

Construction of the test cells for the NNS-1 progressed satisfactorily, and installation of test loops and components is 90% complete.

Preliminary planning was initiated for the NNS-2 test loop.

B. DISCUSSION

1. Non-Nuclear System No. 1 (NNS-1)

The purchase orders for long-lead-time system materials were completed at the beginning of the report period, and in-house fabrication of a zirconium hot trap, for gettering the NaK system oxides, was initiated. The foundations for NNS-1 and NNS-2 NaK (gas-fired) heaters were constructed on the test-facility equipment pad early in September.

Installation of liquid-metals test cells for NNS-1 and NNS-2 began in mid-September and the cell construction and painting was completed by mid-October. An I-beam sub-structure was installed in the test cell to support system components such as the NaK expansion tank and flowmeter, and to support the two mercury radiator assemblies. Electrical power circuits for operation of systems components (pumps, motors, heaters) were installed and checked out.

The fabrication and installation of NNS-1 instrumentation and controls systems was completed at the end of November.

Construction of the NaK loop was initiated during October after receipt of the loop electromagnetic pump and the gas-fired NaK heater. Construction was completed at the close of this report period, except for the mercury boiler which will be delivered in December.

The NaK-loop and mercury-loop cover-gas systems were fabricated, leak-tested, and installed in the test cell preparatory to loop operation. Operational tests of the NaK heater and heater-control system were completed satisfactorily. The NaK hot trap was fabricated, flow-tested with an aluminum dummy element, assembled with Zr element, and installed in the test loop.

The mercury-loop radiator panels were received at the close of the report period, and satisfactorily helium-leak tested. Installation of the air ducting for the radiator is in progress. The blower for radiator heat rejection was received, installed on a support stand on the facility equipment pad, and connecting ducting to the test cell was completed.

The test cell air-exhaust system installation was completed. Catwalks were installed in the test cell to provide easy access to system equipment located in the upper areas of the 20-foot-high cell.

2. Non-Nuclear System No. 2 (NNS-2)

Preliminary planning was initiated for the NNS-2 test loop. The system material requirements will be established and purchase requisitions for long-lead-time items will be issued in December.

C. WORK PLANNED FOR THE NEXT QUARTER

Testing of the NNS-1 will begin early in December. Checkout of the NaK system will occur first to be followed by shake-down tests of the mercury system. Early mercury-system operation will use a nozzle to simulate the turbine. A PDA-X will be installed, when ready, for later operation.

Purchase of all materials and equipment for the NNS-2 will be completed. Fabrication and installation of the test loop, with the associated pneumatic and electrical systems, will be started.

X. NUCLEAR SYSTEMS, GROUND EVALUATION

A. SUMMARY OF ACCOMPLISHMENTS - 1 SEPTEMBER THROUGH 30 NOVEMBER 1961

Construction of the Ground Prototype Test Facility was initiated.

An electrical generating system integration plan was compiled and reviewed.

Title II design for the Flight Prototype Test Facility was initiated.

B. DISCUSSION

1. Nuclear Facility No. 1 (GPTF)

Construction of the GPTF began in October. By the close of the report period, the building site excavation was completed.

Organization, test integration, and support equipment studies continued. An electrical generating system integration plan (EGSIP) was compiled for the GPTF (Aerojet Report No. 0390-52-SD-4) defining Atomics International and Aerojet-General responsibilities with respect to test facility and equipment design, development, installation, and operation. This report was forwarded to NASA, AEC, and AI for review and comments. The plan was reviewed at the November SNAP-8 Coordination Meeting. A preliminary plan was prepared to support the data presented in EGSIP.

A preliminary outline of a hazards report was prepared.

2. Nuclear Facility No. 2 (FPTF)

A contract for the Title I and Title II Design of the FPTF was awarded to the Bechtel Corporation on 1 September 1961. Title I design was

completed by the end of November. Studies of the requirements for facility and test equipment continued.

To facilitate work on the Title II design phase, preliminary studies were conducted on the load bank to be used for alternator power dissipation in the facility.

C. WORK PLANNED FOR THE NEXT QUARTER

EGSIP will be completed and submitted for final approval in December.

Test planning and organization requirements for the GPTF, and preliminary design studies for test support equipment will continue.

Title I design of the FPTF will be reviewed by Atomics International and Aerojet. Title II design will be completed. Construction of this facility is scheduled to begin in April 1962 with an expected completion date in October 1963.

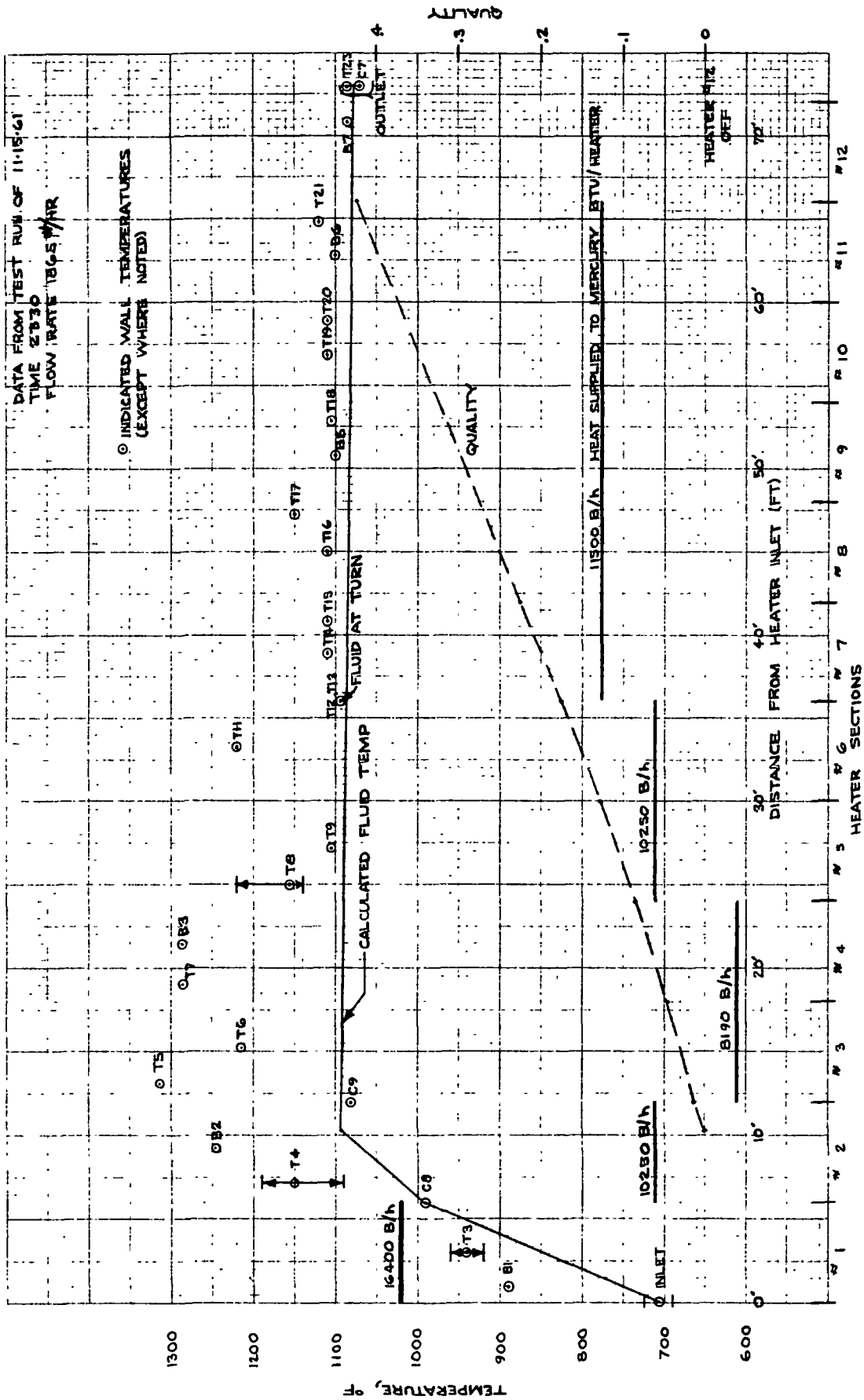
DATA FROM TEST RUN OF 11-15-61
TIME 2330
FLOW RATE 1865 #/HR
INDICATED WALL TEMPERATURES (EXCEPT WHERE NOTED)
QUALITY
HEATER OFF
OUTLET
INLET
FLUID AT TURN
CALCULATED FLUID TEMP
QUALITY
11900 B/h HEAT SUPPLIED TO MERCURY BTU/HEATER
10250 B/h
10250 B/h
8190 B/h
16400 B/h
DISTANCE FROM HEATER INLET (FT)
HEATER SECTIONS
TEMPERATURE, °F

Figure 1

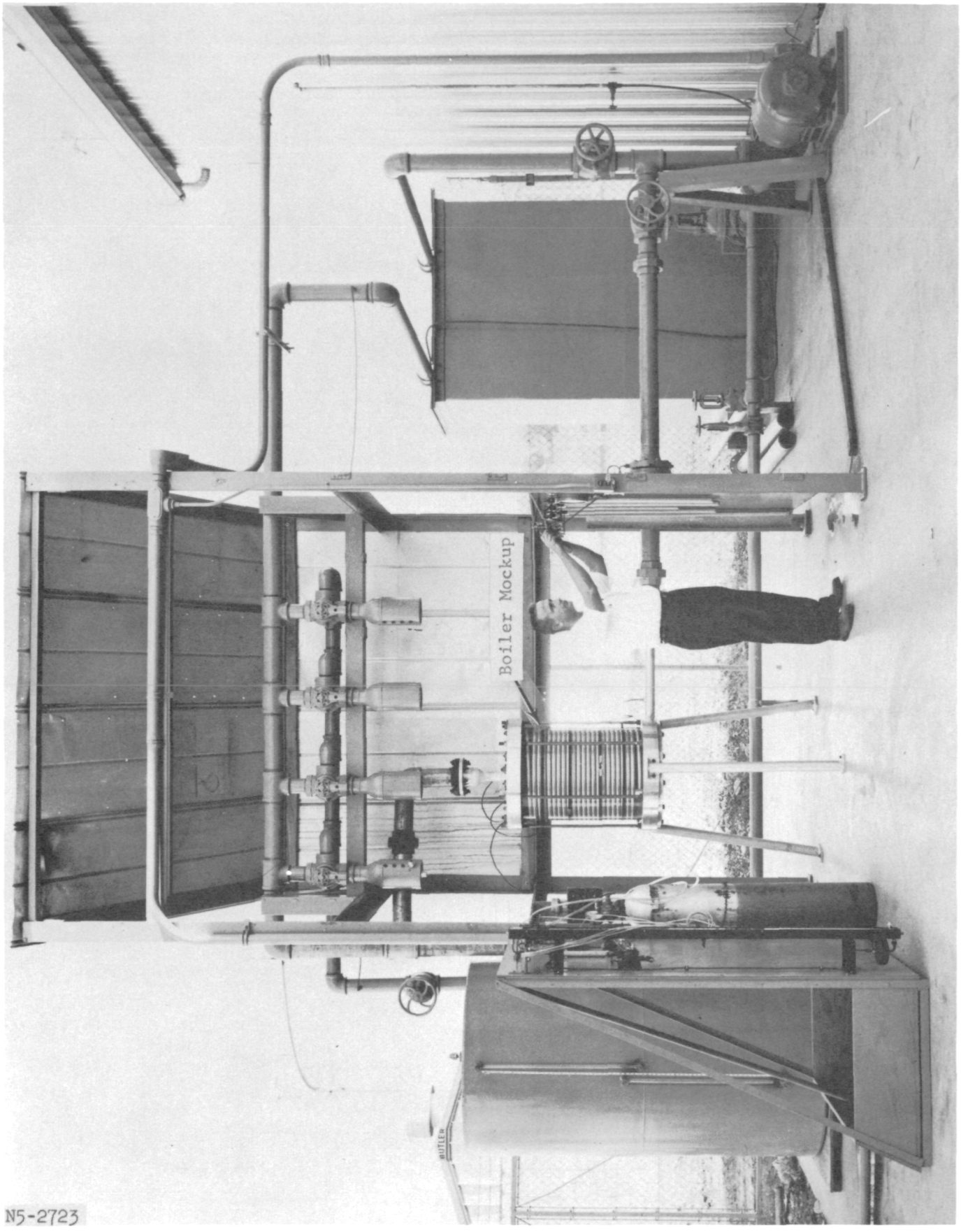

Water Test Loop for Boiler Mockup

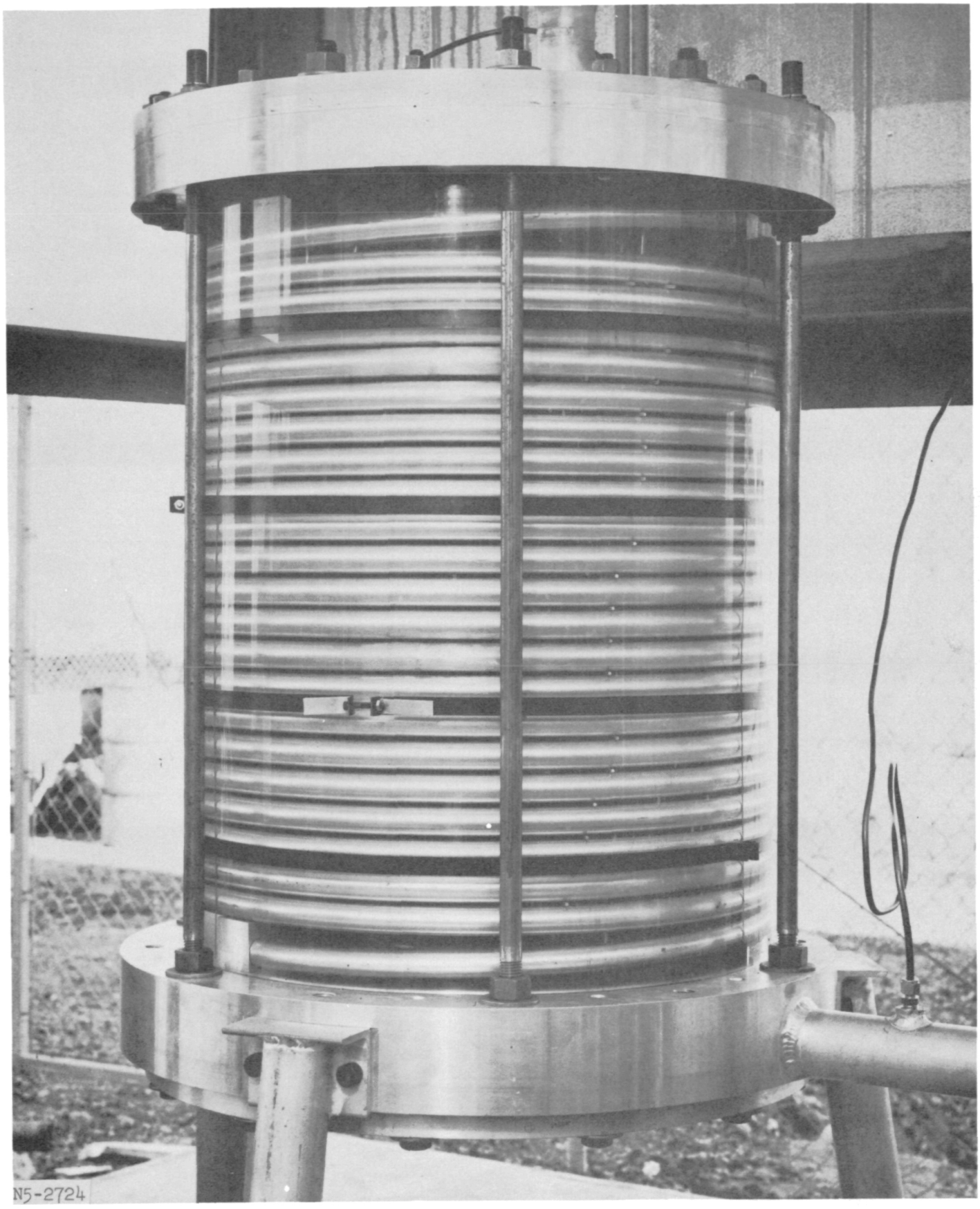

Full-Scale Boiler Mockup

Figure 3

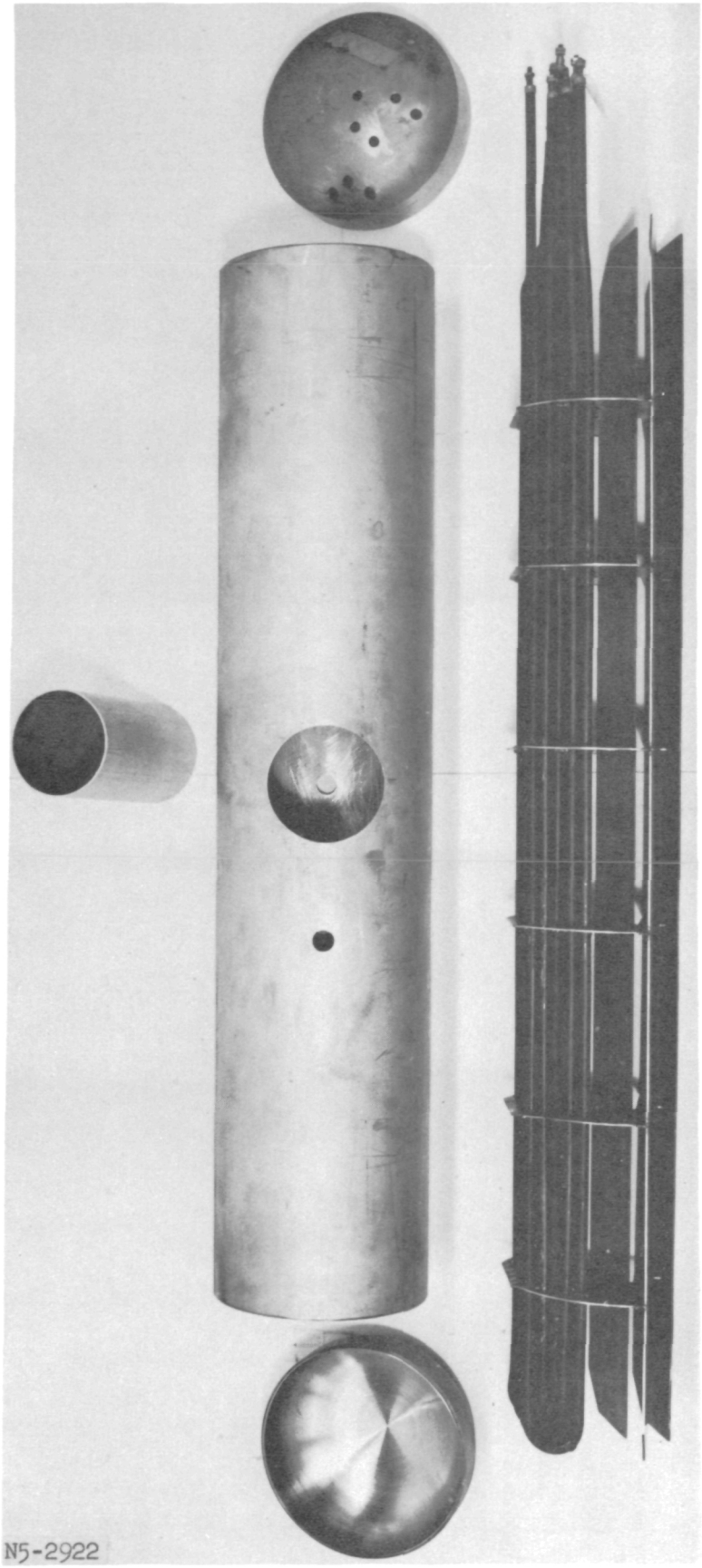

Boiler for 6-tube Condensing Experiment (Disassembled)

Figure 4

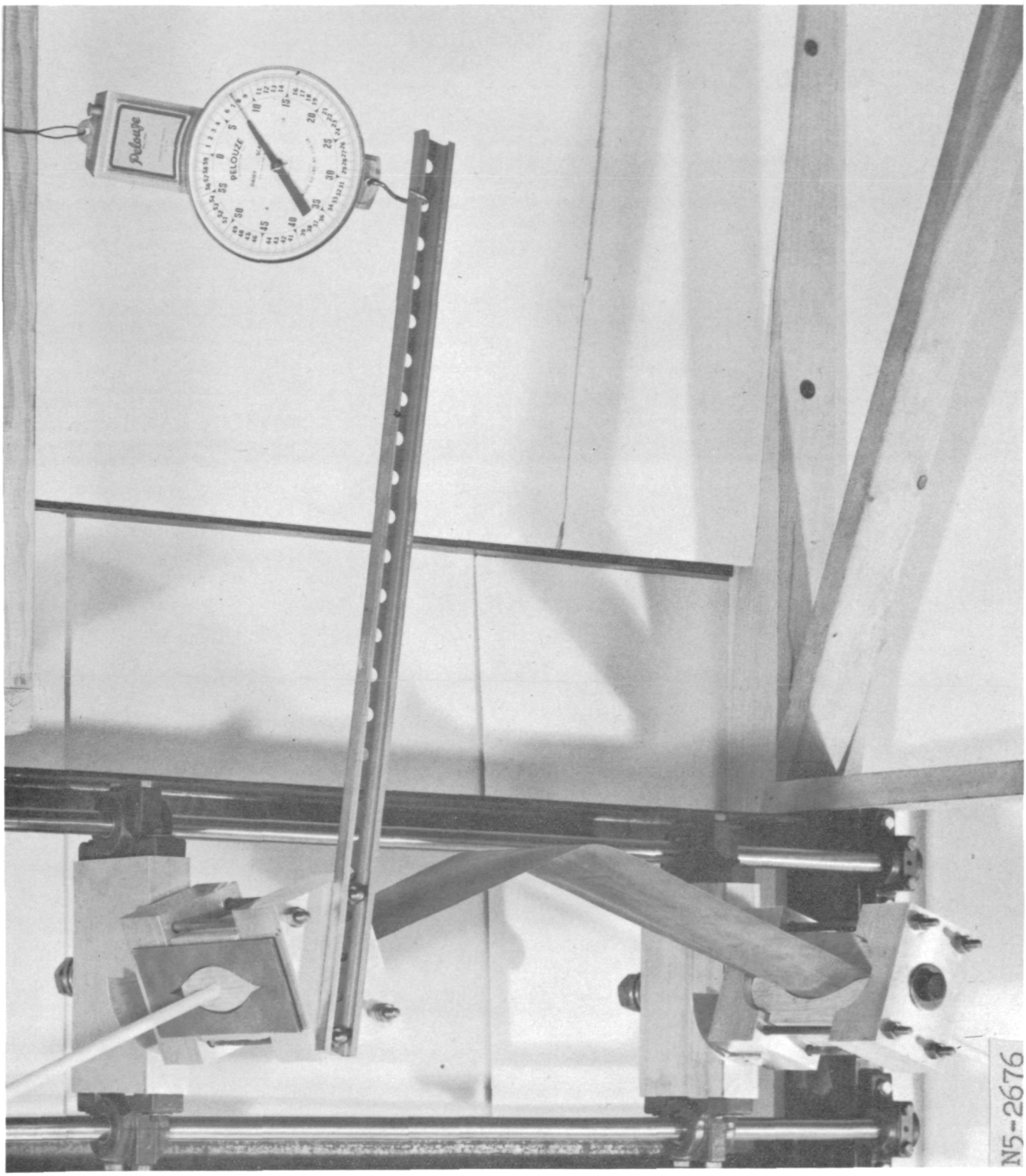

Bend-Test Fixture

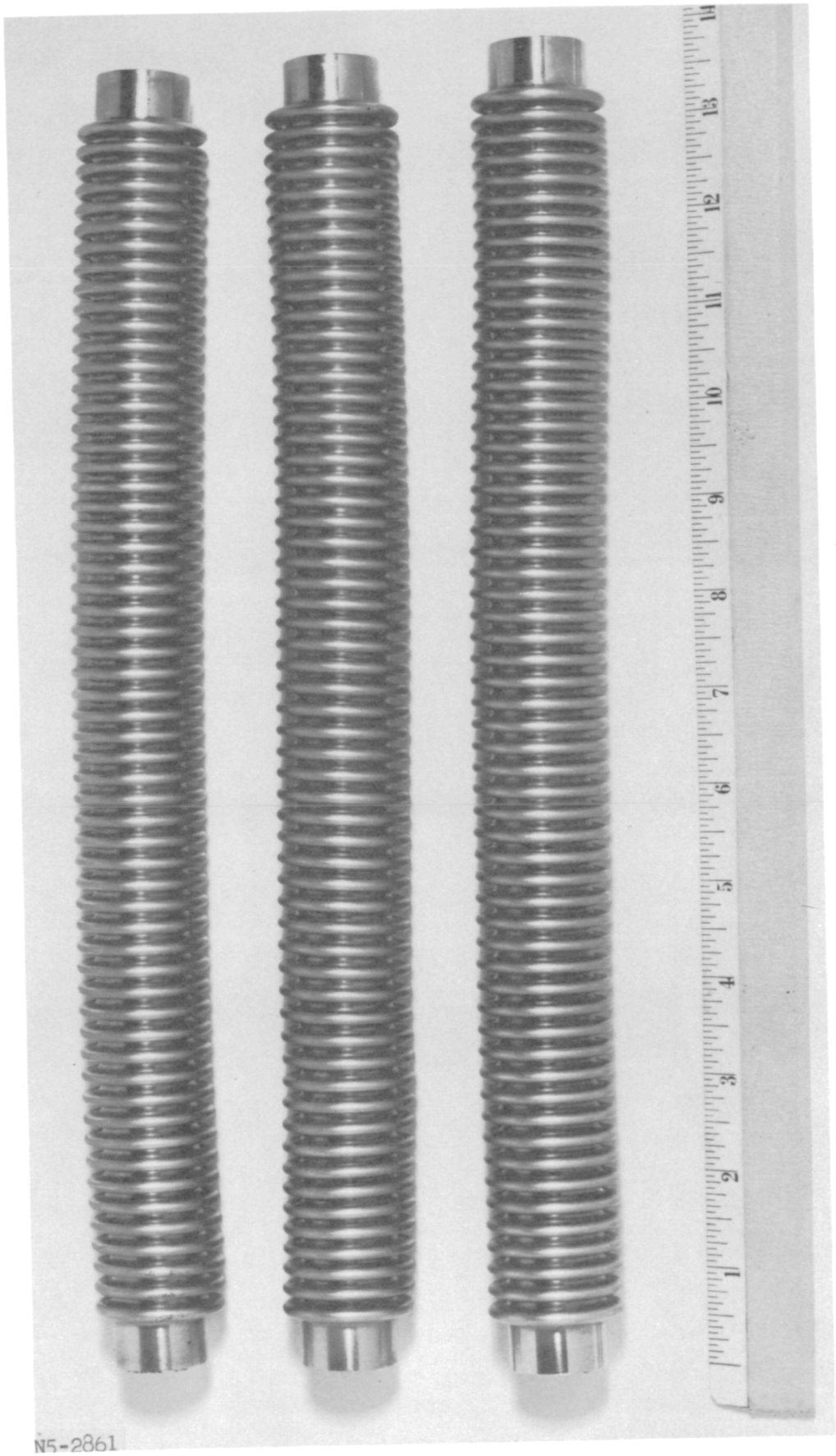

One-Inch Diameter Haynes 25 Bellows

Figure 6

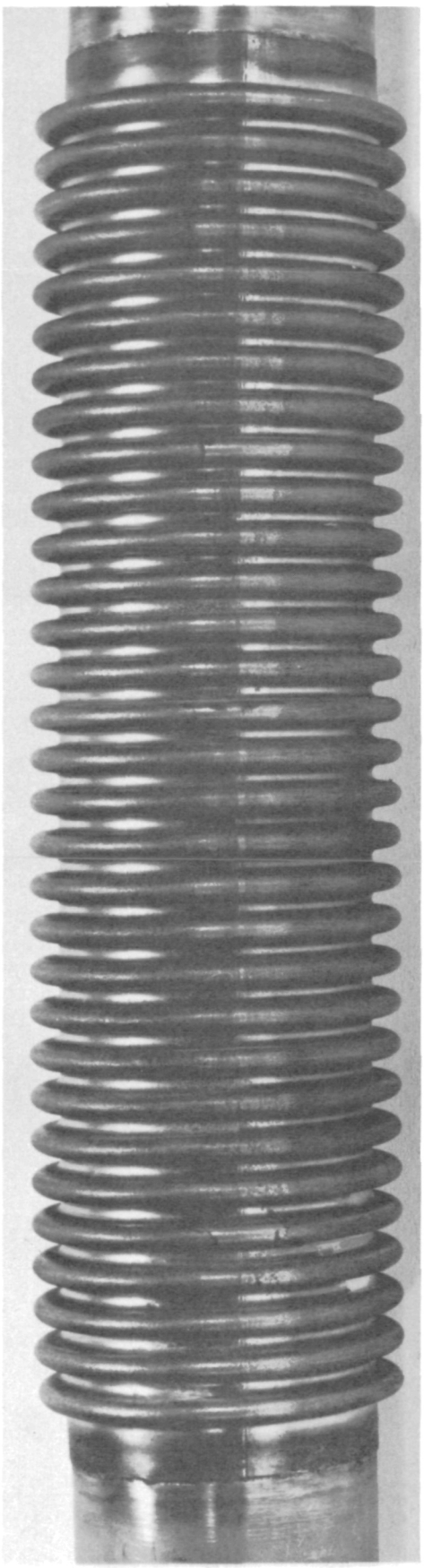

Three-Inch-Diameter Haynes 25 Bellows

N5-2930

Figure 7

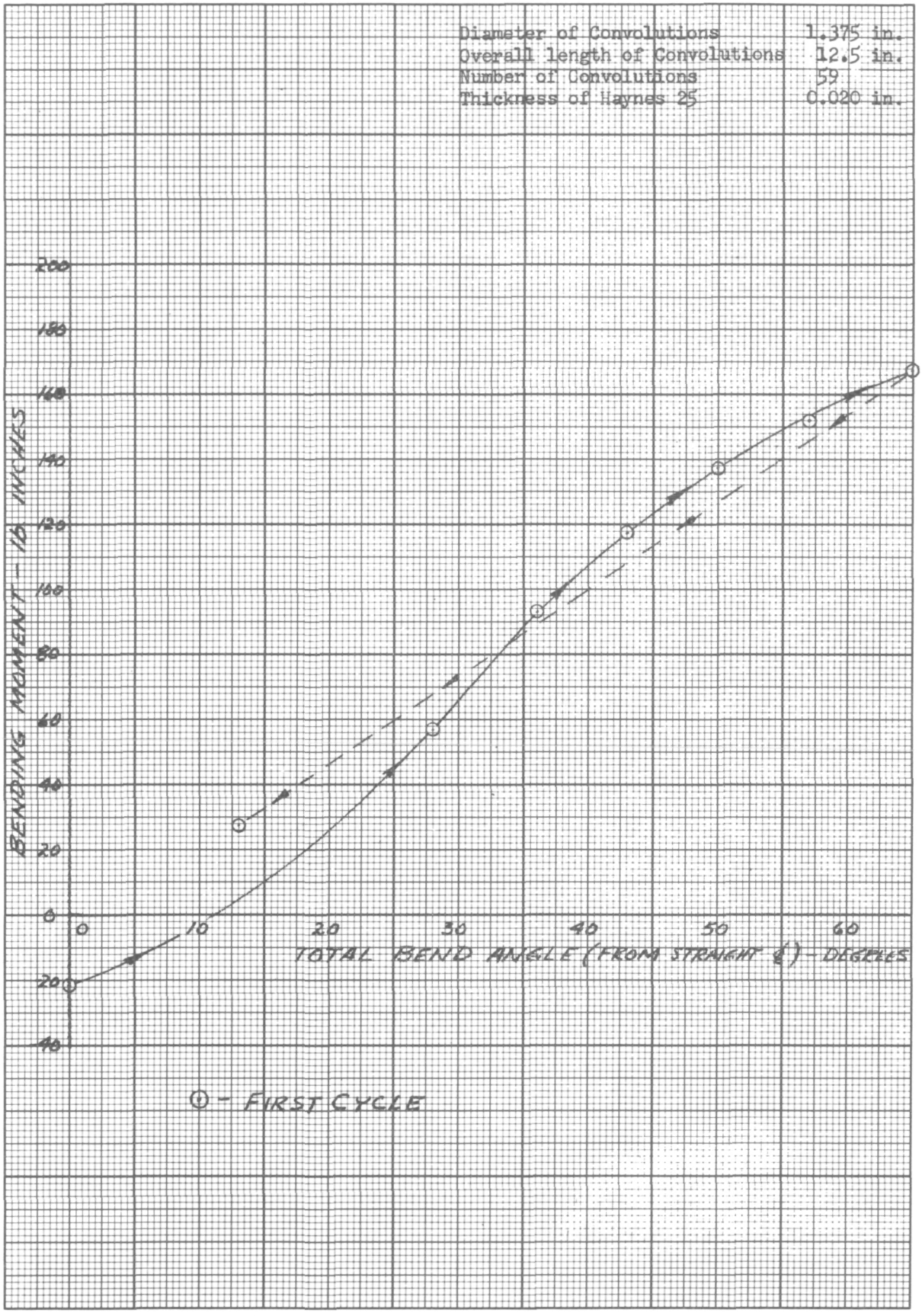

Bend Test Data - One-Inch Haynes 25 Bellows

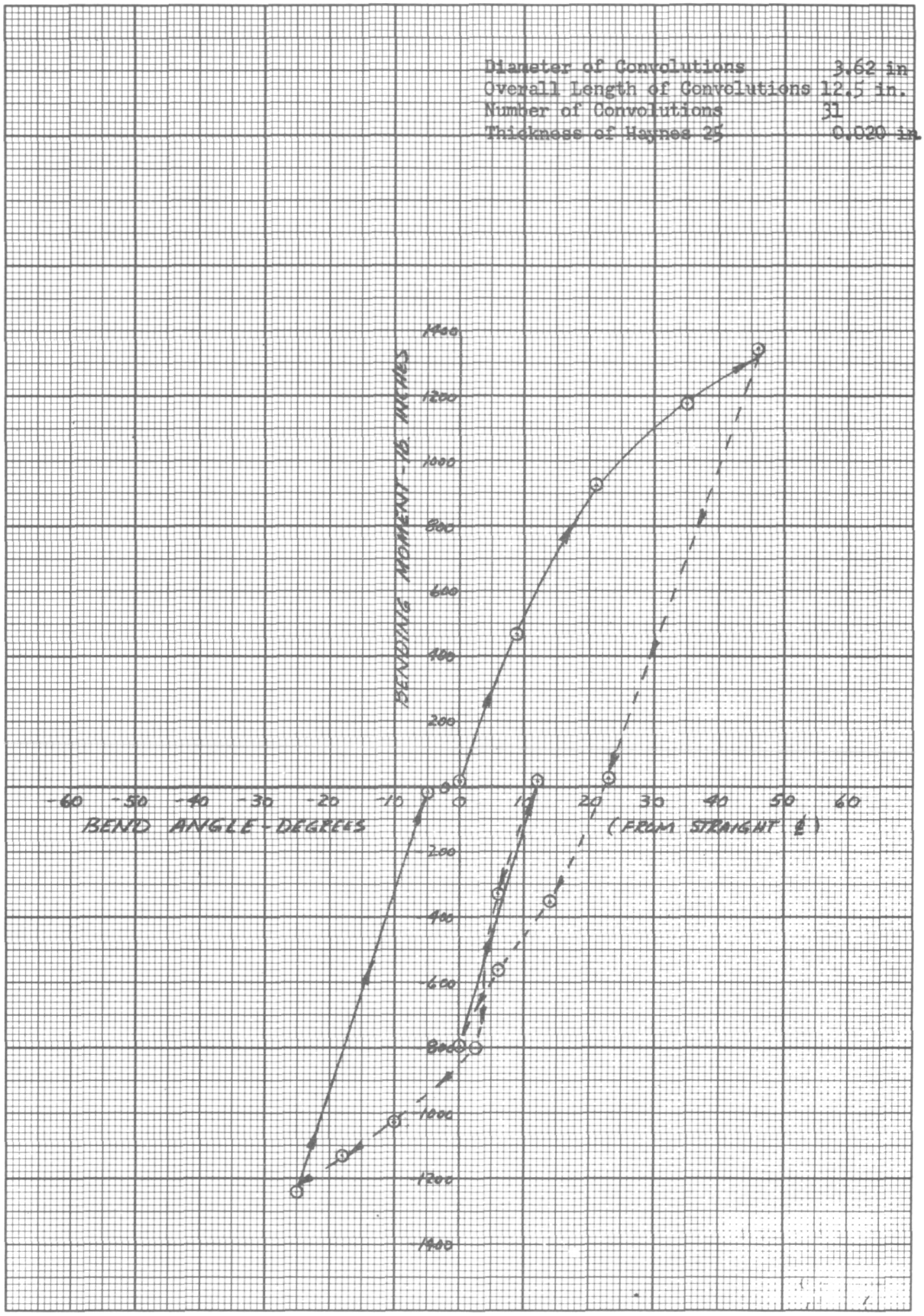

Bend Test Data - Three-Inch Haynes 25 Bellows

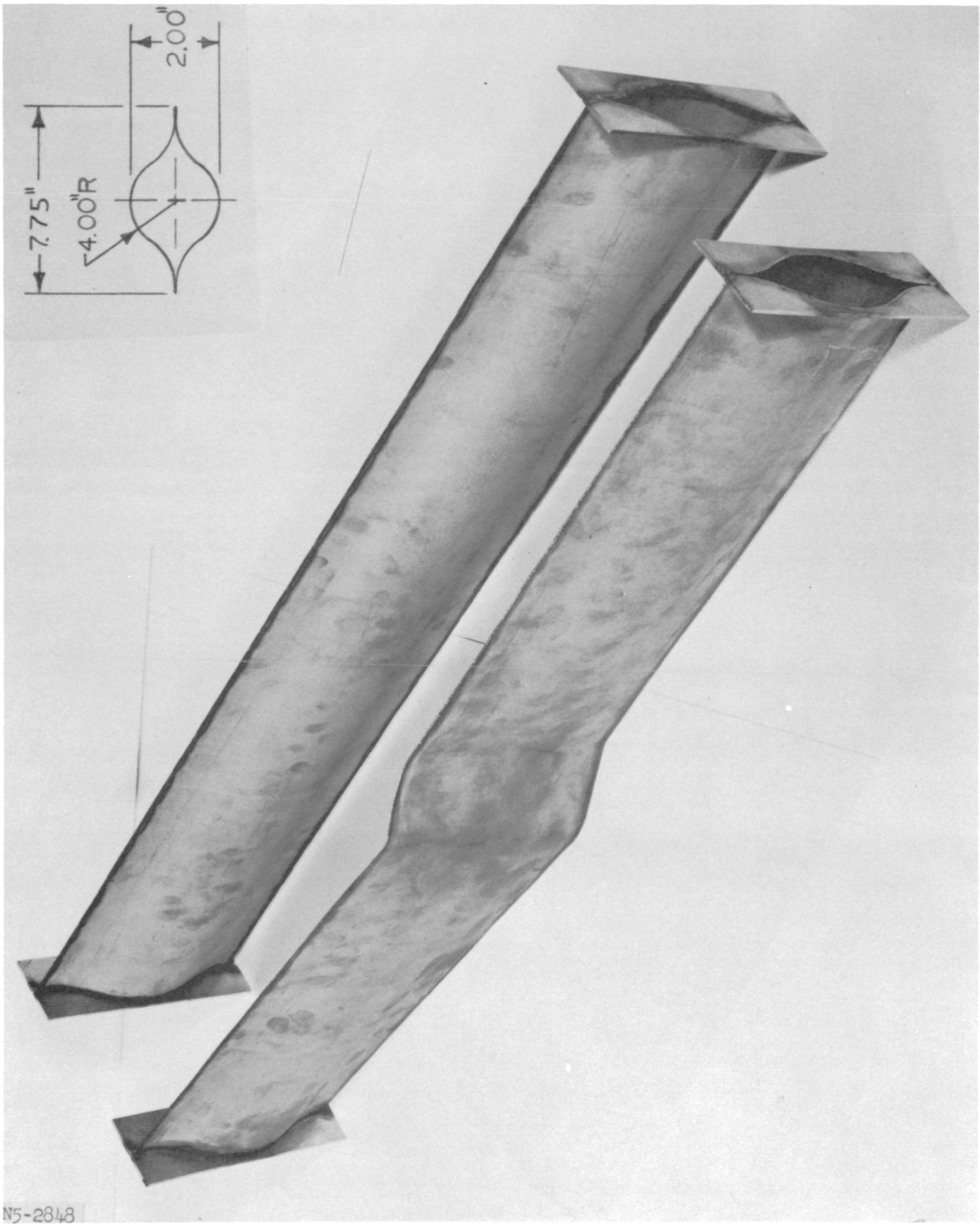

Three-Inch Deflection Joint Made From 0.020-in. Haynes 25

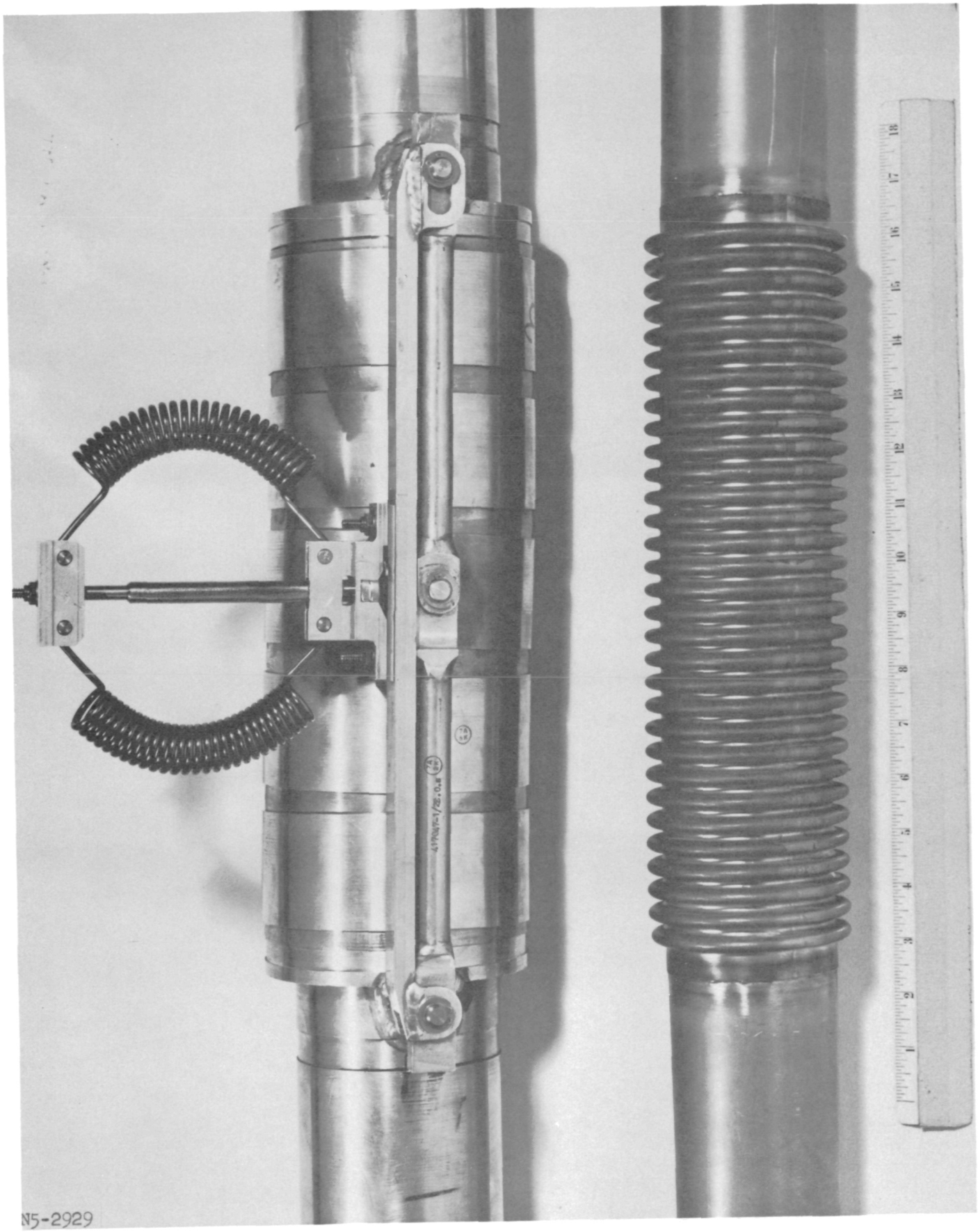

Three-Inch Flexible Joint Assembly

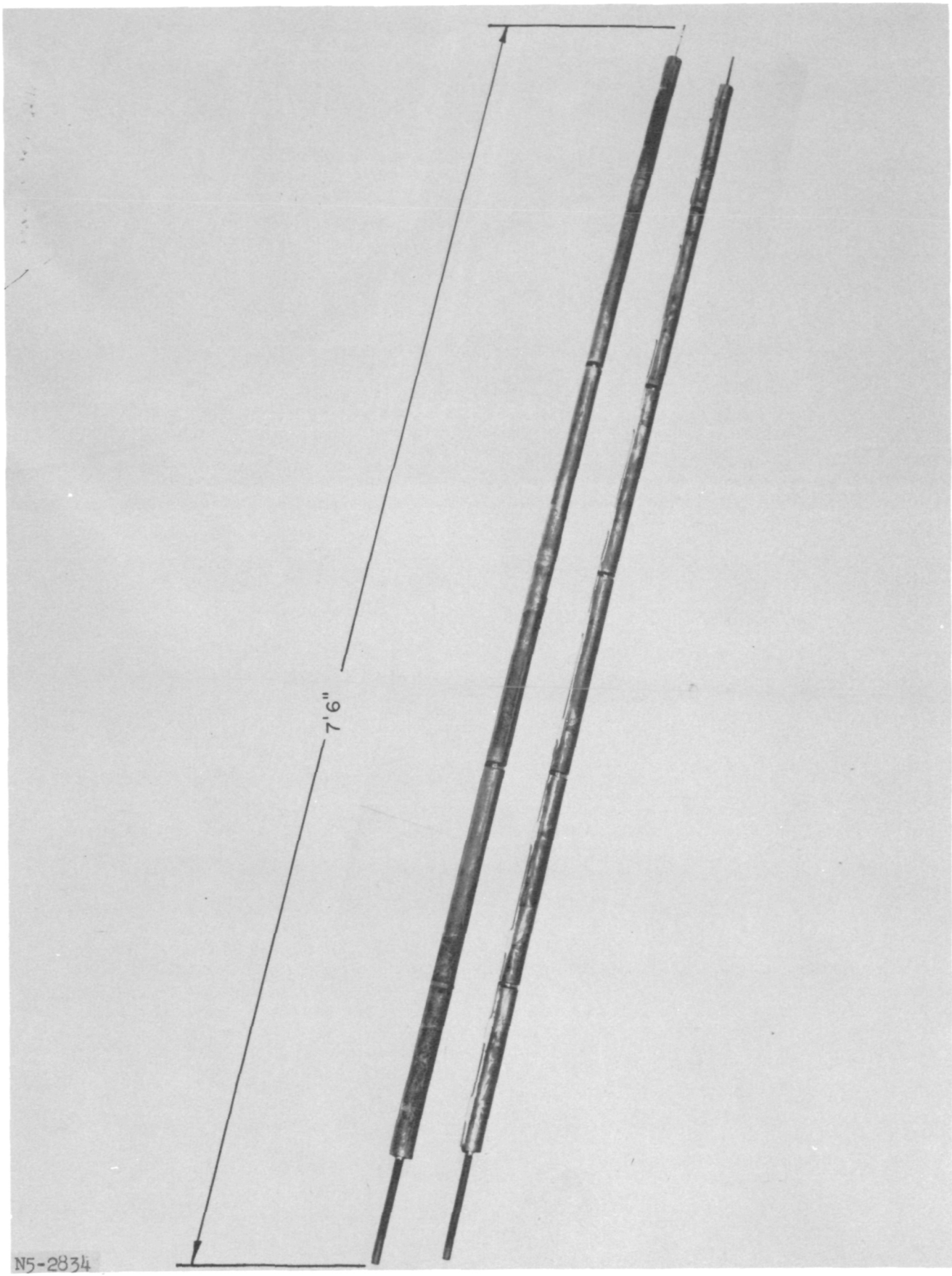

Tapered Radiator Tubes in the "As Cast" Condition

Figure 12

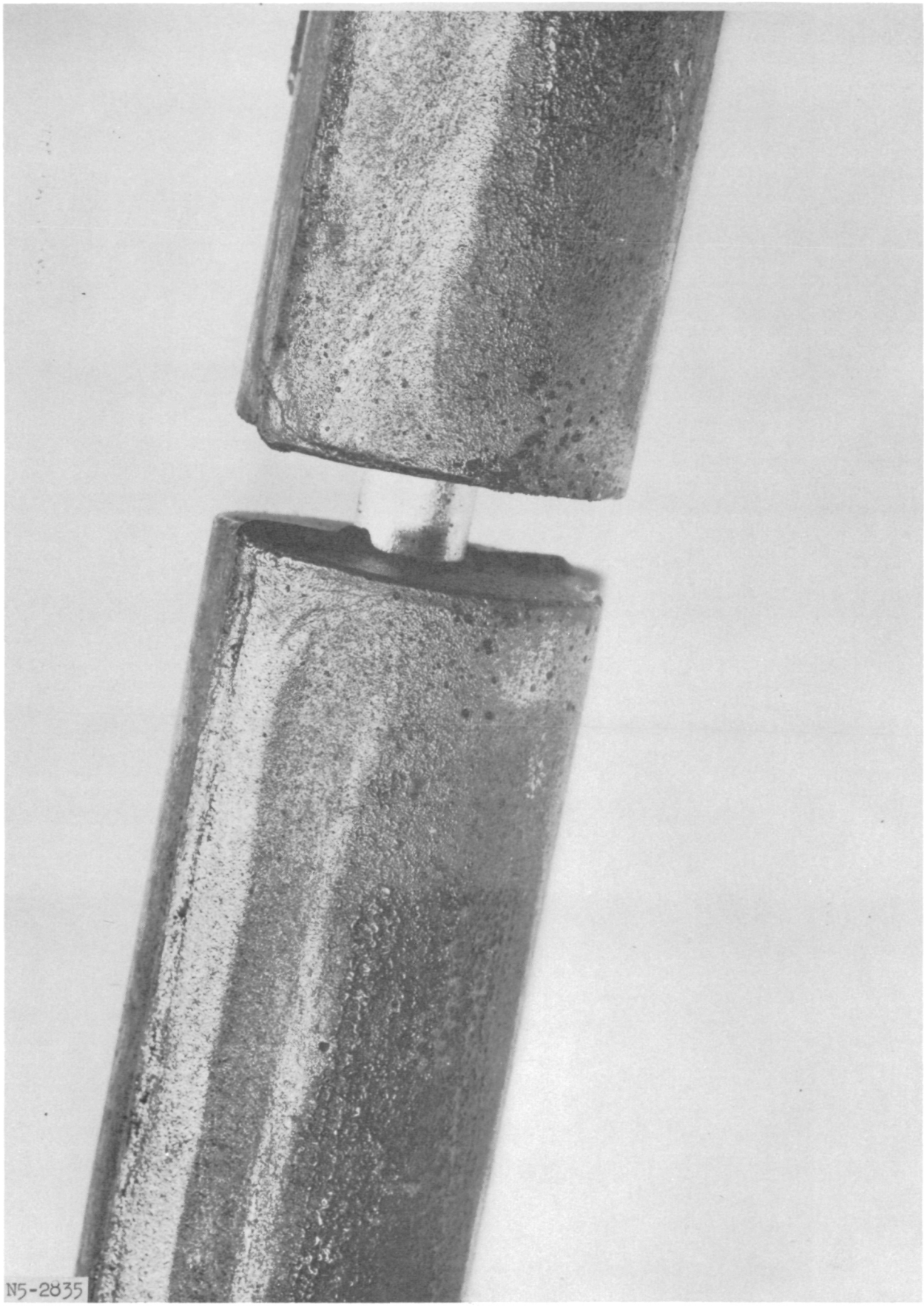

Closeup of Break in Casting to Minimize Shear Stress

Figure 13

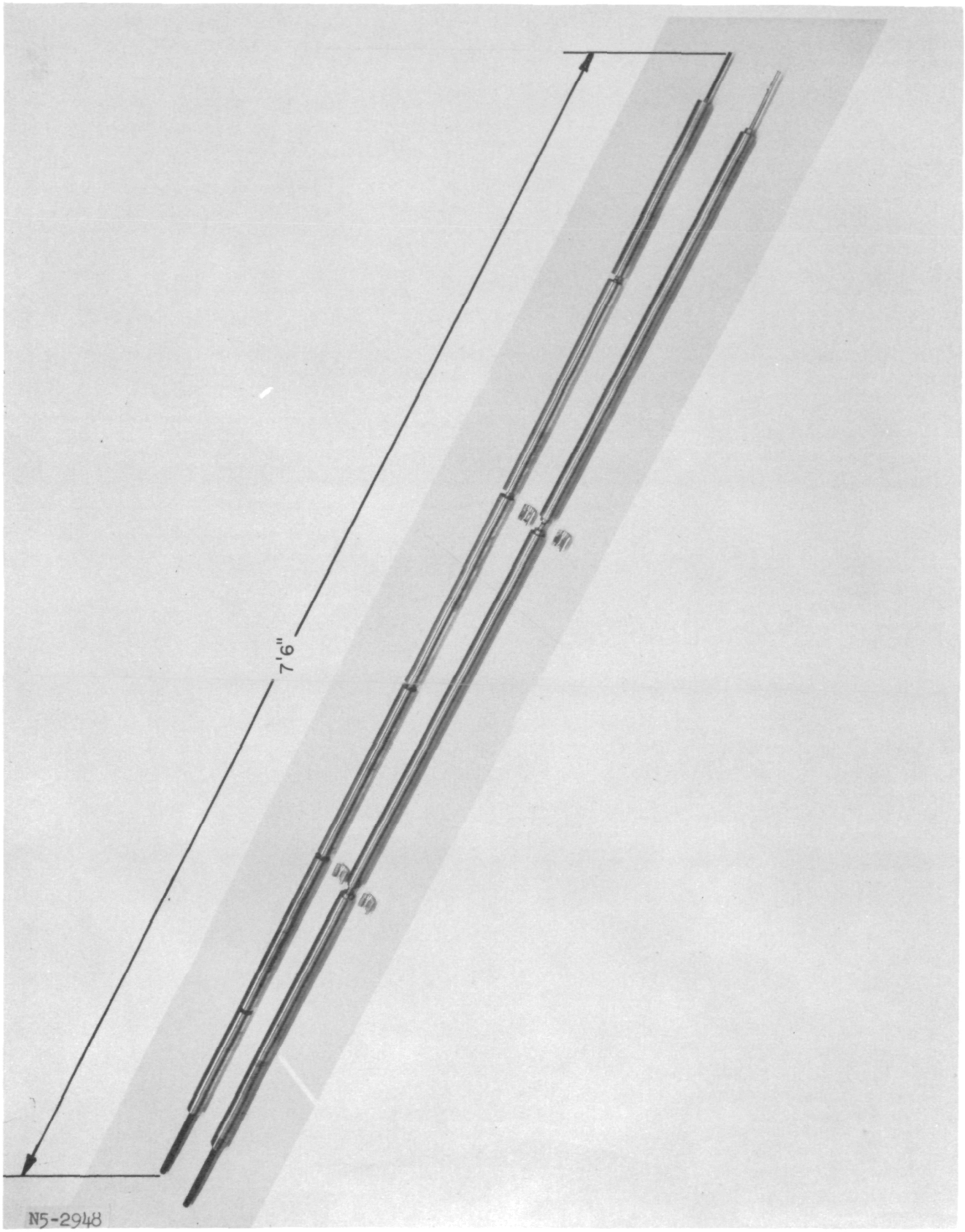

Finished Machined Haynes 25 Tapered Tubes with 0.350-in. Alum. Armor

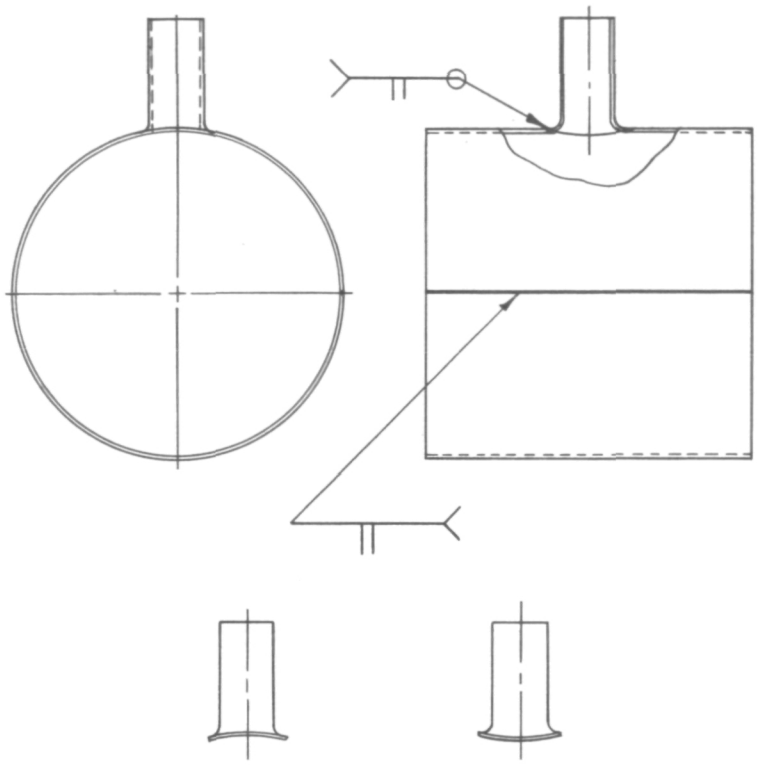

Fig. 15a Flared-Weld Diagram, Tube-to-Vapor Header

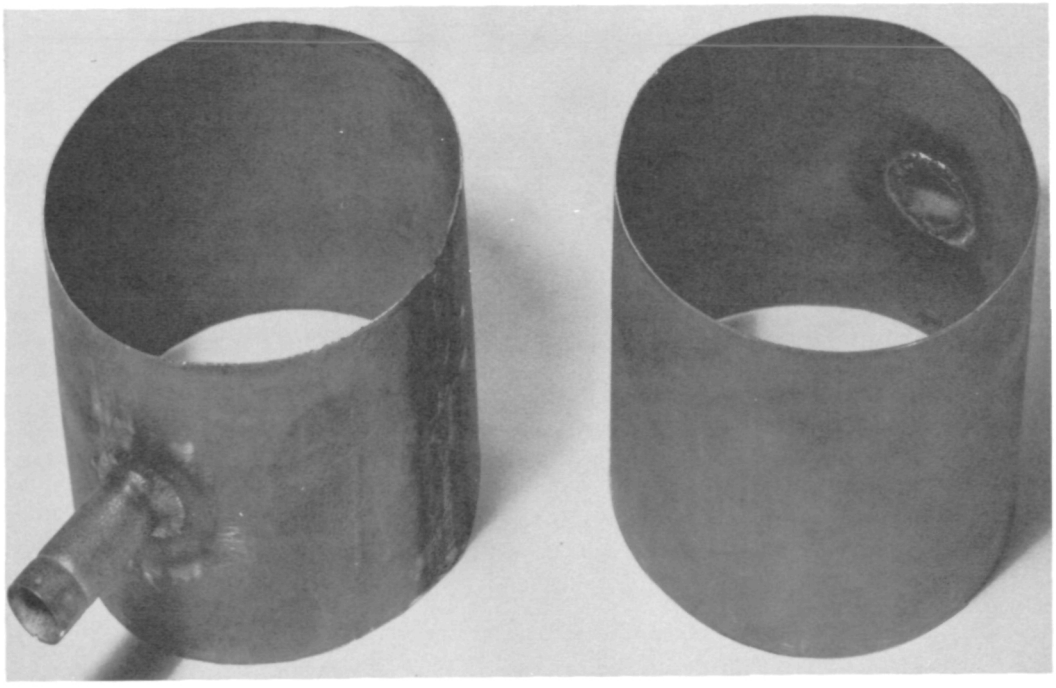

Fig. 15b Tube-to Vapor Header Joint - Flared-Type Weld

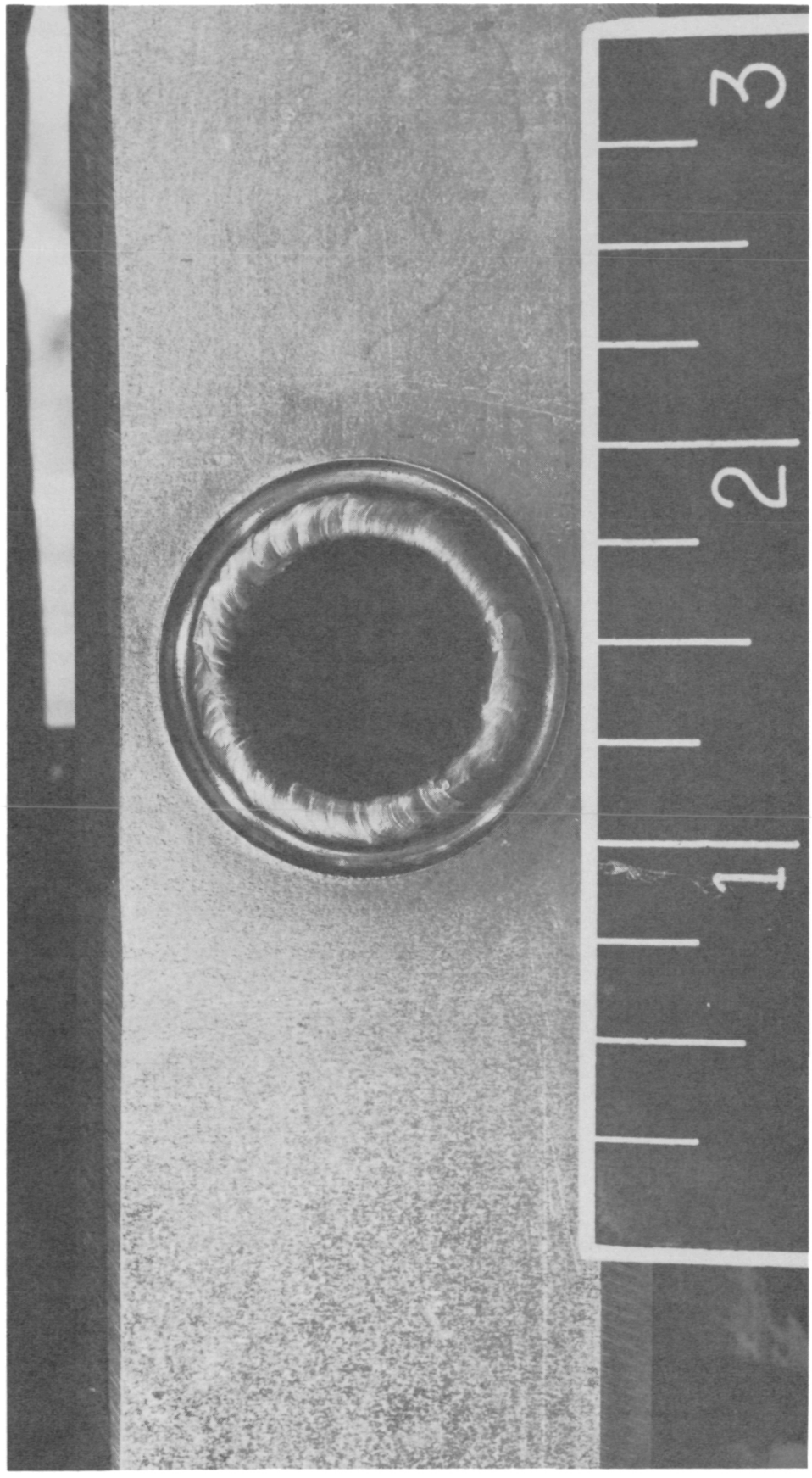

Tube-to-Manifold Plate Weld

Figure 16

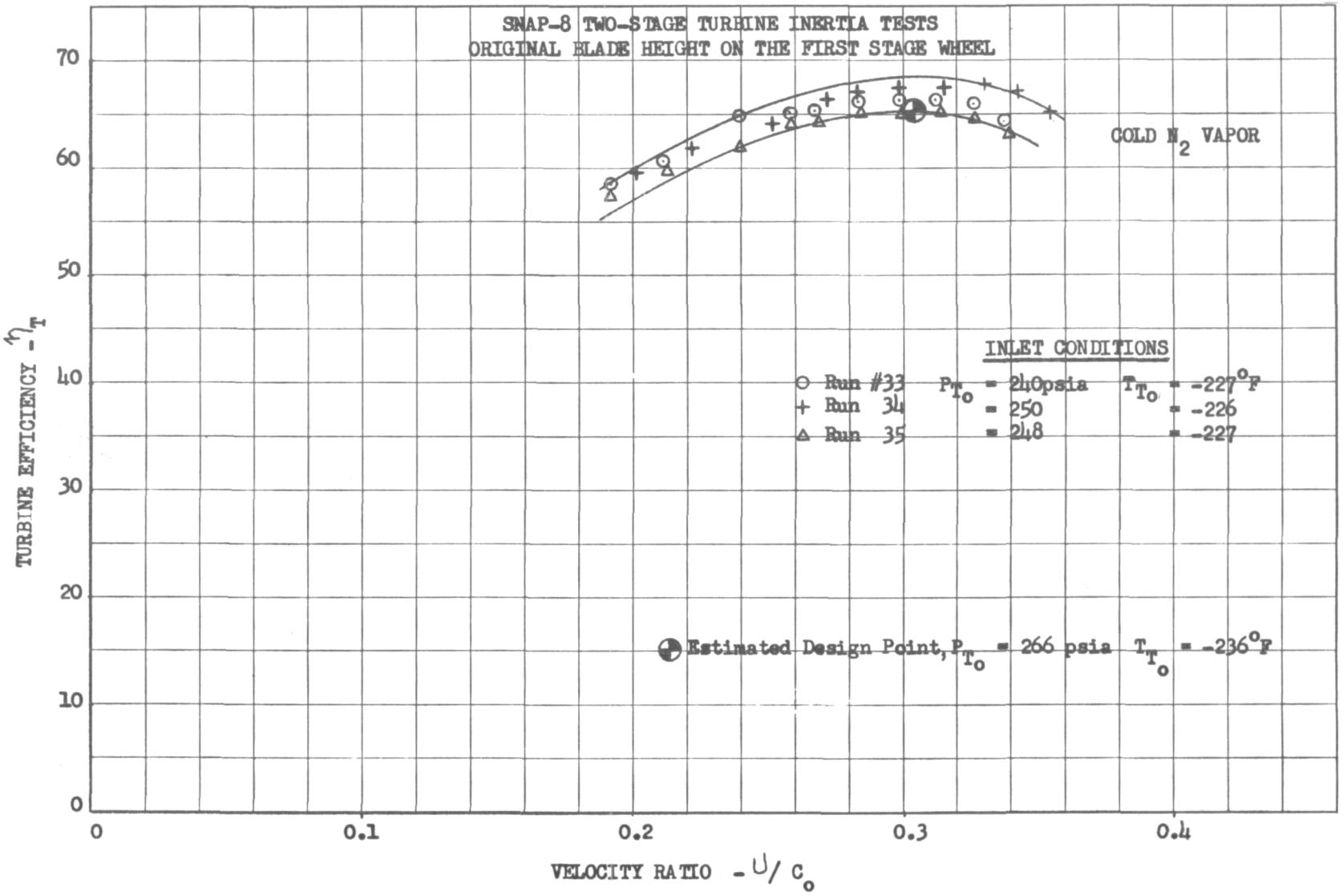
SNAP-8 TWO-STAGE TURBINE INERTIA TESTS
ORIGINAL BLADE HEIGHT ON THE FIRST STAGE WHEEL
COLD N_2 VAPOR
INLET CONDITIONS
○ Run #33 P_{T_o} = 240psia T_{T_o} = -227°F
+ Run 34 = 250 = -226
△ Run 35 = 248 = -227
Estimated Design Point, P_{T_o} = 266 psia T_{T_o} = -236°F
TURBINE EFFICIENCY - η_T
VELOCITY RATIO - U/C_o
0
10
20
30
40
50
60
70
0
0.1
0.2
0.3
0.4

Figure 17

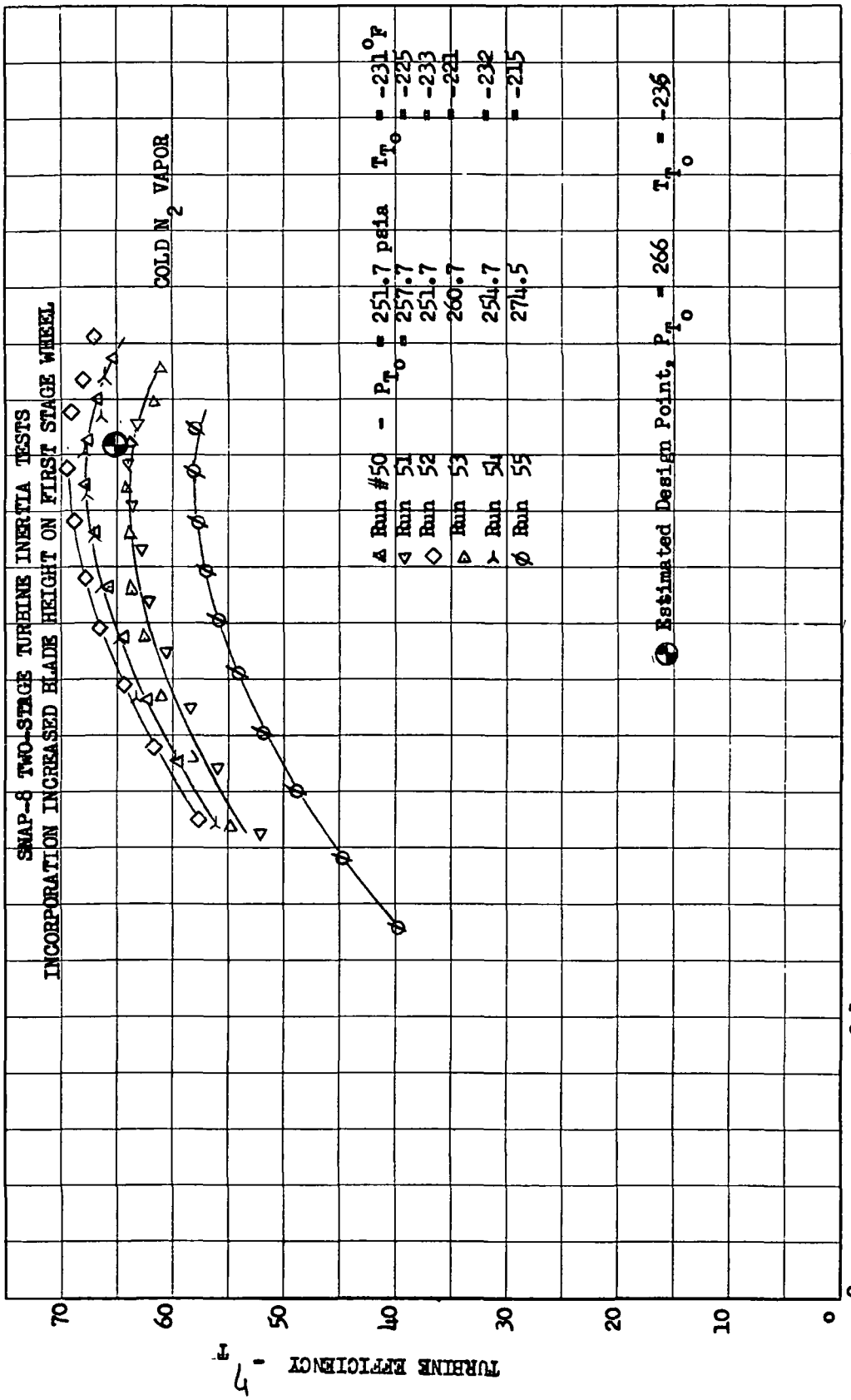
SNAP-8 TWO-STAGE TURBINE INERTIA TESTS
INCORPORATION INCREASED BLADE HEIGHT ON FIRST STAGE WHEEL
COLD N_2 VAPOR
Run #50 - P_{T_o} = 251.7 psia T_{T_o} = -231°F
Run 51 P_{T_o} = 257.7 = -225
Run 52 251.7 = -233
Run 53 260.7 = -221
Run 54 254.7 = -232
Run 55 274.5 = -215
Estimated Design Point, P_{T_o} = 266 T_{T_o} = -236
TURBINE EFFICIENCY - η_T
VELOCITY RATIO - U/C_o
0
10
20
30
40
50
60
70
0.1
0.2
0.3
0.4

Figure 18

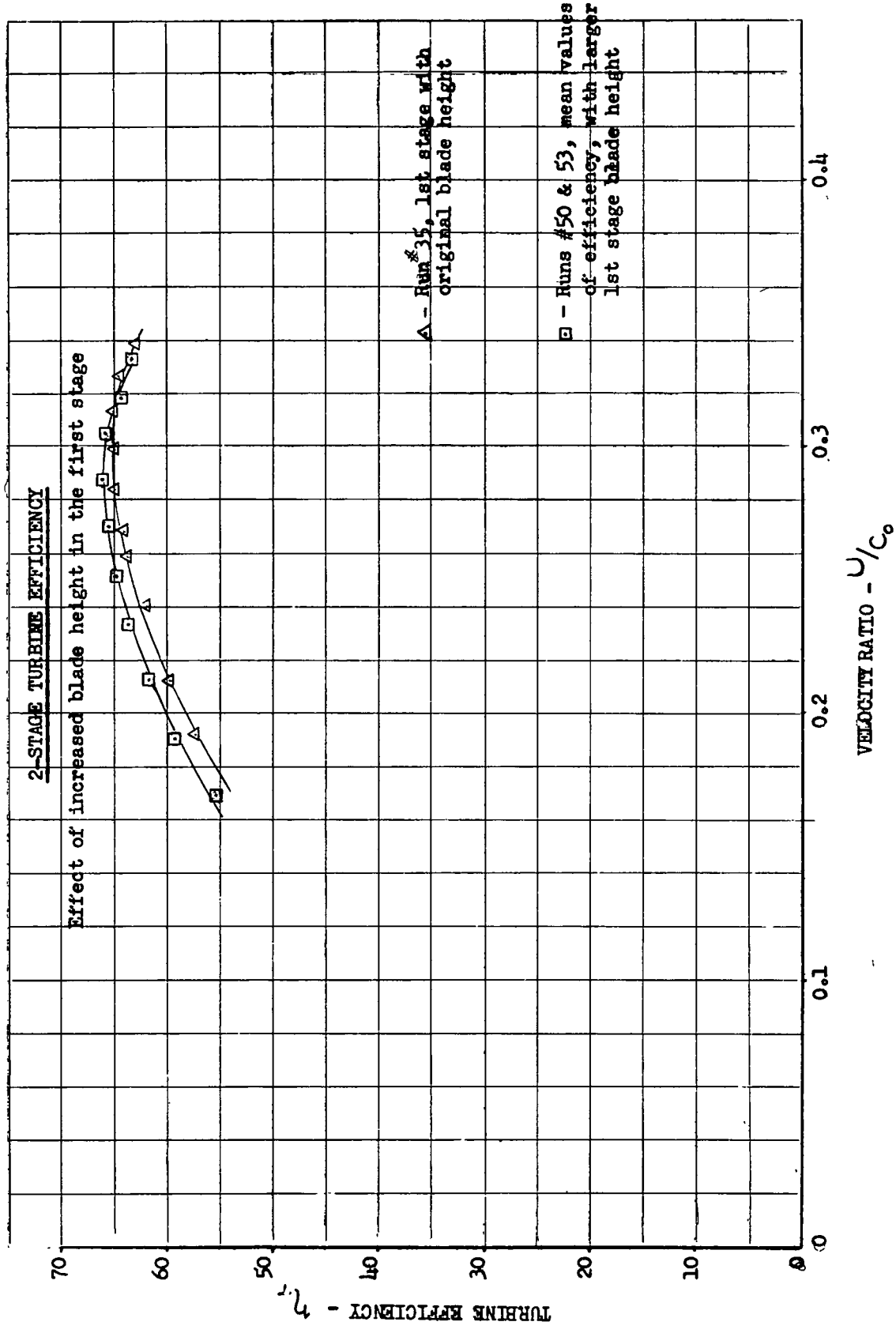
2-STAGE TURBINE EFFICIENCY
Effect of increased blade height in the first stage
Δ - Run #35, 1st stage with original blade height
□ - Runs #50 & 53, mean values of efficiency, with larger 1st stage blade height
TURBINE EFFICIENCY - η_t
VELOCITY RATIO - U/C_o
0
10
20
30
40
50
60
70
0.1
0.2
0.3
0.4

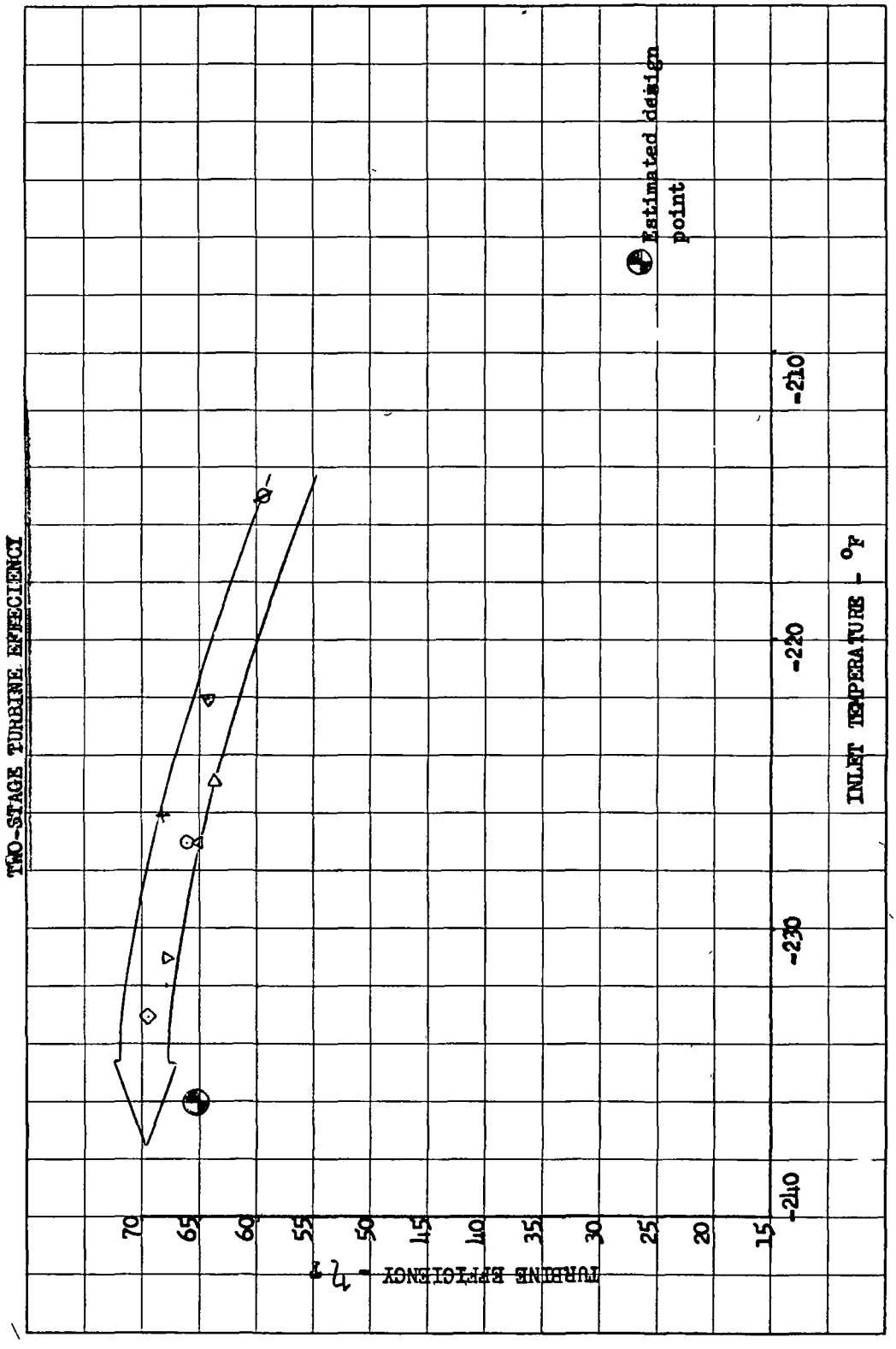
TWO-STAGE TURBINE EFFECIENCY
TURBINE EFFICIENCY - η_T
70
65
60
55
50
45
40
35
30
25
20
15
INLET TEMPERATURE - °F
-210
-220
-230
-240
Estimated design point

Figure 20

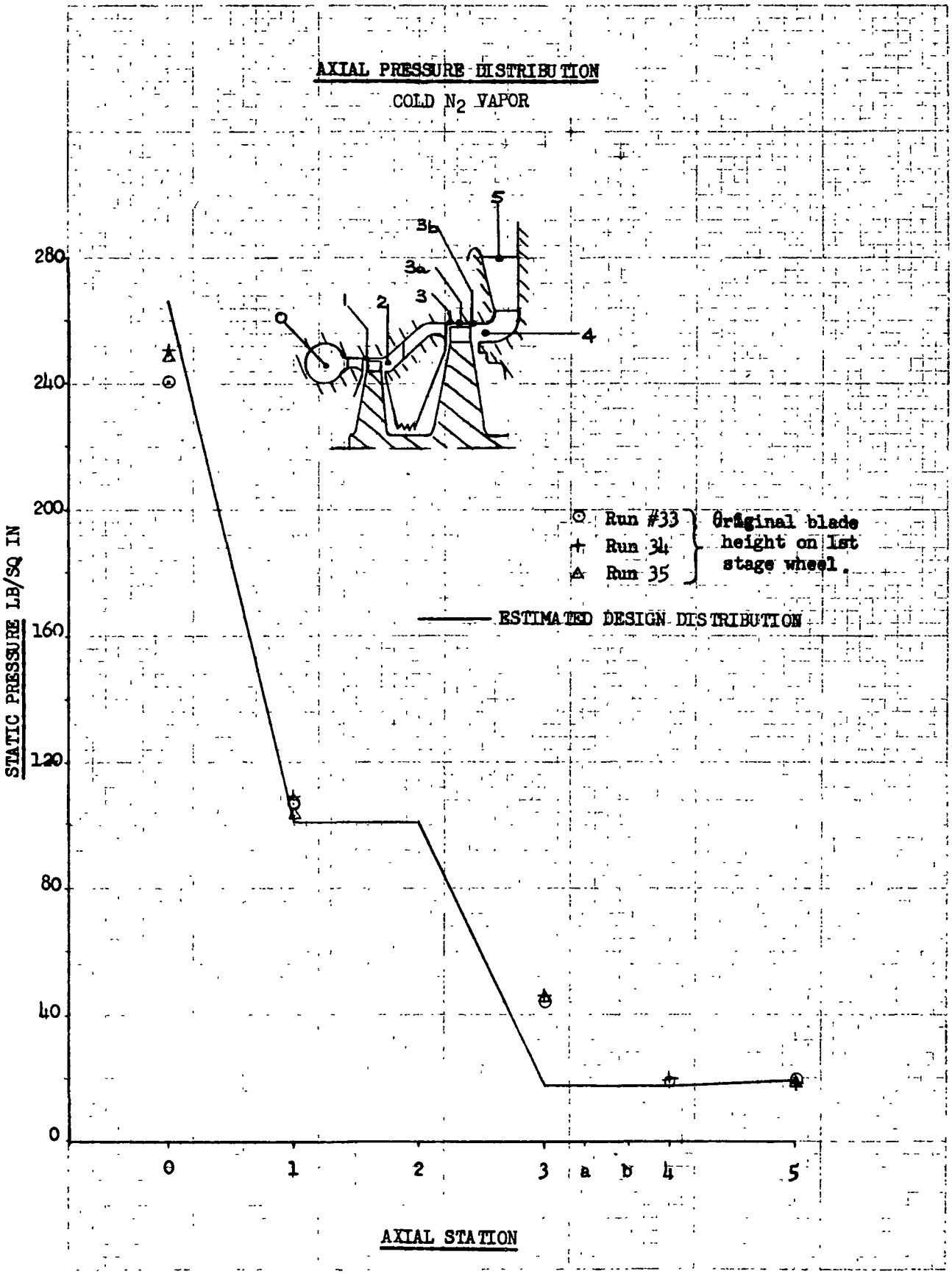
AXIAL PRESSURE DISTRIBUTION
COLD N_2 VAPOR
5
3b
3a
1
2
3
4
280
240
200
160
120
80
40
0
STATIC PRESSURE LB/SQ IN
Run #33
Run 34
Run 35
Original blade height on 1st stage wheel.
ESTIMATED DESIGN DISTRIBUTION
0
1
2
3
a
b
4
5
AXIAL STATION

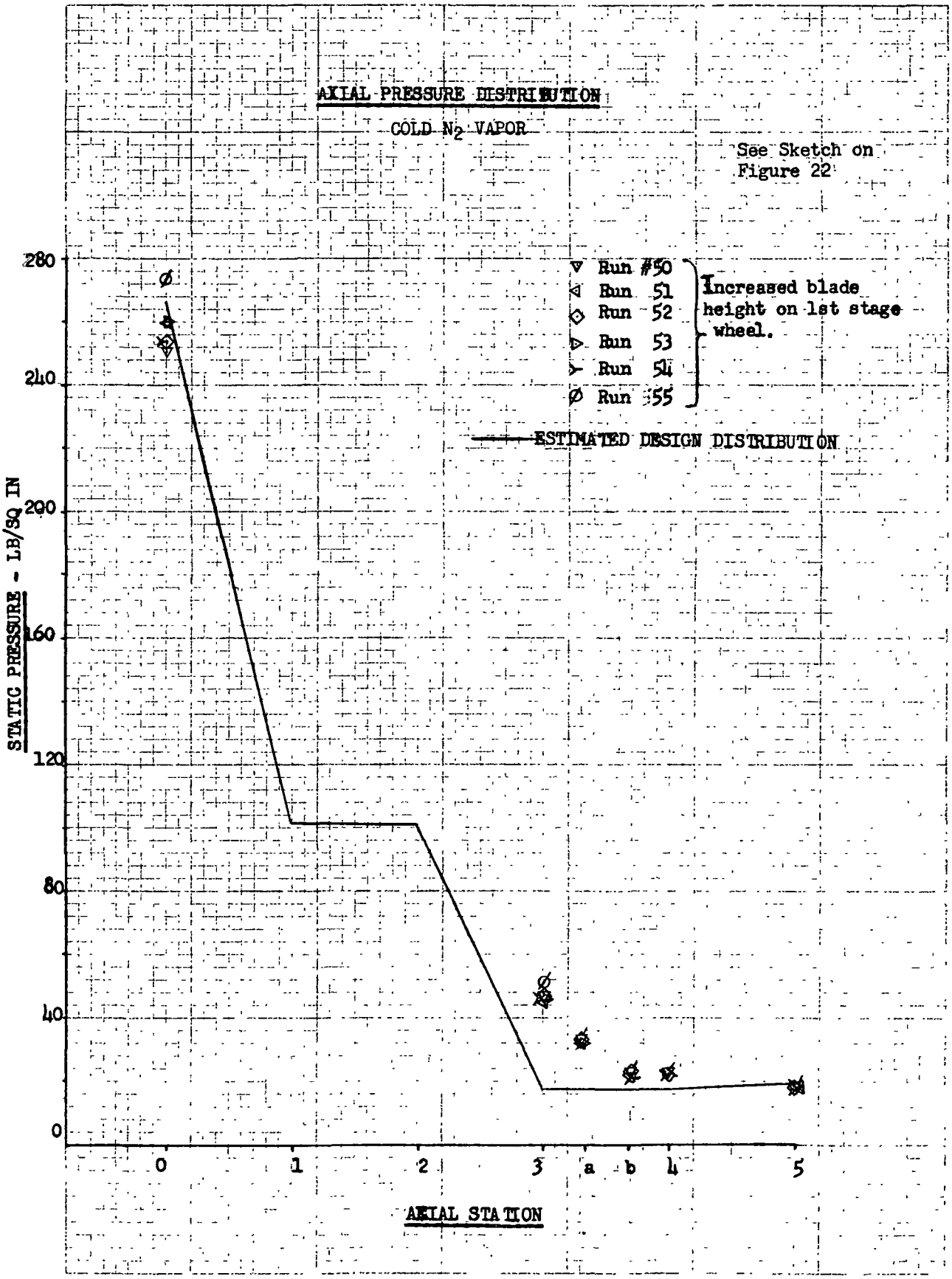
AXIAL PRESSURE DISTRIBUTION
COLD N_2 VAPOR
See Sketch on Figure 22
Run #50
Run 51
Run 52
Run 53
Run 54
Run 55
Increased blade height on 1st stage wheel.
ESTIMATED DESIGN DISTRIBUTION
STATIC PRESSURE - LB/SQ IN
280
240
200
160
120
80
40
0
0
1
2
3
a
b
4
5
AXIAL STATION

UNCLASSIFIED

2-STAGE TURBINE EFFICIENCY

Original Blade Height in First Stage

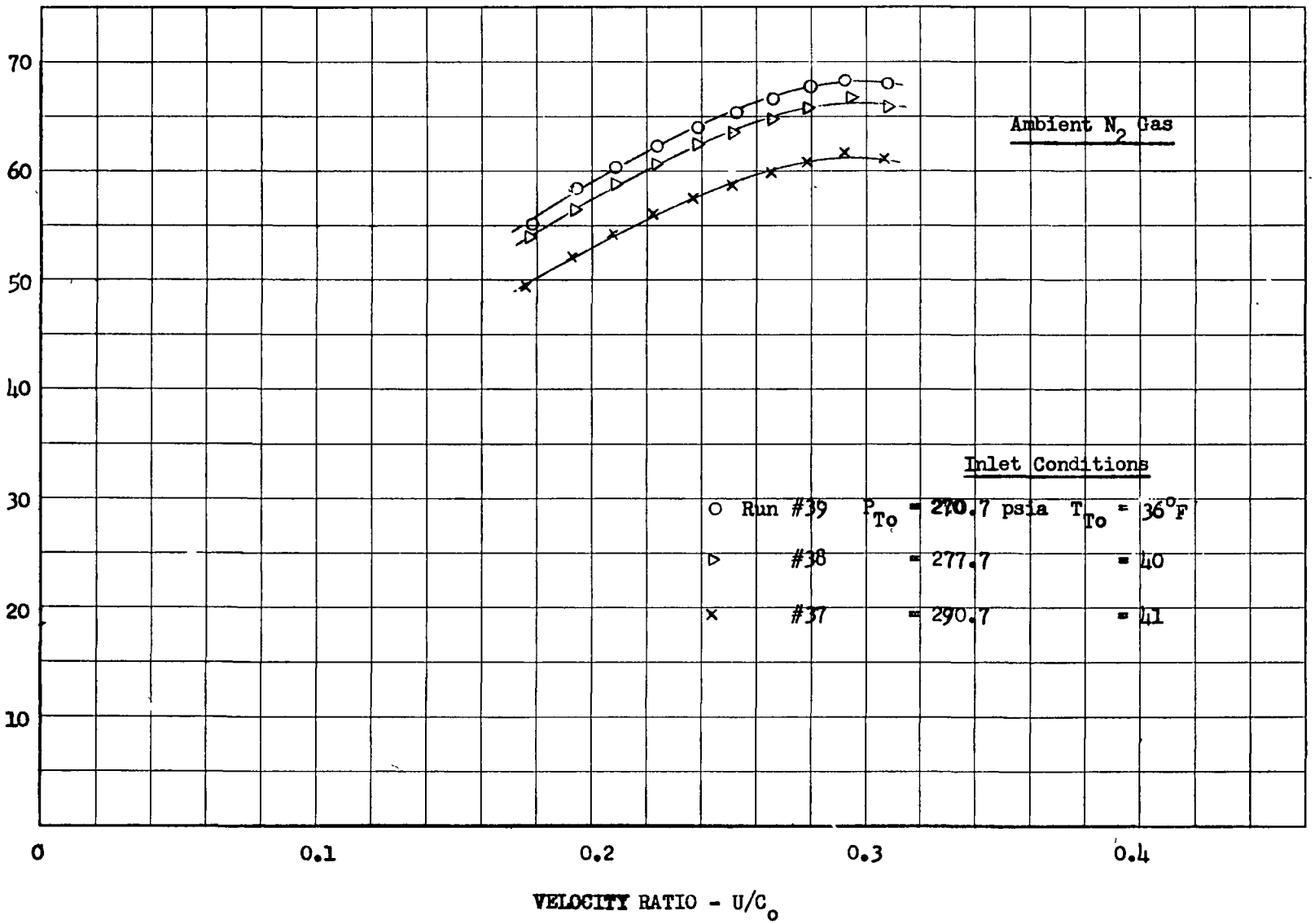

Figure 23

UNCLASSIFIED

2-STAGE TURBINE EFFICIENCY

Effect of increased blade height on first stage

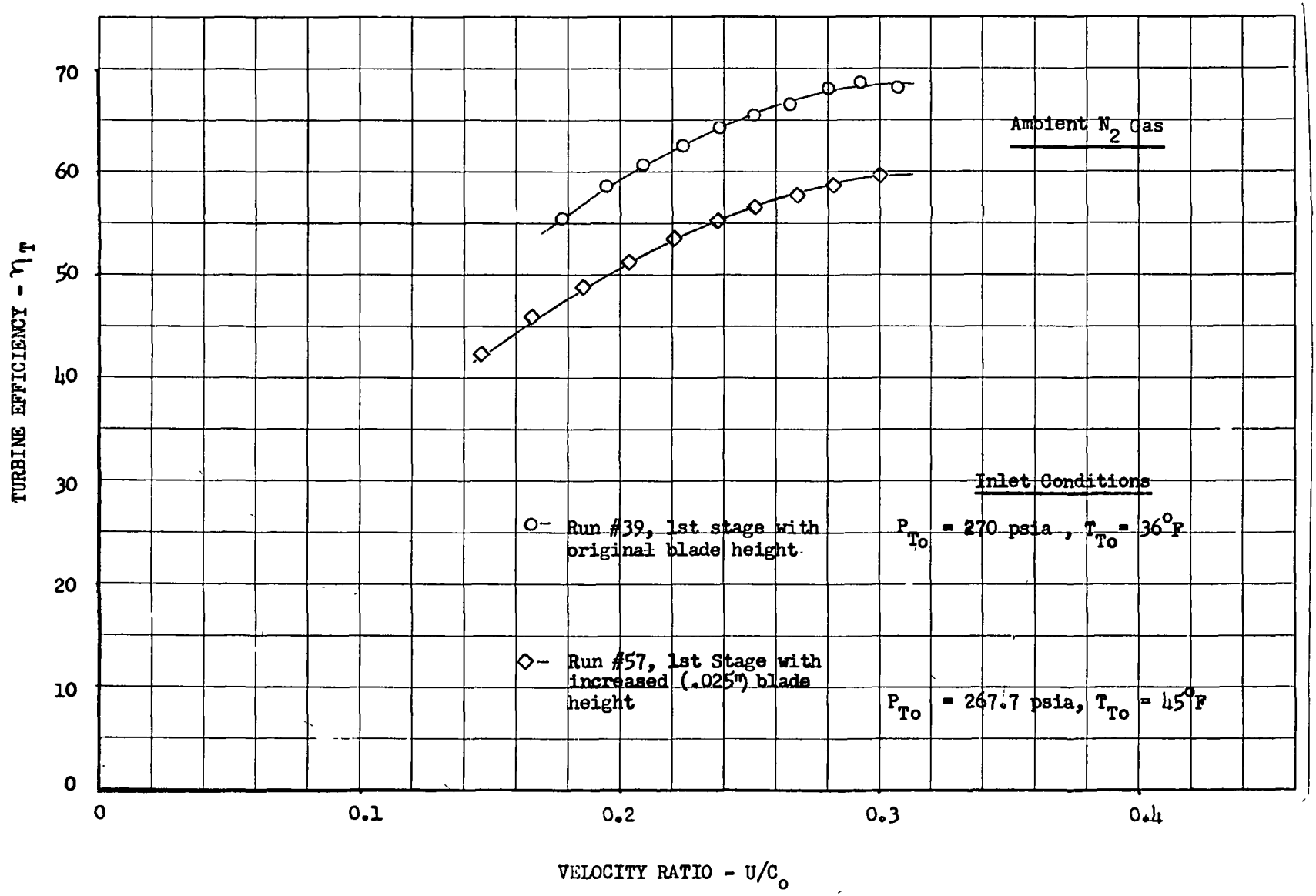

Figure 24

SNAP-8 TWO-STAGE TURBINE INERTIA TESTS

With Increased Blade Height on First Stage Wheel

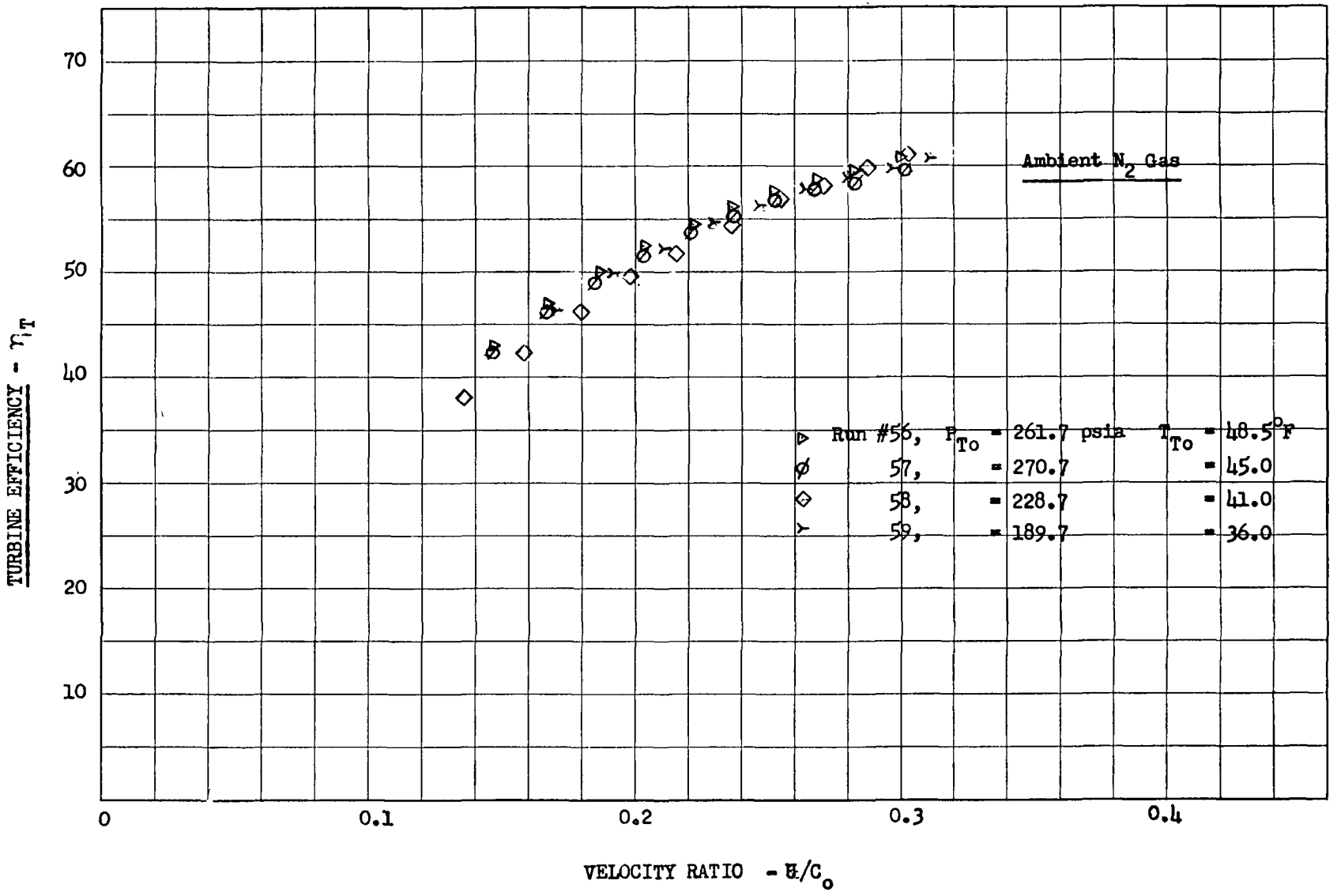

Figure 25

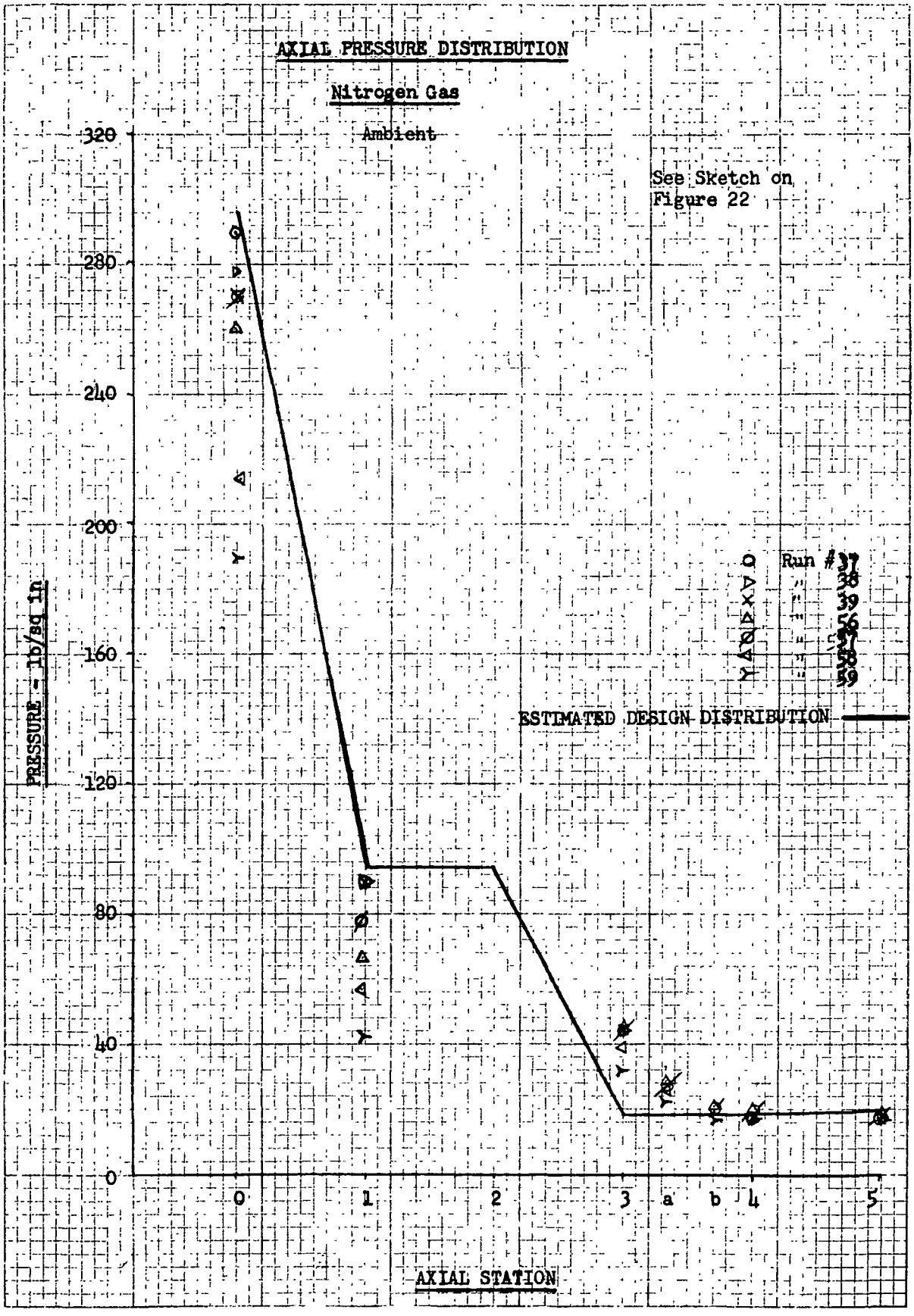
AXIAL PRESSURE DISTRIBUTION
Nitrogen Gas
Ambient
See Sketch on Figure 22
PRESSURE - lb/sq in
320
280
240
200
160
120
80
40
0
Run #37
38
39
56
57
58
59
ESTIMATED DESIGN DISTRIBUTION
0
1
2
3
a
b
4
5
AXIAL STATION

Figure 26

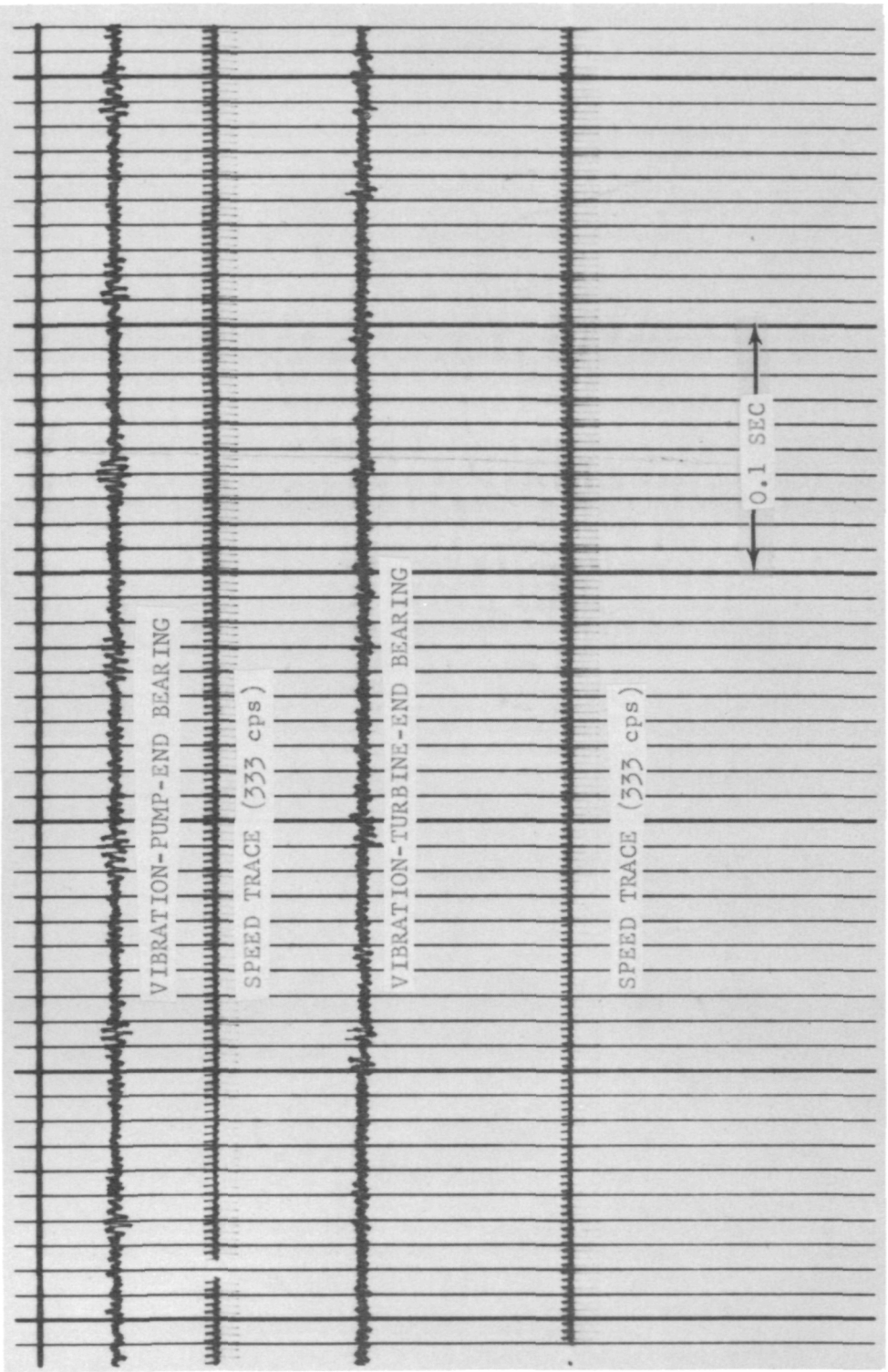

Mercury Bearing Test,
Four-Axial-Groove Bearing - No Evidence
of Half-Frequency Whirl at 20,000 RPM

Figure 27

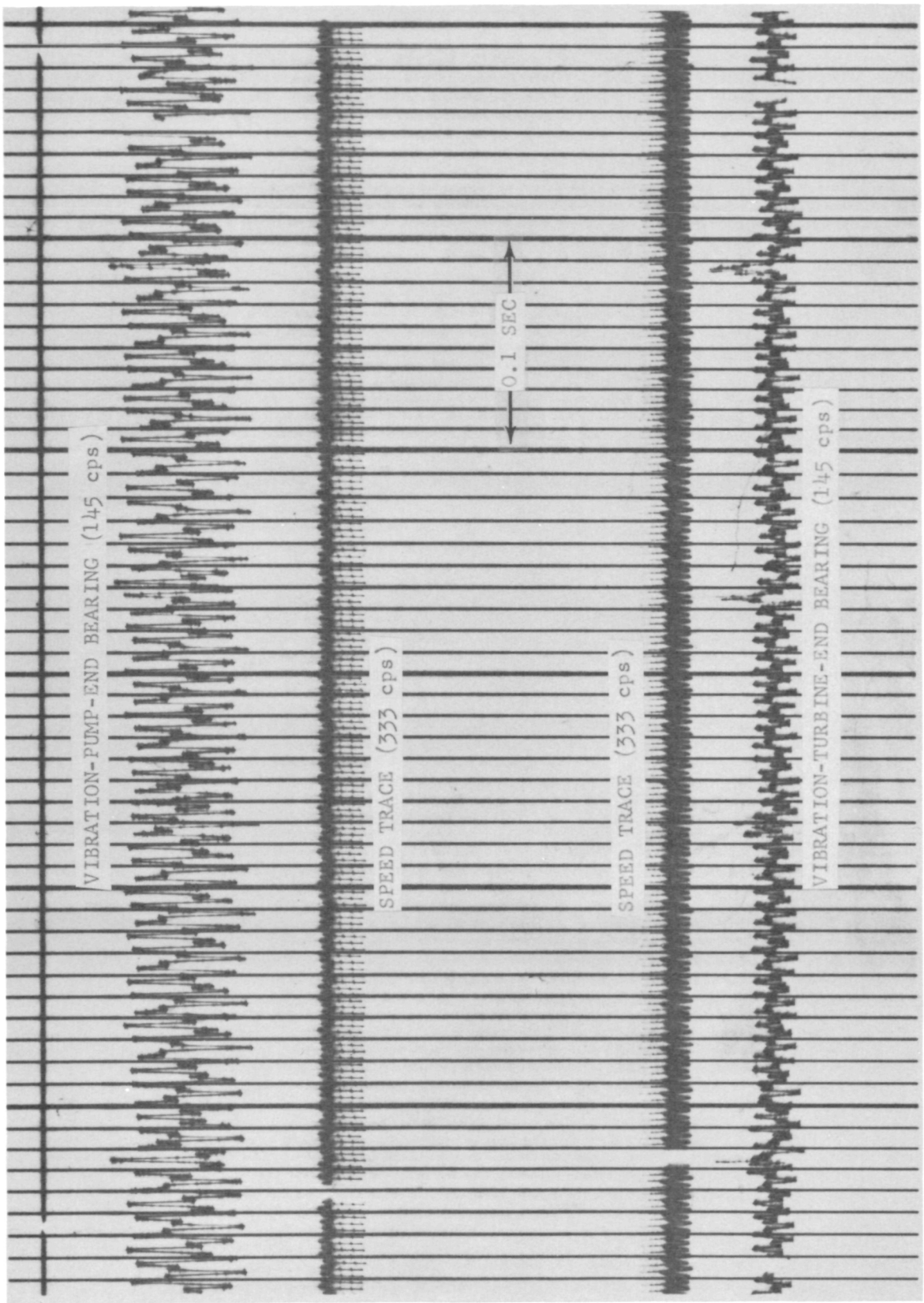

Mercury Bearing Test
Circumferential-Groove Bearing - Half-Frequency
Whirl at 20,000 RPM

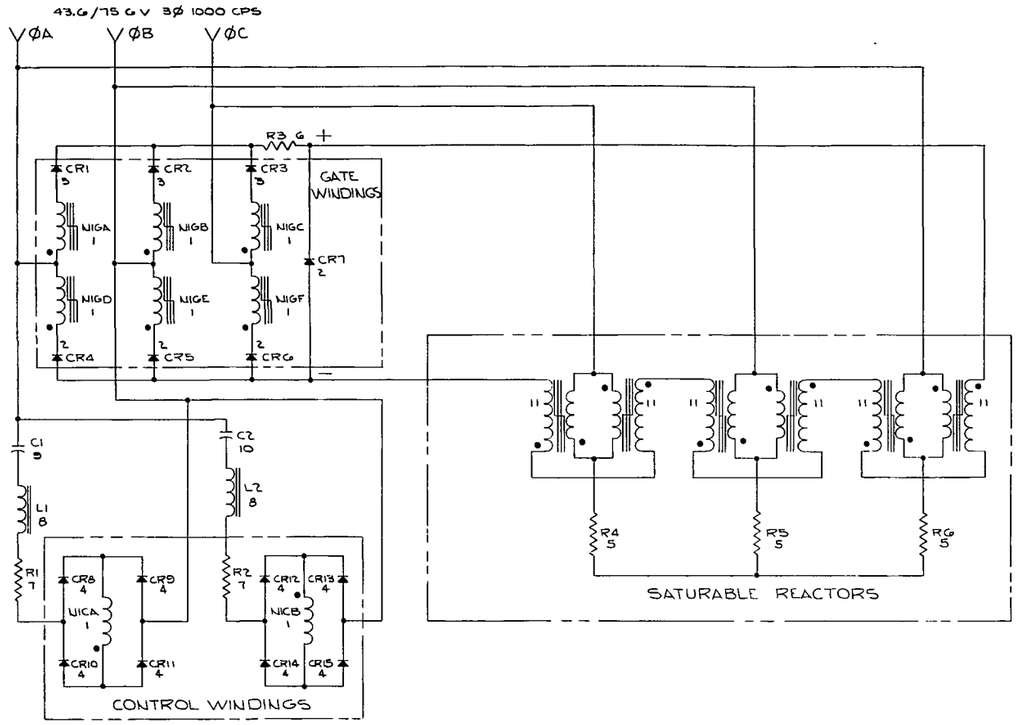

ITEM NO	DESCRIPTION	TYPE OR PART NO	NO REQD
11	SATURABLE REACTORS	079540-1	6
10	CAPACITOR	.018 µF	1
9	CAPACITOR	.033 µF	1
8	INDUCTOR	1.0 H (NOM) 4	2
7	RESISTOR	800 Ω (NOM) 4	2
6	RESISTOR	3	1
5	RESISTOR	3	3
4	DIODE	IN443	8
3	DIODE	IN1202A	3
2	DIODE	IN1202RA	4
1	MAG AMP	079548-1	1

EQUIPMENT LIST

AEROJET	GOVERNMENT

APPLICABLE SPECIFICATIONS

REVISIONS				
SYM	DESCRIPTION	DATE	BY	APPR'D

079556

COPY

PART NO.	DESCRIPTION	MATERIAL	SPECIFICATION	ZONE	QTY REQD PER ASSY
-1	SEE EQUIPMENT LIST	-	-		-

LIST OF MATERIALS

4 TUNING & GAIN ADJUSTMENTS TO BE MADE AT ASSY
3 VALUES OF THESE RESISTORS TO BE DETERMINED BY COGNIZANT ENG
2 ELEC DESIG PER MIL-STD-16
1 ELEC SYMBOLS PER MIL-STD-15.

NOTES

UNLESS OTHERWISE SPECIFIED
DIMENSIONS ARE IN INCHES
DECIMAL TOLERANCE
ANGULAR TOLERANCE
SURFACE ROUGHNESS PER MIL-STD-10
DO NOT SCALE DRAWING

DRAWN LIPENNY 7/8/61
CHECK
DESIGN
PROJECT
TREATMENT
FINISH

TITLE: ELEC. SCHEMATIC, SPEED CONTROLLER (NNS-1)

SIMILAR TO
RELEASE DATE 10-12-61
SCALE
CALC WT
ACT WT
DWG SIZE D
DWG TYPE O

Aerojet-General CORPORATION

DWG NO. 079556
CODE IDENT NO. 70143
SHEET

PART DASH NO.	NEXT	FINAL	QTY REQD PER ASSY	NEXT ASSY	MODEL NO.
				APPLICATION	

UNCLASSIFIED

REVISIONS					
SYM	DESCRIPTION	DATE	BY	APPR'D	
A	DWG REVISED IN ACCORDANCE WITH E O 522586 E O 520385 INCORPORATED IN PART ONLY	11-15-61	HAP	Edgar 11 20 61	

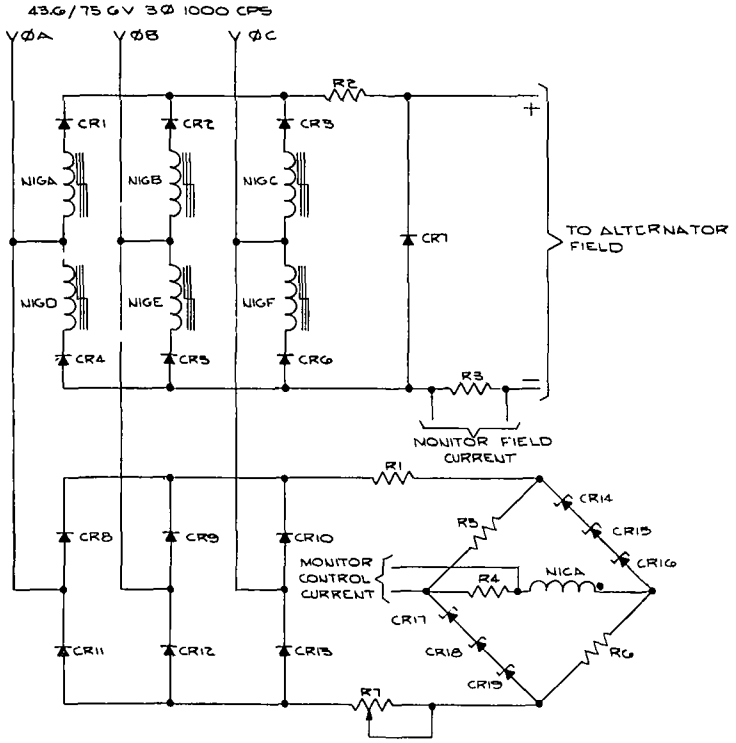

AEROJET	GOVERNMENT
APPLICABLE SPECIFICATIONS	

079553

COPY___ SYM A

NOTES
1. FOR REF SEE ELEC COORDINATION DIAG 081482
2. FOR WIRING DIAG SEE 079545
3. ELEC DESIGNATIONS PER MIL-STD-16
4. ELEC SYMBOLS PER MIL-STD-15
5. △ REMOVED
6. △ REMOVED

[redacted]

00-087-004

PART DASH NO.	NEXT QTY REQD PER ASSY	FINAL QTY REQD PER ASSY	NEXT ASSY APPLICATION	MODEL NO

QTY REQD PER ASSY	PART NO.	DESCRIPTION	MATERIAL	SPECIFICATION	ZONE
		LIST OF MATERIALS			

UNLESS OTHERWISE SPECIFIED
DIMENSIONS ARE IN INCHES
DECIMAL TOLERANCE ANGULAR TOLERANCE
XX ± .03 =
XXX ± .010 —
SURFACE ROUGHNESS PER MIL-STD-10
DO NOT SCALE DRAWING
TREATMENT
FINISH

DRAWN H. PENNY 10 5 61
CHECK
DESIGN N WALDSCHMIDT 10 9-61
PROJECT W D DANIELS 10 11-61

TITLE ELEC. SCHEMATIC, VOLT. REGULATOR (NNS-1)

Aerojet-General CORPORATION

SIMILAR TO | SCALE | CALC WT | ACT WT | DWG SIZE C | DWG TYPE O

DWG NO 079553

RELEASE DATE 10 [illegible] 61

CODE IDENT NO 70143 | SHEET

UNCLASSIFIED

Figure 30

Report No. 0390-04-6

UNCLASSIFIED

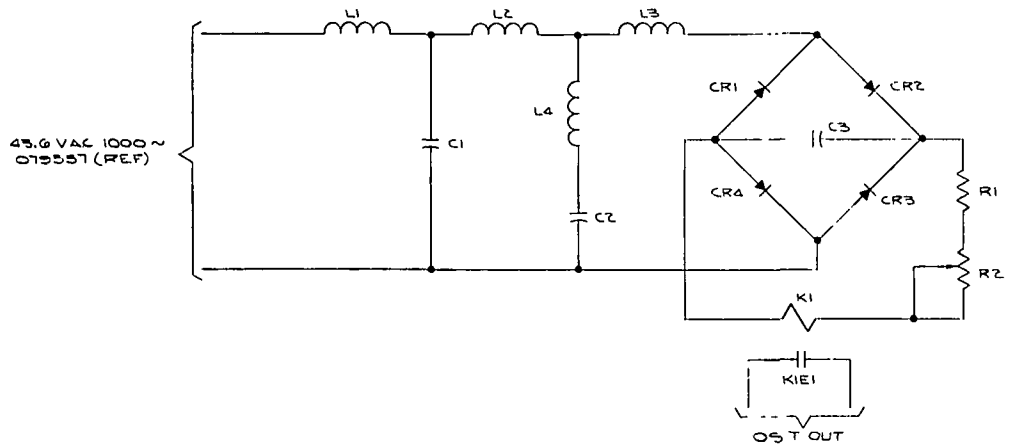

REVISIONS				
SYM	DESCRIPTION	DATE	BY	APPR'D

074659
COPY___ SYM

AEROJET	GOVERNMENT
APPLICABLE SPECIFICATIONS	

QTY REQD PER ASSY	PART NO.	DESCRIPTION	MATERIAL	SPECIFICATION	ZONE
		LIST OF MATERIALS			

NOTES:
6 FOR INSTL ON EDDY CURRENT BRAKE SEE 079544
5 R2 ADJUSTED FOR OVERSPEED TRIP POINT
4 FOR WIRING DIAG SEE 079575.
3 K1 SHOWN IN ENERGIZED POSITION
2 ELEC DESIGNATIONS PER MIL-STD-16
1 ELEC SYMBOLS PER MIL-STD-15.

PART DASH NO.	NEXT ASSY	FINAL QTY REQD PER ASSY	NEXT ASSY	MODEL NO.
			APPLICATION	

UNLESS OTHERWISE SPECIFIED
DIMENSIONS ARE IN INCHES
DECIMAL TOLERANCE .XX ± .03 .XXX ± .010
ANGULAR TOLERANCE ± - —
SURFACE ROUGHNESS PER MIL-STD-10
DO NOT SCALE DRAWING
TREATMENT
FINISH

DRAWN H. PENNY 5 Bec 61
CHECK
DESIGN
PROJECT

TITLE: ELEC. SCHEMATIC, OVER SPEED TRIP FILTER

SIMILAR TO
RELEASE DATE
SCALE
CALC WT
ACT WT
DWG SIZE C
DWG TYPE 0

Aerojet-General CORPORATION

DWG NO. 074659
CODE IDENT NO. 70143
SHEET

08-067-004

UNCLASSIFIED

Report No. 0390-04-6

Figure 31

UNCLASSIFIED

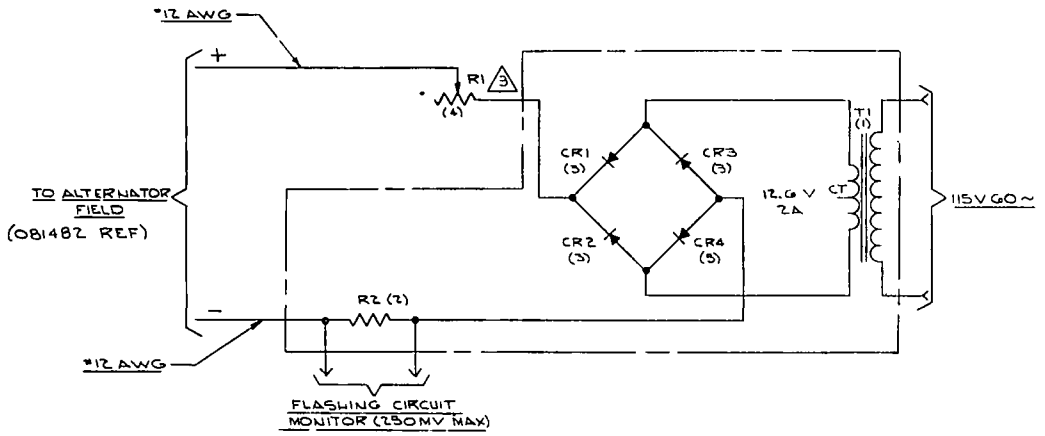

ITEM NO	DESCRIPTION	TYPE OR PART NO	NO REQD
4	POTENTIOMETER	16 Ω, 100W	1
3	DIODE	UT262	4
2	RESISTOR	RS5 .1Ω	1
1	TRANSFORMER	P-8130	1

EQUIPMENT LIST

AEROJET	GOVERNMENT

APPLICABLE SPECIFICATIONS

079573

COPY ____ SYM

QTY REQD PER ASSY	PART NO	DESCRIPTION	MATERIAL	SPECIFICATION	ZONE
		-	-		
		-	-		

LIST OF MATERIALS

UNLESS OTHERWISE SPECIFIED
DIMENSIONS ARE IN INCHES
DECIMAL TOLERANCE ANGULAR TOLERANCE
XX ± .03 ± —
XXX ± .010
SURFACE ROUGHNESS PER MIL-STD-10
DO NOT SCALE DRAWING

DRAWN H PENNY 10-15-64
CHECK
DESIGN
PROJECT

TITLE
ELEC. SCHEMATIC,
FLASHING CIRCUIT

Aerojet-General CORPORATION

SIMILAR TO
RELEASE DATE
SCALE NONE
CALC WT
ACT WT
DWG SIZE C
DWG TYPE 0
DWG NO. 079573
CODE IDENT NO. 70143
SHEET

PART DASH NO.	NEXT	FINAL	NEXT ASSY	MODEL NO.
	QTY REQD PER ASSY		APPLICATION	

TREATMENT
FINISH

△3 THIS POT. FOR REF ONLY, TO BE CONNECTED EXTERNALLY
2 ELEC DESIGNATIONS PER MIL-STD-16
1 ELEC SYMBOLS PER MIL-STD-15

NOTES [redacted]

00-067-004

UNCLASSIFIED

Report No. 0390-04-6

Figure 32

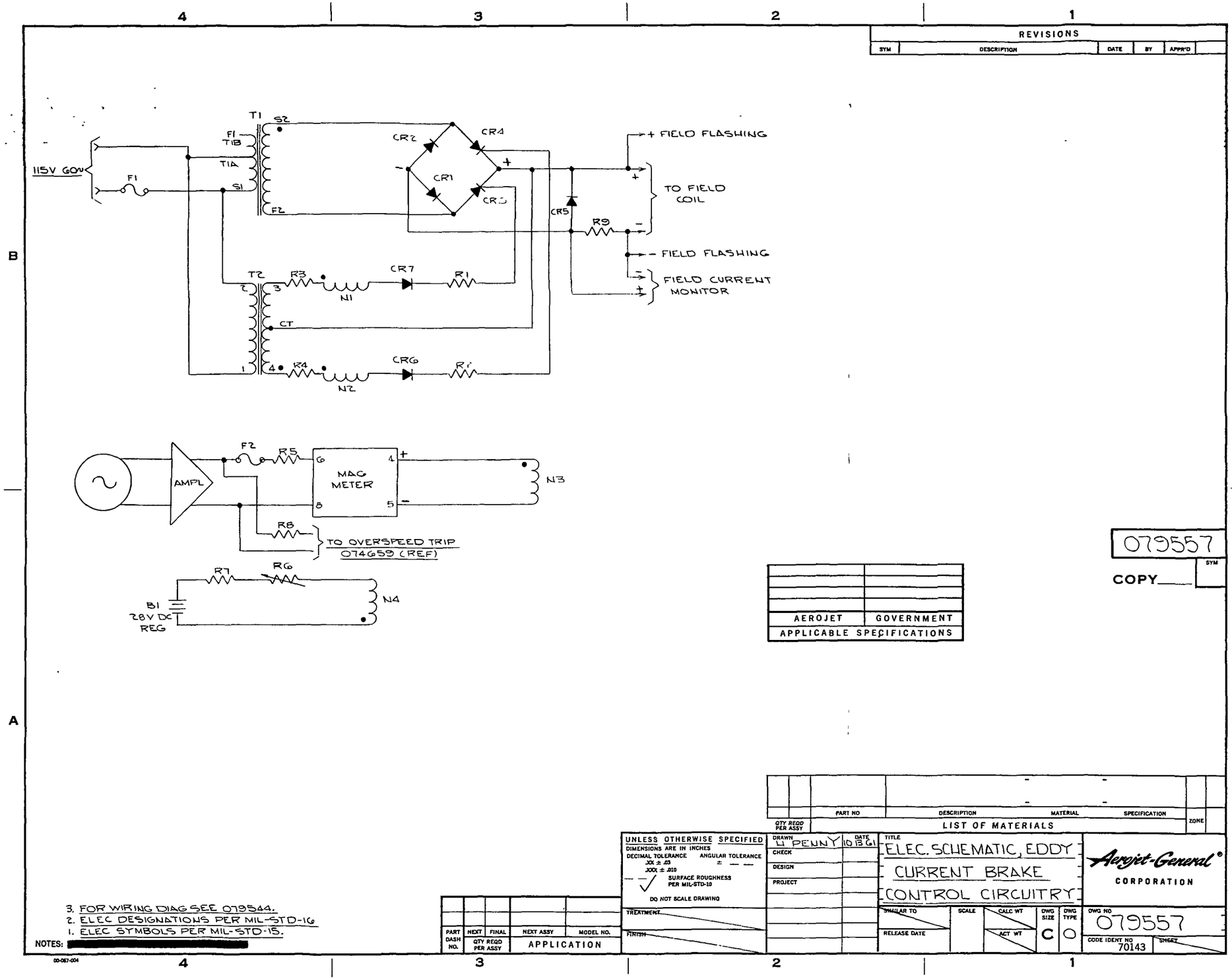

UNCLASSIFIED

Figure 33

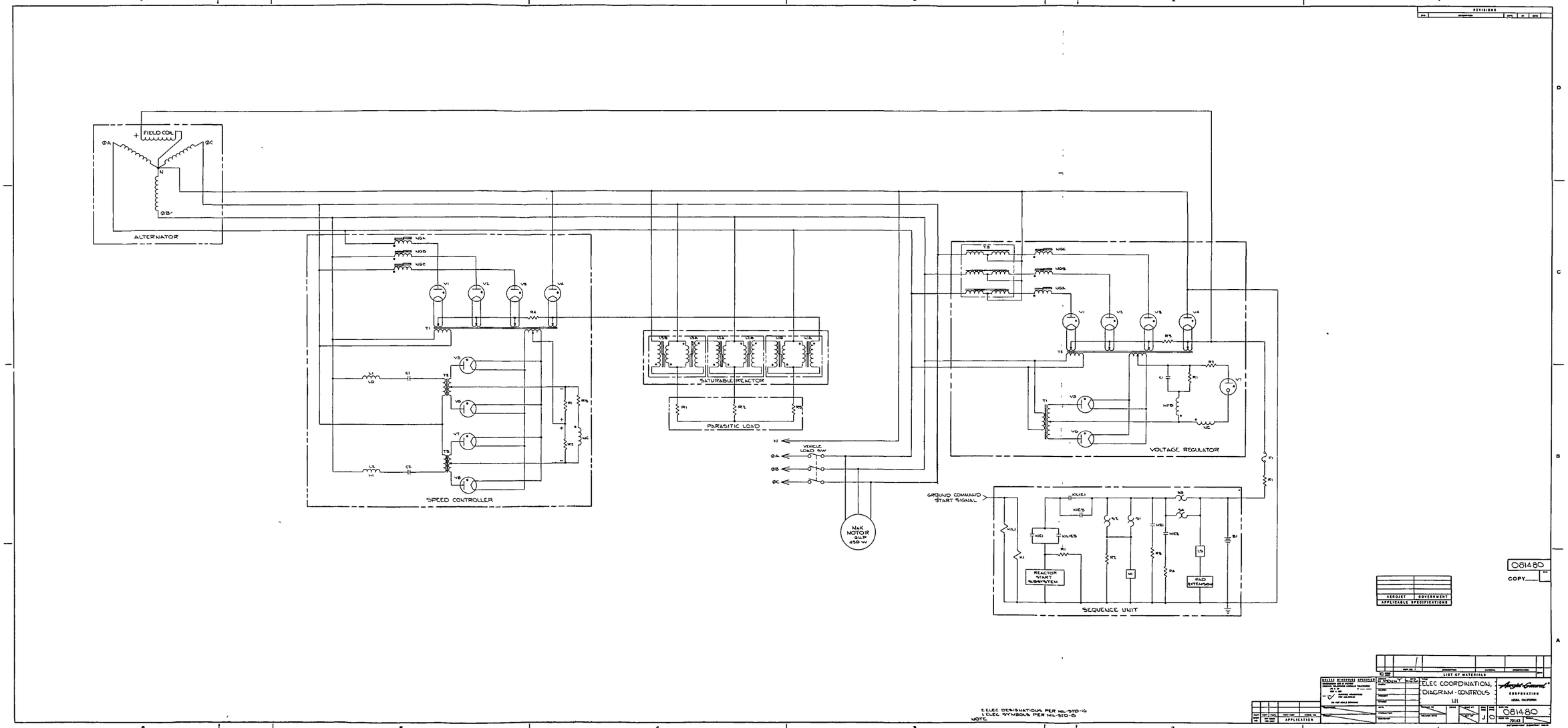
ALTERNATOR
FIELD COIL
ØA
ØB
ØC
N
SPEED CONTROLLER
SATURABLE REACTOR
PARASITIC LOAD
VOLTAGE REGULATOR
VEHICLE LOAD SW
N
ØA
ØB
ØC
NaK MOTOR 6LM 450 W
GROUND COMMAND START SIGNAL
REACTOR START SUBSYSTEM
SEQUENCE UNIT
NOTE
1. ELEC DESIGNATIONS PER MIL-STD-16
2. ELEC SYMBOLS PER MIL-STD-15
REVISIONS
LIST OF MATERIALS
ELEC COORDINATION, DIAGRAM - CONTROLS
Aerojet General CORPORATION AZUSA, CALIFORNIA
0814 80
SIZE J
SCALE NONE
SHEET 1
0814 80
COPY
AEROJET GOVERNMENT
APPLICABLE SPECIFICATIONS

Figure 34

LOOP SECTIONS REMOVED

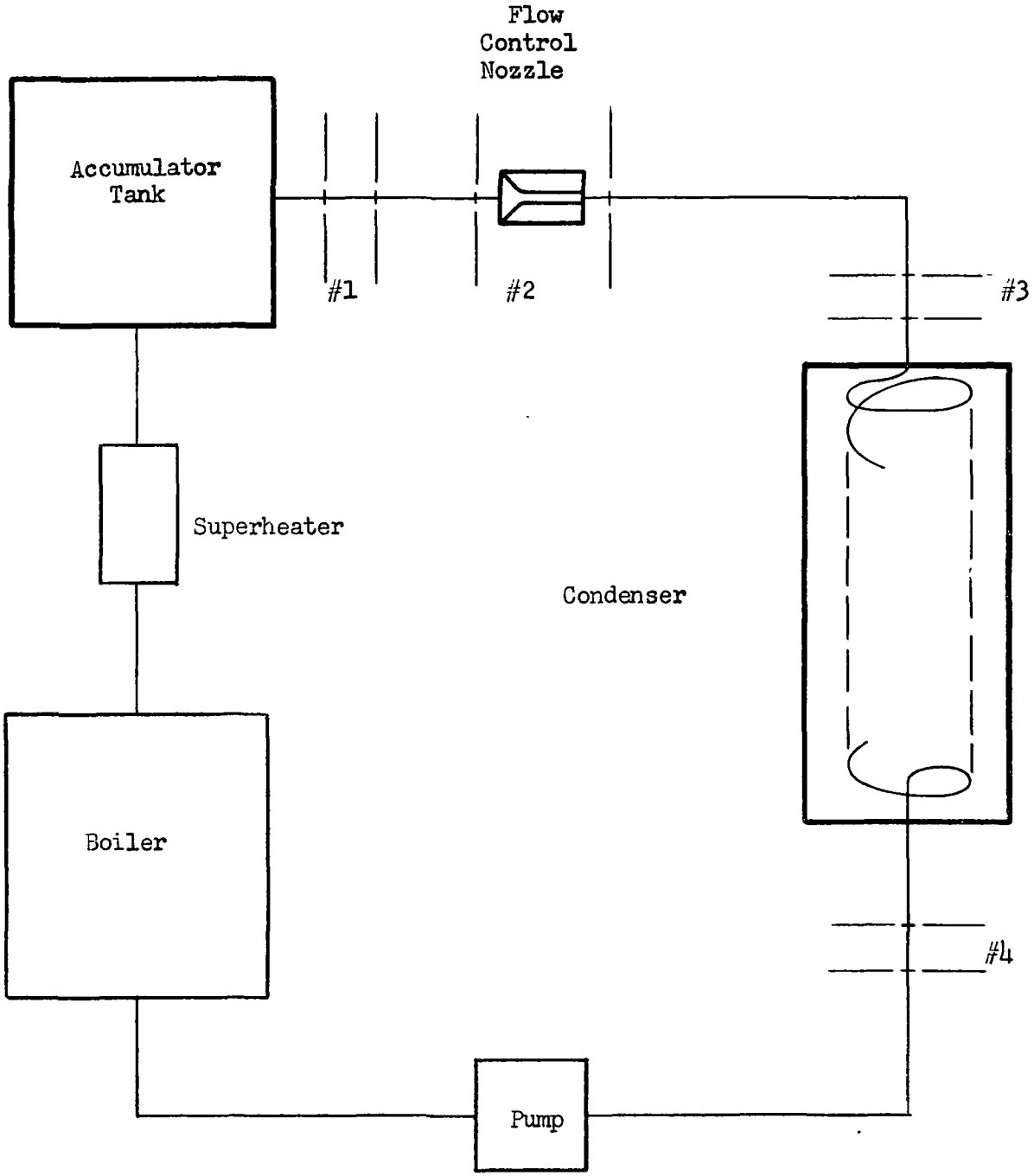

Figure 35

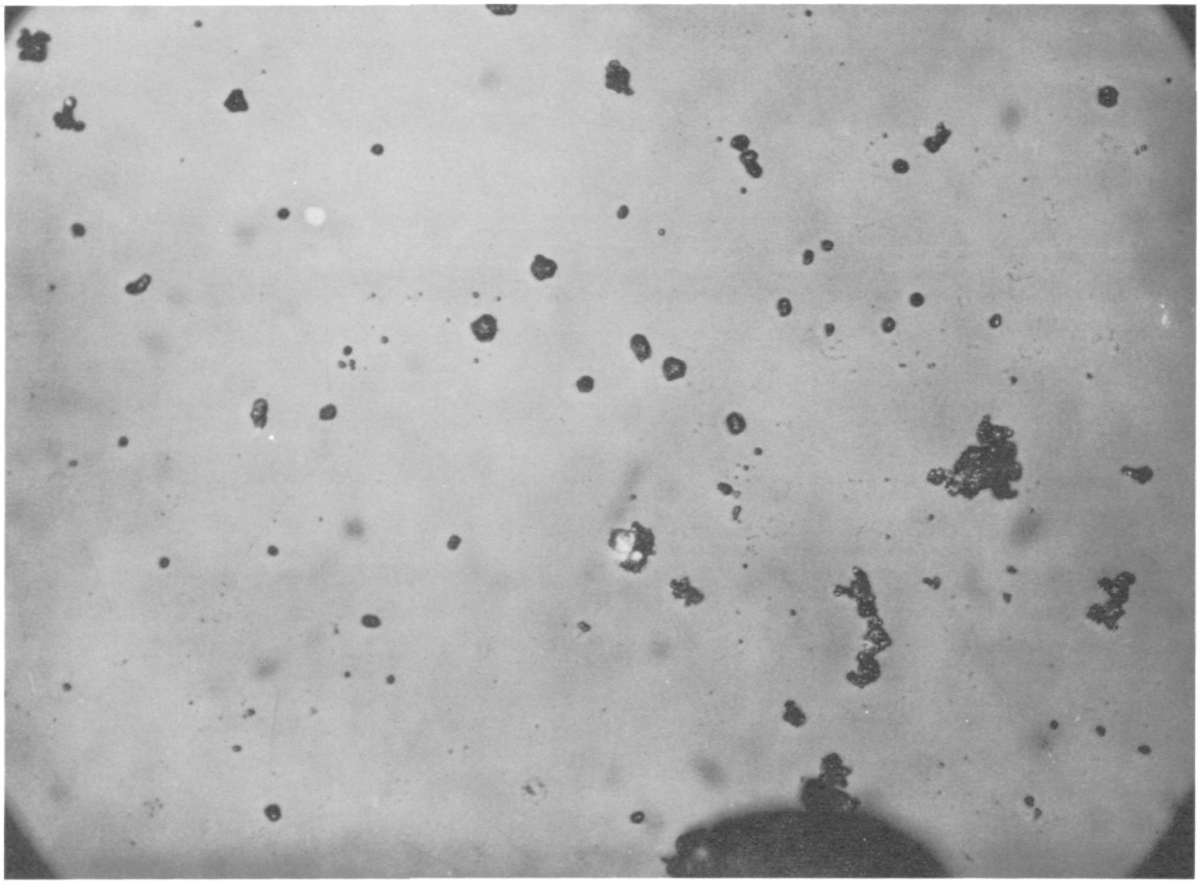

Sample A - Condenser Outlet
(Magnified 1000x)

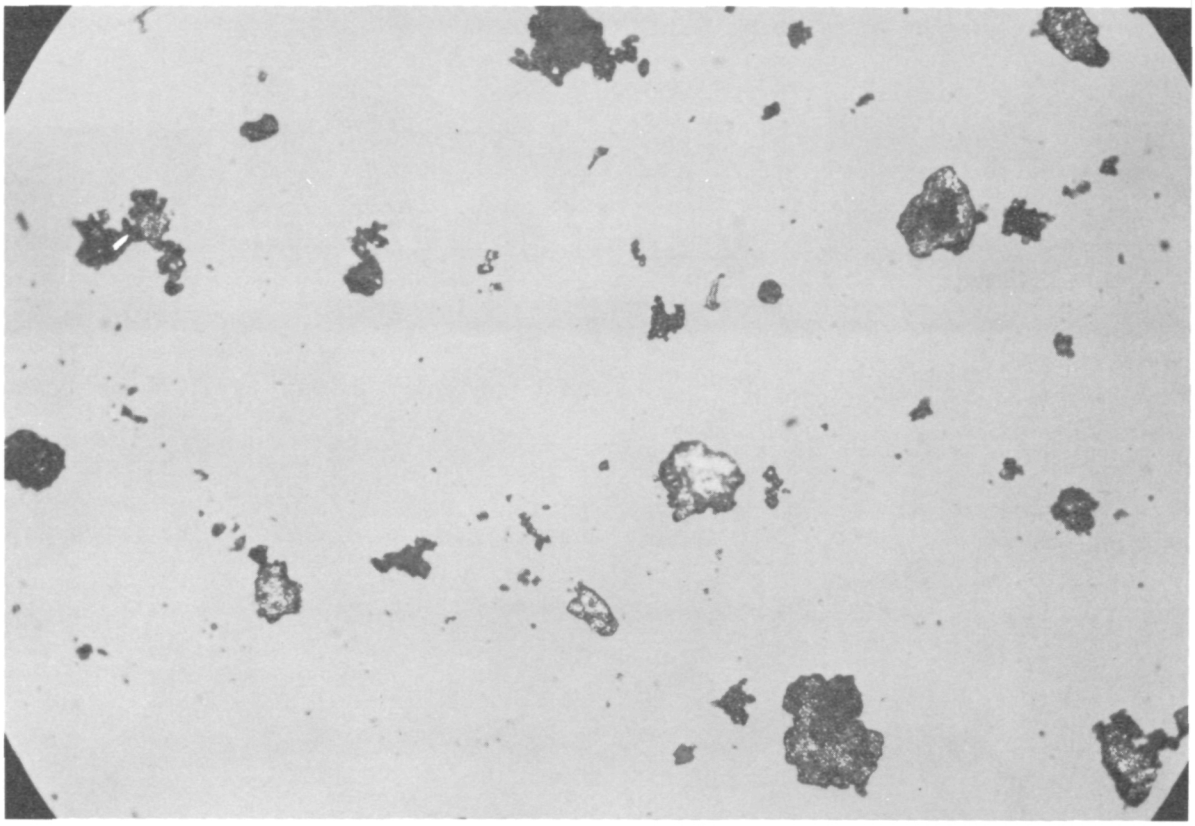

Sample B - Pump Inlet
(Magnified 250x)

publicity release from:

GUERIN, JOHNSTONE, GAGE *inc.*
advertising

1900 BEVERLY BLVD., LOS ANGELES 57, CALIFORNIA • DUNKIRK 5-7451

Don Acklin

for: Industrial Tectonics, Inc.

date: February 6, 1962

for immediate release

NEW TUNGSTEN CARBIDE
MASTER BALLS & SETS FROM STOCK

Sets or individual master balls in tungsten carbide are now available in 31 sizes from stock for gaging, precision measuring, design and production applications. Size range is from 1/16-in. to 1-in. diam. in 1/32-in. increments. Balls are checked at zero gage pressure against master balls calibrated and certified by the National Bureau of Standards. Tolerance is $\pm$0.000010-in., sphericity within 0.000010-in. maximum. Finish is 1-microinch or better, hardness 89-91 Rockwell A. Master balls will not pit, rust or corrode and are resistant to wear, abrasion and impact. Coefficient of expansion is 2.33×10^{-6} in. per ^{o}F. Cost is much lower than comparable gage blocks. Extreme accuracy ideal for space and missile programs and to measure depth of drilled holes, check internal tapers and measure diameters of cylindrical holes. Larger or non-standard sizes and tolerances also available on order. For further information, write to F. E. Schwalbe, Industrial Tectonics, Inc., 3686 Jackson Road, Ann Arbor, Michigan; telephone 663-2451.

-30-

PHOTOGRAPH ENCLOSED

Release No. 3385

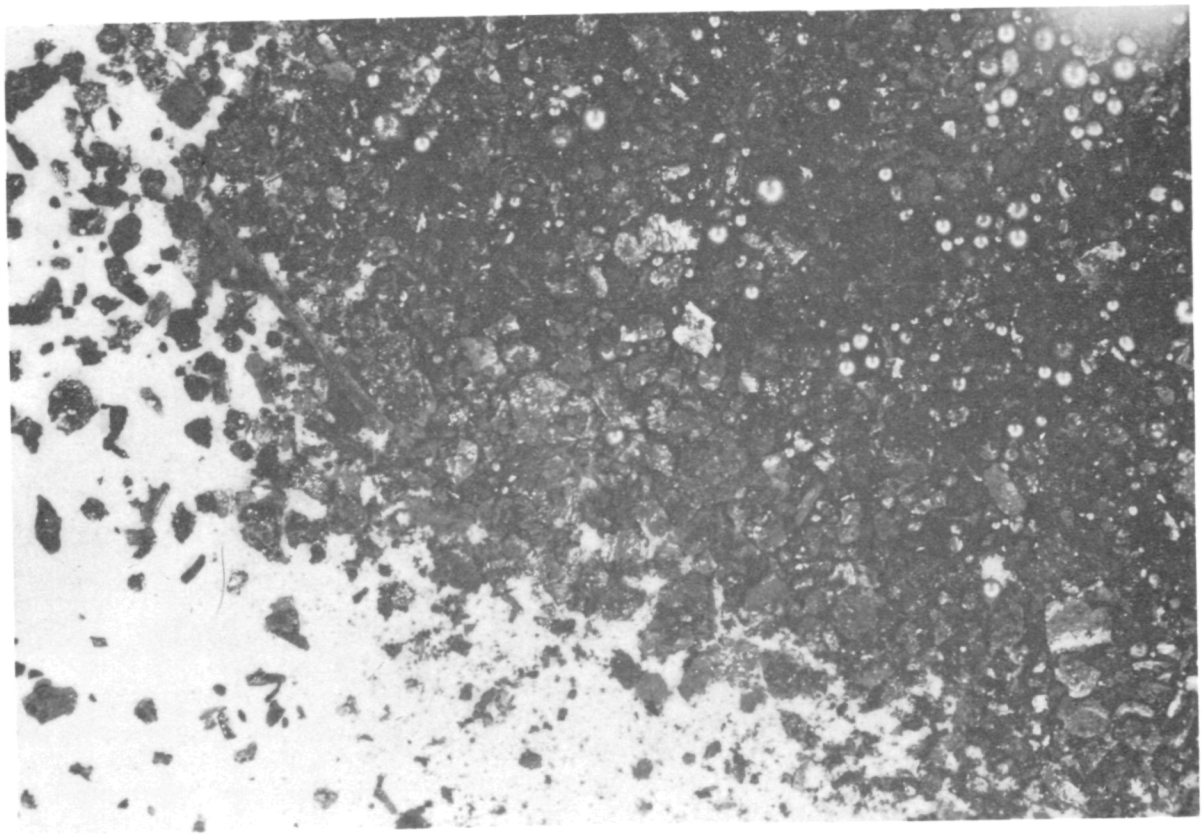

Sample C - Pump Outlet
(Magnified 10x)

Figure 38

Photomicrographs of the Corrosion Layer
Haynes 25 Compatability Capsules
Temperature 1025°F

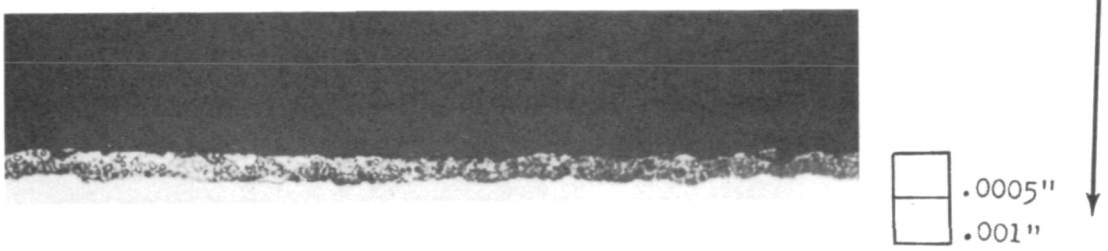

Photo No. 1118 Time-1000 Hrs 500x

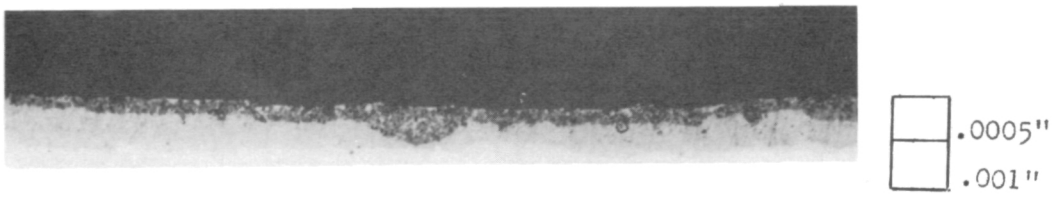

Photo No. 1129 Time-2000 Hrs 500x

Photomicrographs of the Corrosion Layer
Haynes 25 Compatability Capsules
Temperature 1100°F

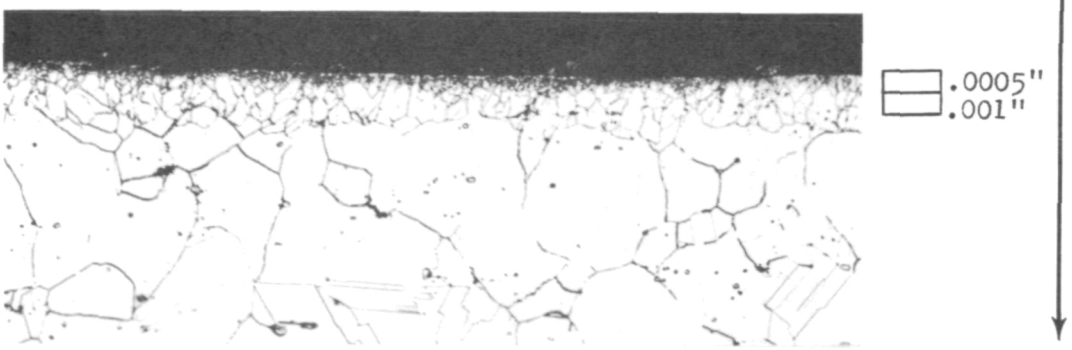

Photo No. 404 Time-500 Hrs 250x

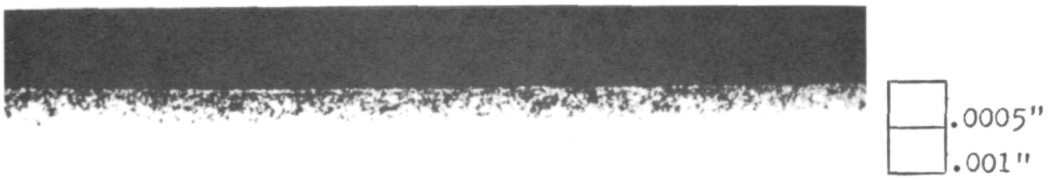

Photo No. 439 Time 1000 Hrs 500x

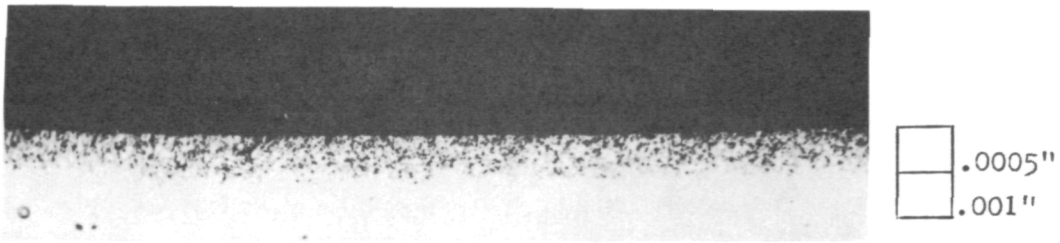

Photo No. 739 Time 2000 Hrs 500x

Photomicrographs of the Corrosion Layer
Haynes 25 Compatability Capsules
Temperature 1175°F

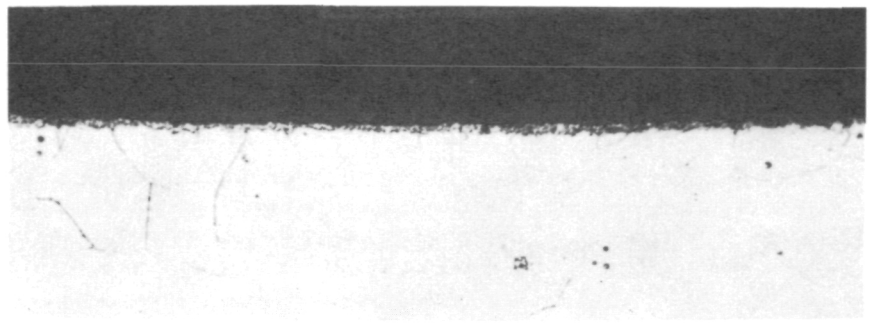

.0005"
.001"

Photo No. 1114 Time 500 Hrs 500x

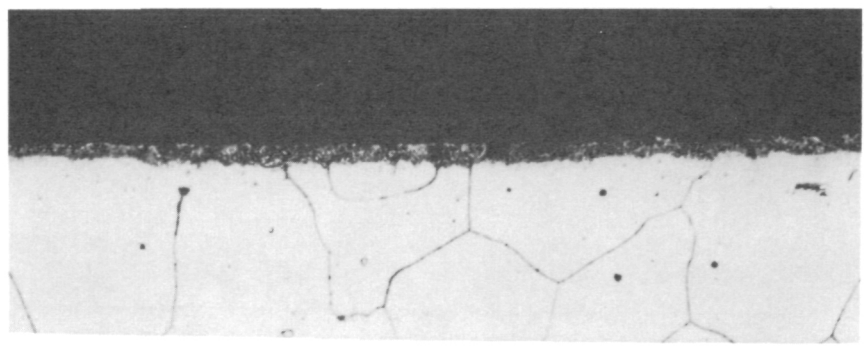

.0005"
.001"

Photo No. 1073 Time 1000 Hrs 500x

MICROHARDNESS SURVEY

HAYNES 25 & 405 STAINLESS STEEL EXPOSED TO MERCURY AT 1025°F

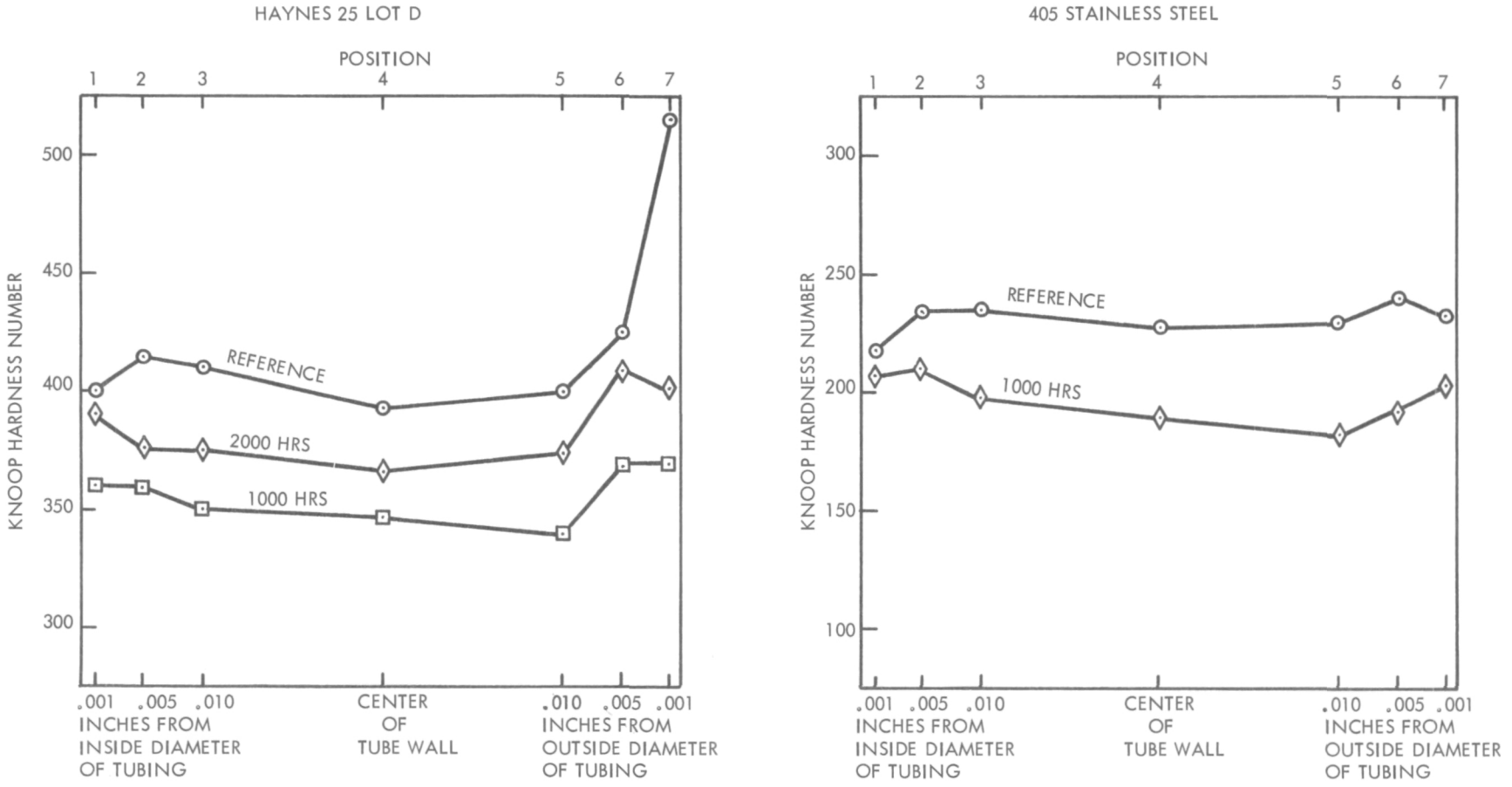

Figure 40

MICRO HARDNESS SURVEY OF HAYNES 25 TUBING EXPOSED TO MERCURY AT 1100°F

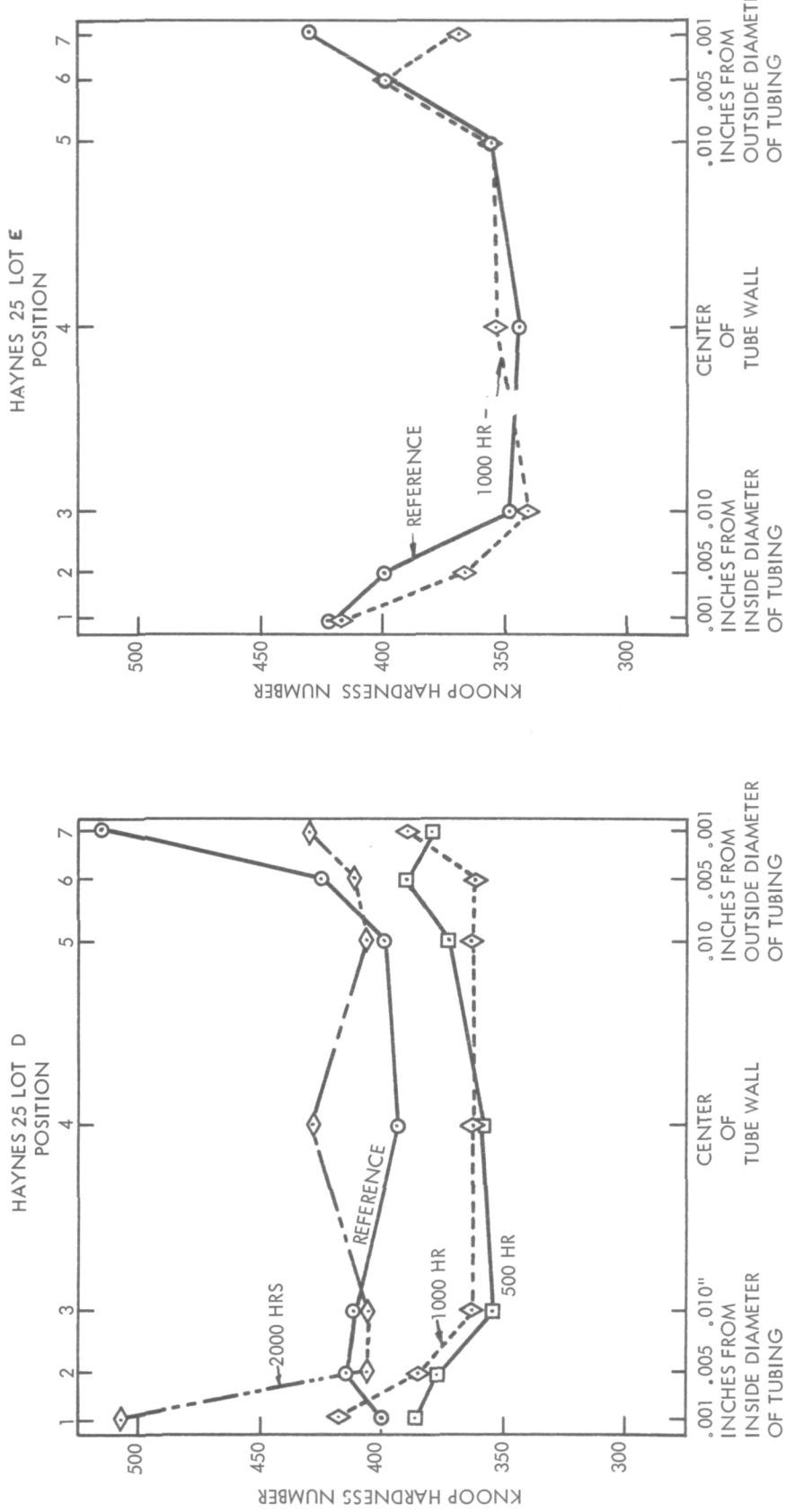

MICROHARDNESS SURVEY; HAYNES 25 EXPOSED TO MERCURY AT 1175°F

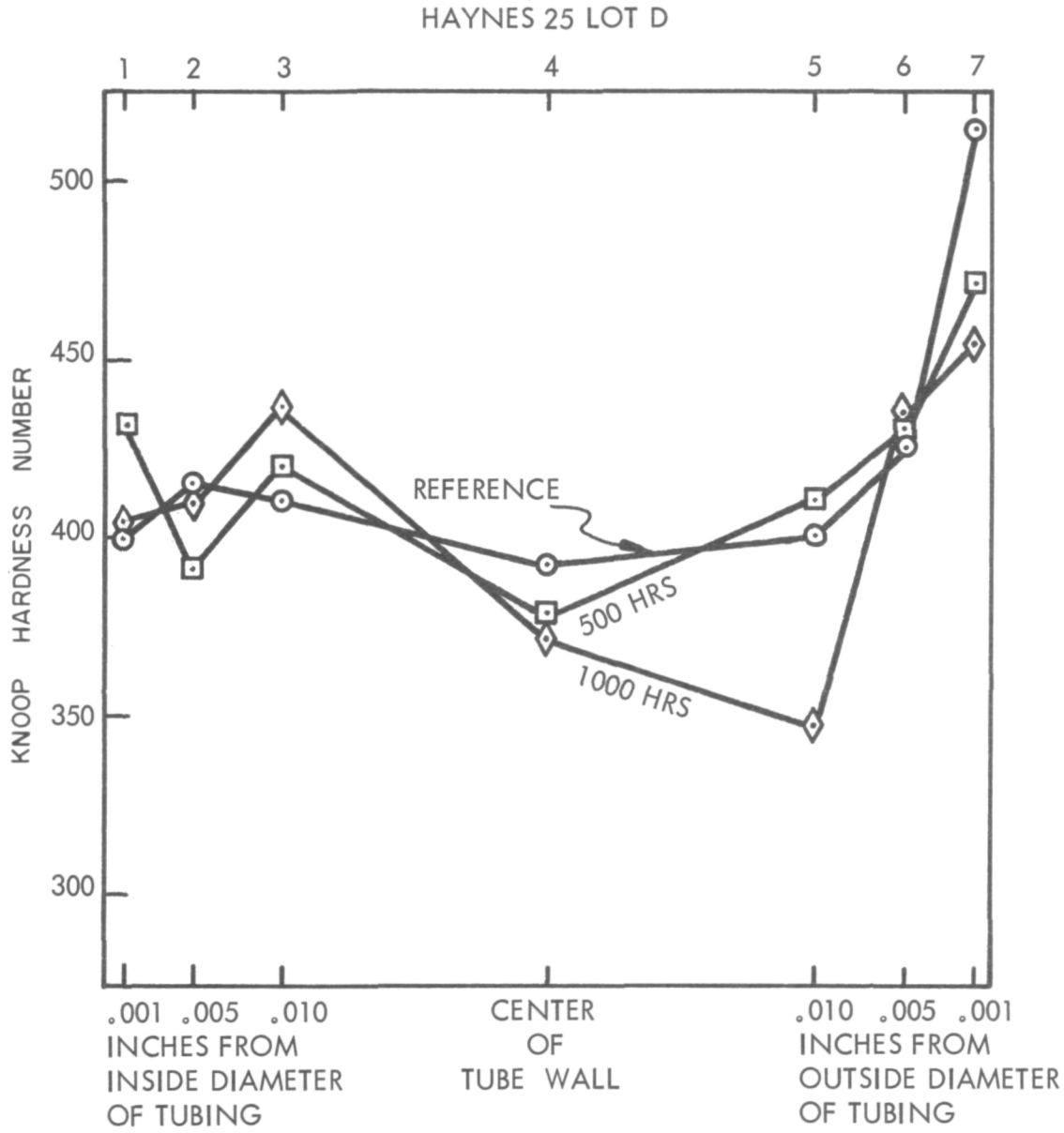

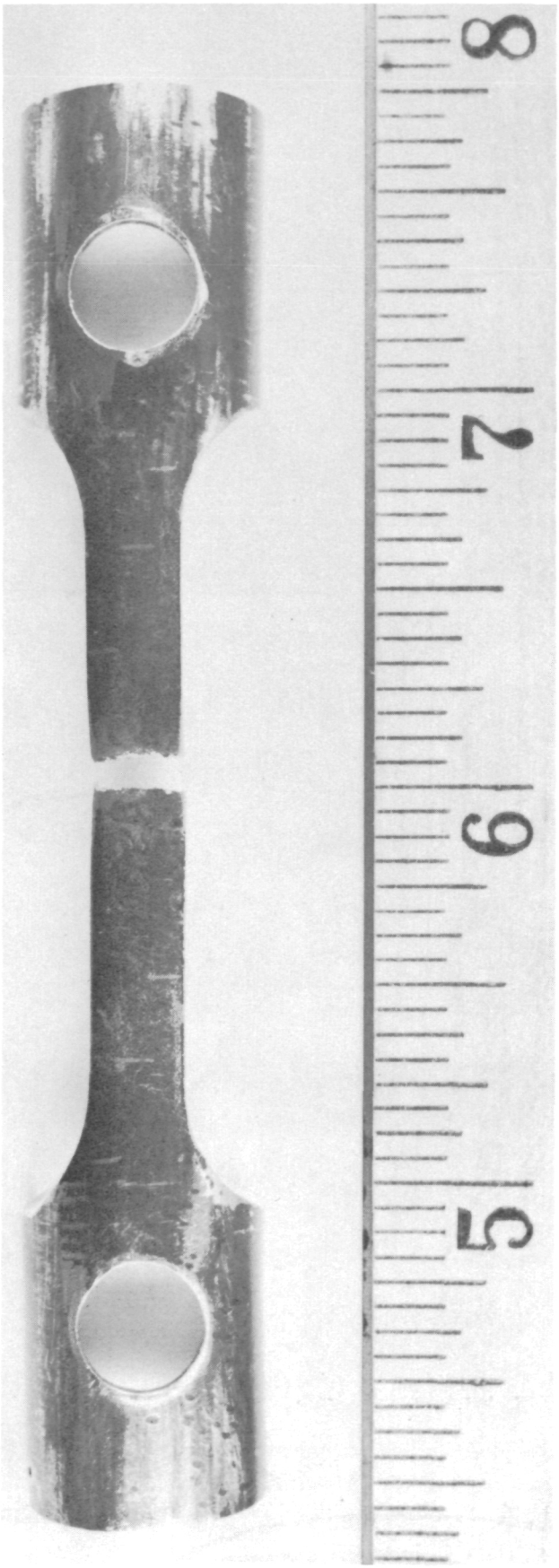

Broken Tensile Specimen from Compatability Capsule Run at 1100°F for 2000 hrs

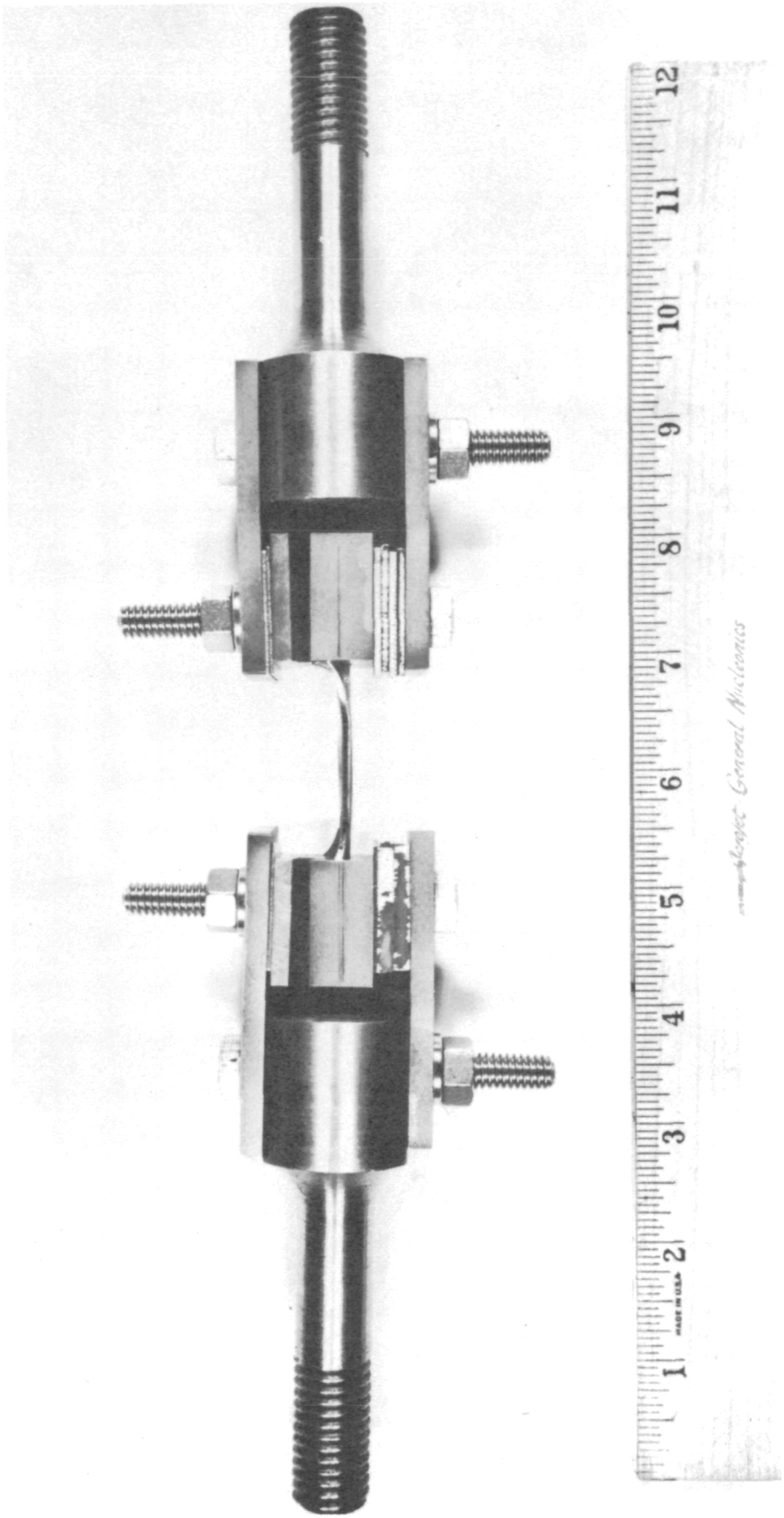

Tensile Test Assembly

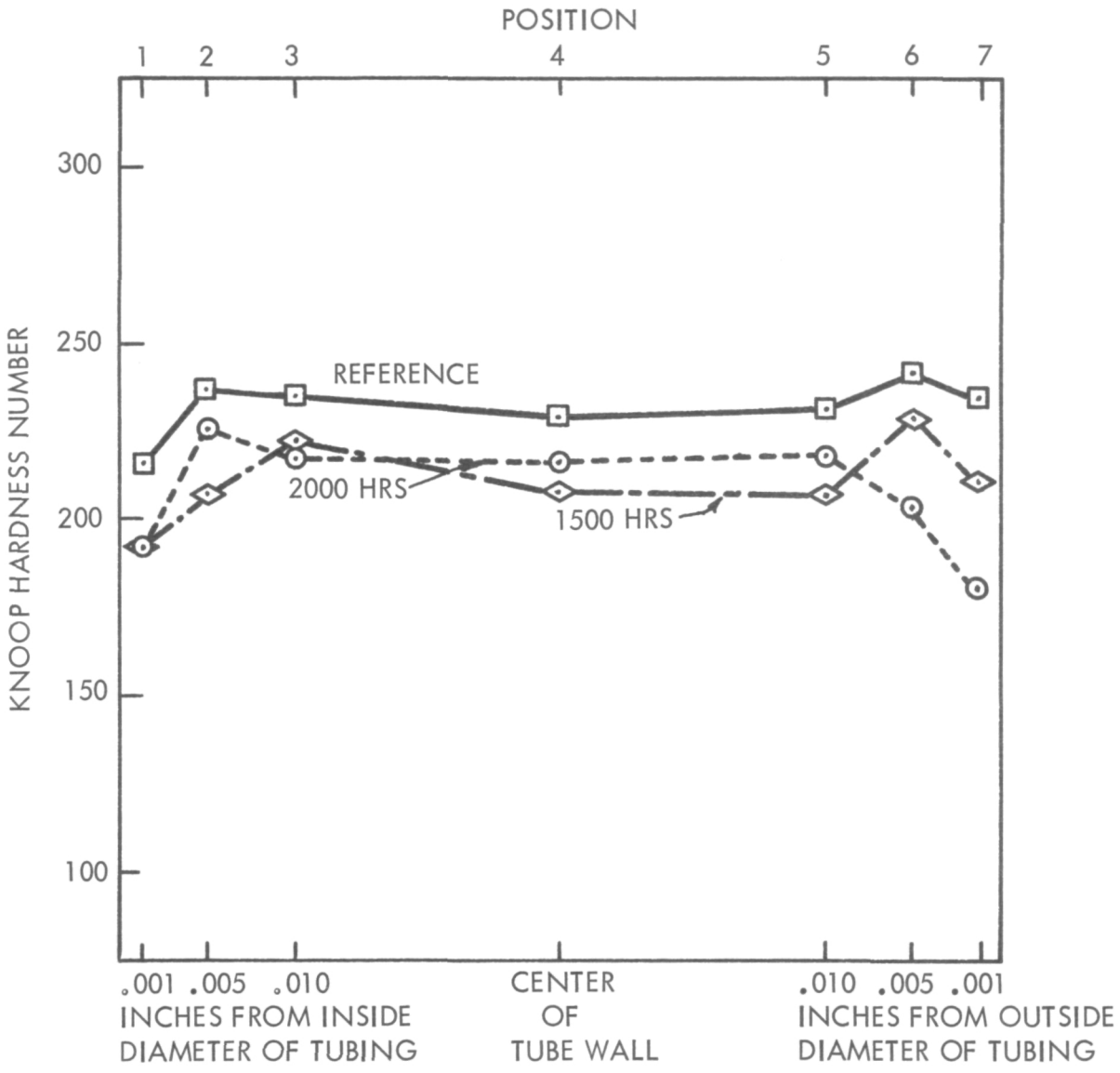

Microhardness Survey of 405 Stainless Steel
Tubing Exposed to Mercury at 1100°F

Figure 45

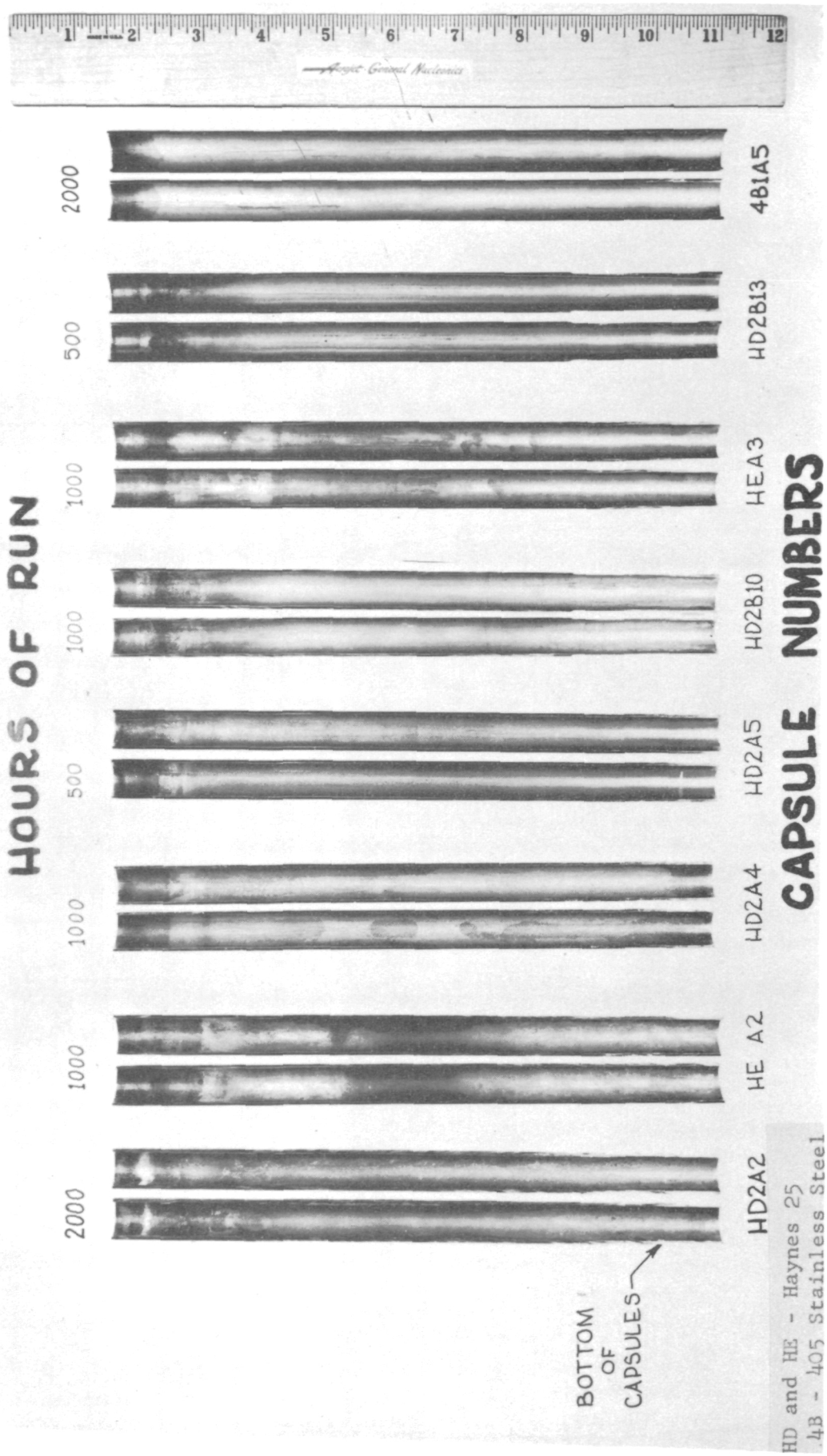

Mercury Compatibility Capsules

CONCENTRATION OF ELEMENTS FOUND IN MERCURY
AFTER 16 HOURS CONTACT WITH HAYNES ALLOY
8187(62Co - 21Cr - 12.5W, 1.5Fe, 3Ni, Si, Mn)

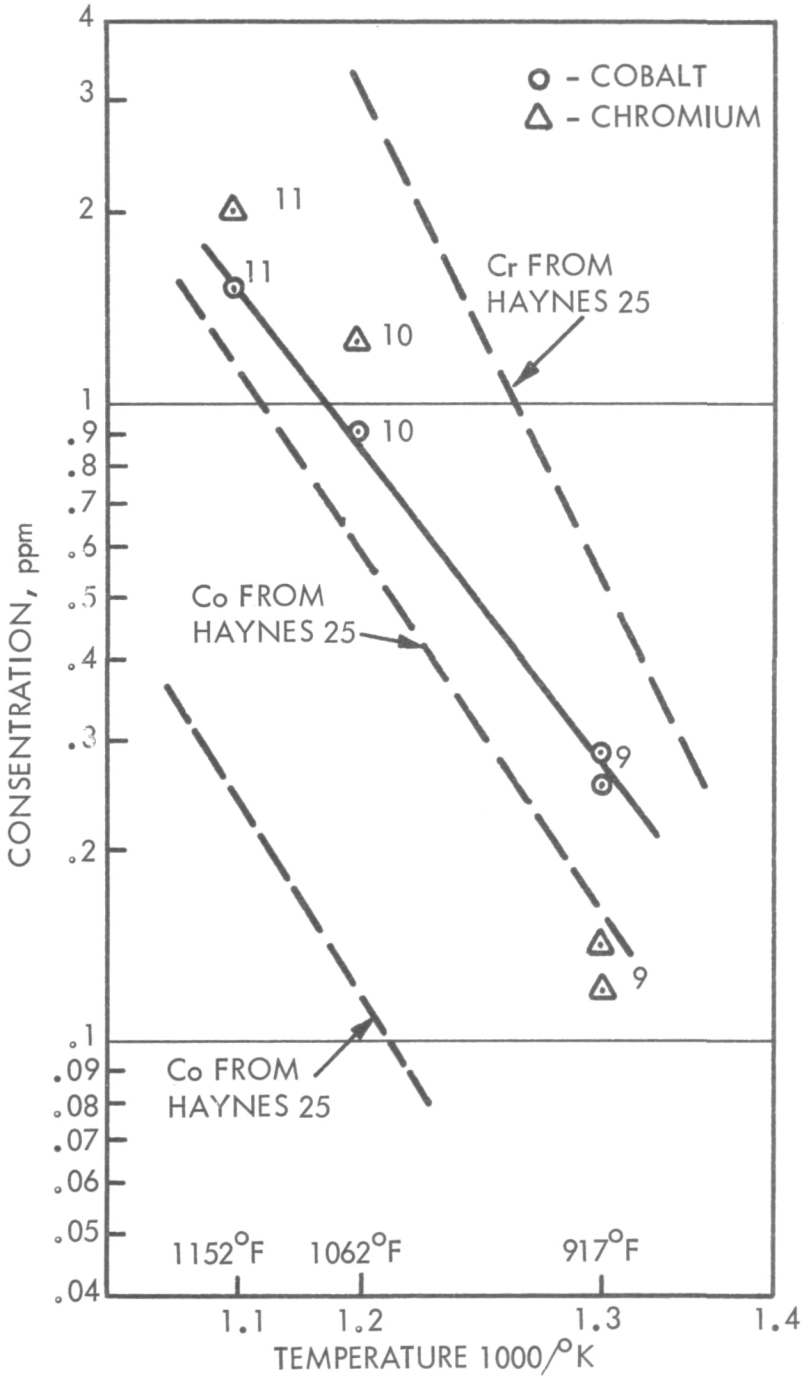

APPENDIX A

IBM 7090 RADIATOR OPTIMIZATION CODE - SNOR

SNOR is composed of 82 inputs consisting of 10 J arrays, 1 I-J array, and 71 single valved quantities. Most of the SNOR inputs are obtained from subroutines.

The SNOR code input is comprised of the following information:

Definition
Number of panels per wing
Number of manifolds per wing
Number of wings
Pitch of condensing tubes
Length of subcooler section of first tube in panel
Length of subcooler section of last tube in panel
Length of tapered section of first tube in panel
Length of tapered section of last tube in panel
Wall thickness of condensing tube
Wall thickness vapor manifold
Wall thickness liquid manifold
Wall thickness vapor bellows
Wall thickness liquid bellows
Distance center line tube to end of liquid bellows
Distance center line tube to end of vapor bellows
Armor factor-vapor manifold
Armor factor-liquid manifold
Density-tube material

Density-armor material
Density-fin material
Thermal conductivity of fin material
Thermal conductivity of armor material
Thermal conductivity of tube material
Thermal conductivity of manifold material
Velocity head factor at a joint in manifold
Velocity head factor at a tube inlet
Velocity head recovery coefficient in liquid manifold
Velocity head recovery coefficient in vapor manifold
Pressure drop correlation
Constants for pressure drop correlation
Density of emissivity coating
Armor factor vapor bellows
Armor factor liquid bellows
Exponent-armor equation
Meteorite puncture rate
Armor thickness correction coefficient for tube thickness
Vehicle diameter
Vehicle porosity
Vehicle temperature
Incident solar flux
Emissivity of armor
Emissivity of tube
Emissivity of manifold
Contact coefficient vapor manifold
Contact coefficient liquid manifold
Effective heat transfer coefficient vapor bellows
Effective heat transfer coefficient liquid bellows
Contact coefficient condensing tubes
Condensing heat transfer coefficient
Bumping factor for heat transfer in liquid
Lowest temperature in array

Highest temperature in array
Number of intervals on fin < 50
Number of intervals on tube < 30
Radiator inlet pressure
Radiator outlet pressure
Radiator inlet quality
Thickness of fin at root
Fin thickness Saper factor
Inside diameter of tapered tube at subcooler joint
Taper factor for inside diameter of condensing tube
Inside diameter of subcooler tube
Thermal conductivity of bellows material
Emissivity of bellows material
J values per parameter
Number of tubes in panel (J values)
Center to center distance between first tube and last tube in adjacent panels
Inside diameter of vapor manifold (J values)
Inside diameter of liquid manifold (J values)
Outside diameter vapor bellows (J values)
Outside diameter liquid bellows (J values)
Weight of vapor bellows per inch of length (J values)
Weight of liquid bellows per inch of length (J values)
Velocity head coefficient vapor bellows (J value)
Velocity head coefficient liquid bellows (J value)
Orifice coefficient first tube of a panel (J value)
Orifice coefficient second tube of a panel (J value)
Orifice coefficient third tube of a panel (J value)
Orifice coefficient fourth tube of a panel (J value)
Orifice coefficient fifth tube of a panel (J value)
Orifice coefficient sixth tube of a panel (J value)
Orifice coefficient seventh tube of a panel (J value)
Orifice coefficient eighth tube of a panel (J value)

The SNOR output comprises the following information:

- Heat rejected from vapor manifolds
- Heat rejected from liquid manifolds
- Heat rejected from condenser tubes
- Total heat rejected from radiator
- Total mercury flow rate
- Weights of all components including:
  - Vapor manifold and bellows
  - Liquid manifold and bellows
  - Condenser tubes
  - Emissivity coating
  - Fins
  - Fluid in tubes
  - Fluid in vapor manifold
  - Total fluid
  - Armor of vapor manifold and bellows
  - Armor of liquid manifold and bellows
  - Armor of tubes
  - Total radiator
- Armor thickness on the following parts:
  - Condenser tubes
  - Liquid manifolds
  - Liquid bellows
  - Vapor manifold
  - Vapor bellows
- Temperatures:
  - Radiator outlet - condensing
  - Radiator outlet - subcooler
- Surface areas:
  - Manifold, bellows, and condenser tubes (without armor)
  - Manifold, bellows, and condenser tubes (with armor)

Condenser tubes (with armor)

Manifold and bellows (with armor)

Fins (both sides)

Total length of manifolds and condenser tubes

Distance of interface from tube inlet for each tube for each panel

Heat rejection per tube for each tube for each panel

Flow rate per tube for each tube for each panel

Tube outlet temperature for each tube for each panel

Tube inlet pressure for each tube for each panel

Tube outlet pressure for each tube for each panel

Vapor manifold fluid quality for each tube for each panel

The subroutines include the following programs:

GEOMETRY - Comprises 35 inputs and calculates the following:

Unarmored outer surface area of all fluid carrying tubes

Total length of all tubes

Armored surface area of all condenser tubes

Armored surface area of all manifold and bellows

Total heat transfer surface area

Armor thickness on condenser tubes

Armor thickness on liquid bellows

Armor thickness on vapor bellows

Armor thickness on liquid manifolds

Armor thickness on vapor manifolds

Tapered length of each condenser tube

Straight length of each condenser tube

Total length of each condenser tube

C/C distance of each tube from vehicle center line

Center line distance of first condenser tube in first panel to vehicle center line

Center line distance of last condenser tube in last panel to vehicle center line

Tapered length of longest condenser tube

C/C distance from first condenser tube in first panel to last condenser in last panel

Number of vapor manifolds per wing

Number of liquid manifolds per wing

Number of condenser tube groups per wing

FMRCAL - Calculates view factors from each manifold and bellows section to the plane of the radiator.

FMVCAL - Calculates view factors from each manifold and bellows section to the vehicle.

CM12QS - Calculates coefficients in manifold or bellows network analysis equations.

MRWCAL - Calculates wall resistance of each manifold and bellows section from tube ID to armor OD.

QPTFAB - Uses RADIAT and CUMINT to build a three dimensional array of heat rejection per unit length as a function of condenser tube temperature at ID, distance of condenser tube center line from vehicle center line, armored condenser tube OD.

RADIAT - Calculates heat rejection per inch of length of tube, fin surface and total, the temperature distribution in fin, fin base temperature, fin efficiency.

CUMINT - A trapezoidal integration procedure for integrating dp/dx, heat rejection/unit length of fin, heat rejection/unit length of tube, and other position dependent variables.

QPT4LØ - For a given point on a given condenser tube (i.e., a specified c/c dist of the condenser tube to the vehicle center line, a specified condenser tube ID, and a specified temperature on the ID of the condenser tube at this point). QPT4LØ interpolates in the array set up by QPTFAB and calculates the value of $Q = QP/T_1^4$ at this point.

QPCALC - For a given point in a given condenser tube (as above, with the fluid temp initially set = temp at ID on condenser tube) QPT4LØ is used to give QPX/T_1^4. The film drop is then calculated (based on h from HCØNDR) and the heat flux is iterated on until a convergence of 0.01% is reached.

TUBCAL - For each condenser tube an initial interface position is assumed. QPCALC is used to calculate the heat rejection at each point from the tube entrance to the interface. CUMINT is then used to sum these heat rejections. The enthalpy change is then used to find the coolant flow rate. The flow rate and tube dimensions are used to find the velocity gradient which in turn determines the pressure gradient. Pressure at each pt. is determined from dP/dx with CUMINT. The pressures are used to reset the sat. temp at each pt. and recalculate the heat rejection and flow rate. The iteration continues until flow rate converges to 0.05%. The outlet pressure is then calculated and the interface position reset and the iteration continued until outlet pressure converges to within 1% of the ΔP through the tube.

If the interface is pushed out the end of the tube, an artificiality is introduced which repositions the interface within one diameter of the end of the tube and linearly decreases the outlet pressure for this case.

The heat rejection from the subcooled fluid (i.e., interface to tube outlet) is calculated and the outlet temperature is iterated upon until the calculated outlet temperature on consecutive passes agrees within $0.1^{\circ}F$.

The total heat rejection and flow rate through all condenser tubes is then summed. The pressure distribution through the vapor and liquids manifolds and bellows is determined and the new pressure distribution used in each subsequent iteration with TUBCAL until the following convergence criteria are met:

Total flow rate in consecutive passes agrees within 1%.

Flow rate through each condenser tube in consecutive passes agrees within 1%.

VECALC - Calculates the following for each vapor bellows:

Heat rejection

Outlet enthalpy

Outlet pressure

VMPCAL - Calculates the following for each section of vapor manifolding:

Heat rejection

Outlet flow rate and enthalpy

Outlet pressure

LMPCAL - Calculates the following for each section of liquid manifolding:

Heat rejection

Outlet flow rate and pressure

LBCALC - Calculates the following for each liquid bellows:

Heat rejection

Outlet flow rate and pressure

After the flow rate (total and in individual condenser tubes converges within 1%), WEIGHT is called.

WEIGHT - Calculates:

Weight of fluid in all vapor manifolds	(WFVM)
Weight of fluid in all liquid manifolds	(WFLM)
Weight of fluid in all condenser tubes	(WFLT)
Fin surface area (both sides)	(FS)
Weight of all condenser tubes	(WTT)
Weight of all vapor manifolds	(WVM)
Weight of all liquid manifolds	(WLM)
Weight of armor on all condenser tubes	(WATT)
Weight of armor on all vapor manifolds	(WAUM)
Weight of armor on all liquid manifolds	(WALM)
Weight of all fins	(WFT)
Weight of all fluid (WFVM + WFLM + WFLT)	(WFLD)
Weight of emissivity coating	(WEC)
Weight of radiator	(WRT)

APPENDIX B

MERCURY SOLUBILITY DATA FOR HAYNES ALLOY 8187

MERCURY SOLUTIBILITY DATA FOR HAYNES ALLOY 8187

OPERATING DATA

Run No.	Material	Temp. °F	Wt. Hg-g	Surf. to Vol. Ratio	Appearance of Hg After Run	Appearance of Specimen After Run
9	Blank	917	75.0	--	Clean	
9	8187	917	75.0	2	Light scum	No wetting; slightly discolored
9	8187	917	75.0	2	Light scum	No wetting; slightly discolored
10	Blank	1062	--	--	Clean	
10	8187	1062	75.0	2	Capsule leaked. No data.	
10	8187	1062	75.1	2	Scum	No wetting; discolored
11	Blank	1152	75.0	--	Clean	
11	8187	1152	75.4	2	Capsule leaked. No data.	
11	8187	1152	75.0	2	Heavy scum; dark particles.	Slight wetting below Hg surface

ANALYTICAL DATA

					Quantitative						Semiquantitative												
Run No.	Material	Temp °F	Tube No.	Sample wt-g	Fe(2) mg	Fe(2) ppm	Cr mg	Cr ppm	Co mg	Co ppm	Na mg	Mg mg	Al mg	Si mg	Ca mg	Ti mg	Mn mg	Ni mg	Cu mg	Mo mg	Ag mg	Ba mg	Pb mg
--	(1) Reagent Blank	--	C-6	--	<.001	--	.0006	--	--	--	--	.001	.002	.01	.003	--	--	--	.0007	--	--	--	--
--	(1) Mercury Blank	--	C-5	--	<.001	--	.001	--	--	--	--	.001	<.002	.01	.004	--	--	--	.005	--	.0002	--	--
9	Blank	917	A-4	14.8821	.0033	--	.0009*	--	--	--	--	.004	.005	.03	.009	--	--	--	--	--	<.001	.0008	--
9	Haynes 8187	917	B-5	12.3505	.0072	--	.0024	.12	.0035	.28	--	.007	.03	.035	.015	.001	.002	.002	.0006	.001	<.001	.0005	--
9	Haynes 8187	917	B-6	17.4835	.010	--	.0034	.14	.0043	.25	.021	.003	.04	.03	.01	.001	.001	.004	.0006	.003	<.001	.002	--
10	Haynes 8187	1062	B-2	20.2972	.005	--	.026*	1.23	.018	.89	--	.004	.008	.025	.006	.002	--	.015	.0018	--	<.001	--	--
10	Blank	1062	B-7	24.7038	.005	--	.0010*	--	--	--	.018	.006	.013	.035	.02	.001	--	--	.0007	.003	<.001	.002	--
11	Haynes 8187	1152	B-3	13.3495	<.005	--	.028*	2.0	.020	1.5	.015	.0035	.01	.025	.007	.001	.001	.02	.002	--	<.001	.0008	--
11	Blank	1152	A-2	19.3823	.0048	--	.0009*	--	--	--	.015	.006	.009	.035	.01	.001	--	--	.0012	--	<.001	--	0.2
--	(1) Reagent Blank	--	A-3	--	.0034	--	.0007	--	--	--	--	.0025	.003	.015	.004	.001	--	--	.0009	--	<.001	--	--

Notes:

(1) All analyses semi-quantitative (± 50%). Submitted as group. Remaining 8 samples analyzed as group.
(2) Blank too high. No significant results.
* Indicates value used to calculate blank correction.

Report No. 0390-04-6

DISTRIBUTION LIST

	No. of Copies
National Aeronautics and Space Administration 801 Nineteenth Street, N.W. Washington 25, D.C. Attention: Dr. Fred Schulman Program Director Via: BuWeps Rep., Azusa	2 plus repro
BuWeps Representative, Azusa	1
National Aeronautics and Space Administration 1512 H St., N.W. Washington 25, D.C. Attention: George Deutsch	1
National Aeronautics and Space Administration Lewis Research Center 21000 Brookpark Road Cleveland 35, Ohio Attention: Henry O. Slone Nuclear Engine Projects Office	2
National Aeronautics and Space Administration Lewis Research Center 21000 Brookpark Road Cleveland 35, Ohio Attention: Louis Rosenblum Materials & Structures Division	1
National Aeronautics and Space Administration Lewis Research Center 21000 Brookpark Road Cleveland 35, Ohio Attention: Robert E. English Nuclear Systems Division	1
National Aeronautics and Space Administration Lewis Research Center 21000 Brookpark Road Cleveland 35, Ohio Attention: Irving Johnsen Fluid System Components Division	1

DISTRIBUTION LIST (cont.)

	No. of Copies
National Aeronautics and Space Administration Lewis Reaearch Center 21000 Brookpark Road Cleveland 35, Ohio Attention: George Mandel Library	1
National Aeronautics and Space Administration Western Operations Office 150 Pico Boulevard Santa Monica, California Attention: Mr. John Keeler	1
National Aeronautics and Space Administration Jet Propulsion Laboratories California Institute of Technology 4800 Oak Grove Drive Pasadena, California Attention: John Paulson	2
National Aeronautics and Space Administration Lewis Research Center 21000 Brookpark Road Cleveland 35, Ohio Attention: B. Lubarsky Nuclear Systems Division	1
National Aeronautics and Space Administration Marshall Space Flight Center Huntsville, Alabama Attention: Russell H. Shelton	1
National Aeronautics and Space Administration Marshall Space Flight Center Huntsville, Alabama Attention: Dr. Ernst Stuhlinger	1
National Bureau of Standards Department of Commerce Washington 25, D.C. Attention: C. W. Beckett	1
Rocketdyne 6633 Canoga Avenue Canoga Park, California Attention: R. B. Dillaway	1

DISTRIBUTION LIST (cont.)

	No. of Copies
Pratt & Whitney Aircraft East Hartford Connecticut Attention: Wm. H. Podolny	1
Flight Propulsion Laboratory Department General Electric Company Cincinnati 15, Ohio Attention: Morris A. Zipkin	1
Thompson Ramo-Wooldridge, Inc. New Devices Laboratories 7209 Platt Avenue Cleveland 4, Ohio Attention: J. E. Taylor	1
Allison Division General Motors Corporation Indianapolis 6, Indiana Attention: T. F. Nagey	1
National Aeronautics and Space Administration 1512 H. Street, N.W. Washington 25, D.C. Attention: W. H. Woodward	1
Atomics International P.O. Box 309 Canoga Park, California Attention: Carl E. Johnson	1
Atomics Energy Commission Germantown, Maryland Attention: Lt. Col. G. M. Anderson	1
National Aeronautics and Space Administration Marshall Space Flight Center Huntsville, Alabama Attention: Arthur Thompson	1
National Aeronautics and Space Administration Lewis Research Center 21000 Brookpark Road Cleveland 35, Ohio Attention: Richard P. Geye Sunflower Project Officer	1

DISTRIBUTION LIST (cont.)

	No. of Copies
Director, USAF Project RAND The RAND Corporation 1700 Main Street Santa Monica, California Attention: Library Via: Air Force Liaison Office	1
Electro-Optical Systems Pasadena, California Attention: Mr. Joseph Neustein	1
Internal Distribution	42